A Spatiotemporal Model of Condition to Derive a Novel Starvation Mortality Index That Improves a State-space Stock Assessment Model for Atlantic Cod on the Southern Grand Bank of Newfoundland

by

© **S. J. W. W. M. M. P. Weerasekera**

A thesis submitted to the School of Graduate Studies in partial fulfillment of the requirements for the degree of Master of Science.

Centre for Fisheries Ecosystems Research, Fisheries and Marine Institute

Memorial University of Newfoundland

March 2024

St. John's, Newfoundland and Labrador, Canada

Abstract

Atlantic cod on the Southern Grand Bank (SGB) collapsed in the early 1990's and a fishing moratorium has been in place since 1994. I investigate how fish condition influences the natural mortality rate (M) and the prospects for rebuilding the SGB cod stock. I developed a body condition model and derived a starvation mortality rate (M_K) index. I modelled weight as a function of length, with deviations (i.e., change in condition) for survey strata, year, month, length, and their interactions. The M_K index was higher in the spring than in the fall, higher for cod between 55–80 cm in length and for cod larger than 120 cm, and higher during 1991–1993 when the stock experienced a substantial decline. The M_K index was incorporated into an age-based state-space stock assessment model (SSAM) as a component of M. This led to a significant decrease (62%) in the size of the cohort process errors (i.e., their standard deviation). This reduction suggests that M_K significantly improved the model of stock productivity. Therefore, I conclude that M_K explains a substantial portion of the variation in M, and that starvation mortality is an important component of the productivity of SGB cod.

To my loving wife, son and daughter

General summary

This thesis's primary focus is to estimate an index of starvation-induced mortality rate for cod on the Southern Grand Bank (SGB) by examining changes in body condition. I used length and gutted-weight (total body weight minus stomach contents and internal organs) data and developed a body condition model to derive a starvation mortality index. The index was higher in the spring than in the fall, higher for cod between 55–80 cm in length and for cod larger than 120 cm, and higher during 1991–1993 when the stock experienced a substantial decline. I incorporated this index into an age-based stock assessment model as a component of natural mortality. This substantially reduced the uncertainty in population dynamics not explained by the model, indicating that this index improved the model of stock productivity. In conclusion, this index explains a substantial portion of the variation in natural mortality, and proves to be an important component of the productivity of SGB cod.

Acknowledgements

I would like to express my sincere gratitude to my supervisor, Prof. Dr. Noel Cadigan, for his expert advice and extraordinary support throughout my study. The training strategy he employs for his students is unique. In particular, his guidance, encouragement, and motivation for proper scientific writing were simply outstanding, which greatly boosted my confidence in true scientific writing. He truly molds his students into independent scientists, and that is something to be admired.

I extend my heartfelt thanks to Dr. Kunasekaran Nirmalkanna, a postdoctoral fellow of Prof. Cadigan, for his immense support in modeling work and explanations of significant statistical modeling concepts.

My sincere thanks also go to Dr. Paul M. Regular and Dr. Rick M. Rideout of Fisheries & Oceans Canada, for providing their expert knowledge in developing, reviewing, and contributing to the research papers I produced based on my thesis.

I am thankful to my external thesis reviewers, Dr. Divya Varkey of Fisheries & Oceans Canada and Dr. Matthew Robertson of Fisheries and Marine Institute of Memorial University of Newfoundland, for their valuable suggestions to improve the thesis text.

I am also deeply thankful for the generous funding provided for this research by the Ocean Frontier Institute, through an award from the Canada First Research Excellence Fund. Without their generous financial support during my program, this research work

would not have been possible.

My sincere gratitude also goes to my parents for their love and unconditional support throughout my life and my studies. Finally, but not least, special thanks go to my loving wife, son, and daughter for their incredible support, love, and endurance throughout this journey. This effort would not have been successful without their understanding and support.

Co-authorship statement

The research presented in this thesis was conducted by S. J. W. W. M. M. P. Weerasekera under the guidance of his supervisor, Dr. Noel G. Cadigan. Dr. Cadigan was responsible for the initial development of research ideas. The model described in Chapter 2 was initially developed by Dr. Kunasekaran Nirmalkanna, a Postdoctoral Fellow at the Marine Institute of Memorial University. The model implementation and further analysis and refinements were conducted by S. J. W. W. M. M. P. Weerasekera. For Chapters 3, 4, and 5, the initial modeling work was supported by Dr. Cadigan. The model implementation and further analysis were done by S. J. W. W. M. M. P. Weerasekera. Chapters 2 and 3 of the thesis produced a research paper co-authored by Dr. Noel G. Cadigan and Dr. Kunasekaran Nirmalkanna of the Marine Institute of Memorial University, and Dr. Paul M. Regular and Dr. Rick M. Rideout of Fisheries & Oceans Canada. Dr. Nirmalakanna reviewed the methodology part of the paper. Dr. Cadigan reviewed the initial draft of the manuscript. Dr. Regular and Dr. Rideout provided comments for the improvement of the manuscript and also contributed to the discussion text. The paper was submitted to Fisheries Research and is currently under review. The second research paper is being compiled based on Chapters 4 and 5. Dr. Cadigan reviewed the first draft of the manuscript. Further review of the manuscript is being conducted by Dr. Regular and Dr. Rideout. The paper will be submitted to Fisheries Research or other journal.

Table of contents

List of tables

List of figures

List of abbreviations

AIC	Akaike Information Criterion
BIC	Bayesian Information Criterion
DFO	Fisheries and Oceans Canada
EEZ	Exclusive Economic Zone
ICNAF	International Commission for Northwest Atlantic Fisheries
LWR	Length Weight Relationship
MSE	Mean Squared Error
NAFO	Northwest Atlantic Fisheries Organization
NOAA	National Oceanic and Atmospheric Administration
RMSE	Root Mean Squared Error
RV	Research vessel
SA	Spatial Autocorrelation
SGB	Southern Grand Bank
SSAM	State-space Stock Assessment Model
SSB	Spawning Stock Biomass
SSM	State-Space Model
TA	Temporal Autocorrelation
TMB	Template Model Builder
VPA	Virtual Population Analysis

Chapter 1

Introduction

I first provide an overview of Atlantic cod population demographics. I then provide an overview of the history of cod fisheries in the Northwest Atlantic and the status of the cod fishery in the Northwest Atlantic and Atlantic Canada in general, followed by specific information for Southern Grand Bank (SGB) cod. This stock is also referred to as 3NO cod in the literature, but I usually refer to it as SGB cod.

1.1 Overview of Atlantic cod

Atlantic cod widely occupy the continental shelves of the Northwest and Northeast Atlantic Ocean (Sundby, 2000; COSEWIC, 2003; DFO, 2021), primarily at depths less than 500 m (Righton and Metcalfe, 2004). Additionally, cod can be found along inshore-offshore gradients (Rose, 2019). Overall, this distribution spans from about 40°N (south of Georges Bank in the US) to 80°N (to the north of West Spitsbergen) (Sundby, 2000; Rose, 2019) (Figure 1.1). In Newfoundland and Labrador, Atlantic cod occupy the waters spanning from Cape Chidley (i.e., northern tip of Labrador) southeast to the Grand Bank off eastern Newfoundland (COSEWIC, 2003). The biogeographic distribution of cod is primarily influenced by temperature (Coutant, 1987; Sundby, 2000; Mieszkowska et al., 2009). The ambient temperature within their distribution

range typically ranges from 1°C to 11°C for the stocks in the the West Greenland and northern Labrador, and southern part of the North Sea, the Irish and the Celtic Seas, respectively (Sundby, 2000). Nevertheless, they are sometimes found in water less than -1°C and over 20°C (Drinkwater, 2005; Mieszkowska et al., 2009). Atlantic cod from the Labrador and northeast Newfoundland shelves (i.e., NAFO 3K and northern 3L) to the northern Grand Banks are consistently distributed more to the north in warm ocean periods and more to the south in cold periods (DeYoung and Rose, 1993; Rose et al., 1994). In Labrador, cod are widely distributed within the temperature range of -1.0 to 3.5°C, whereas on the northeast Newfoundland shelf, this range is 2.0 to 3.5°C. On the northern Grand Bank, most of the cod inhabit cooler waters (-1 to 0.5°C) (Rose et al., 1994).

Atlantic cod is a moderately long-lived fish with a maximum recorded age of 25 years (O'Brien et al., 1993; Mieszkowska et al., 2009; Froese and Pauly, 2023). It reaches adulthood at an average length of 65.4 cm, which can vary between 31 cm and 74 cm (Froese and Pauly, 2023). The maximum recorded length and weight are 200 cm (O'Brien et al., 1993; Mieszkowska et al., 2009; Froese and Pauly, 2023) and 96 kg (O'Brien et al., 1993; Froese and Pauly, 2023), respectively. The growth of cod is correlated with food availability, temperature (Brander, 1995; Morgan et al., 2007, 2018), and other factors (Brander, 1995). Brander (1995) investigated the effect of temperature on growth for 17 North Atlantic cod stocks and found that the temperature effect on growth rate declines with age and is only significant up to age 4. Average weight-at-age 4 ranged from 0.6 kg in Labrador (2°C) to 7.3 kg in the Celtic Sea (11°C) (see Figure 1.2). Brander also established an exponential relationship between cod growth and temperature, indicating approximately a 30% increase in the weight-at-age 4 for every 1°C rise in temperature. According to Jobling (1988), an increase in cod growth rate can be supported by temperature up to a maximum of 14°C, but it declines above that threshold.

Atlantic cod is considered an early to medium-maturing fish compared to other fish species (Trippel, 1995; Myers et al., 1997; Link and Sherwood, 2004). Thus, cod shows a wide range of age and size of maturity (Wright and Rowe, 2004). In general, A_{50} (age at which 50% of fish in a population is assumed to be matured) varies between two (O'Brien et al., 1993; Trippel, 1995; Myers et al., 1997; Link and Sherwood, 2004; Mieszkowska et al., 2009) and seven years (Trippel, 1995; Myers et al., 1997; Link and Sherwood, 2004). A_{50} can vary across different locations and among populations (Trippel, 1995; Myers et al., 1997; Link and Sherwood, 2004), and even between females and males (Link and Sherwood, 2004). For instance, in the Northeast Arctic region, Ajiad et al. (1999) reported A_{50} values of 6.9 and 6.4 years, respectively for female and male cod. In contrast, Fahay (1999) reported A_{50} of 1.7 years for females and 1.9 years for males in Georges Bank. The highest A_{50}'s recorded for both female and male cod on the Icelandic north coasts were 7.3 and 6.6 years, respectively (Marteinsdottir and Begg, 2002). A summary of reported A_{50} values for various regions can be found in Table 3 of Link and Sherwood (2004).

Atlantic cod is a highly fecund species (Link and Sherwood, 2004; Wright and Rowe, 2004; Mieszkowska et al., 2009), meaning they produce a large number of eggs, which usually is directly proportional to the body size of the fish (Fudge and Rose, 2008; Rideout and Morgan, 2010a). Larger and older females may produce a relatively higher number of eggs compared to smaller females (Lambert et al., 2005). However, Atlantic cod are broadcast spawners, releasing their eggs into the water to disperse with the current. Consequently, only a very small percentage of these eggs, as low as 1 in 10 million, survive to maturity (Duarte and Alcaraz, 1989; Link and Sherwood, 2004; Wright and Rowe, 2004).

Habitat suitability for cod primarily depends on the food availability and temperature, particularly during early life stages. Habitat characteristics are critical as they settle to the bottom and live in their juvenile stage for one to four years. They prefer a

heterogeneous nearshore habitat such as in eelgrass (*Zostera marina*) beds (COSEWIC, 2003), where they find protection from predators. Juvenile cod tend to exhibit seasonal movements and migrations after age four (COSEWIC, 2003). Adult cod's habitat is quite diverse (COSEWIC, 2003; Grabowski and Grabowski, 2004). Usually, they move farther offshore to deeper habitats (Dalley and Anderson, 1997; Anderson and Gregory, 2000; Grabowski and Grabowski, 2004), while older juvenile cod still prefer to remain in coastal waters (Clark and Green, 1990; Gregory and Anderson, 1997; Cote et al., 2003; Grabowski and Grabowski, 2004).

Atlantic cod have more complicated spawning dynamics than was previously understood as a simple and random process (Zemeckis et al., 2014). Depending on the geographic location, spawning time can vary between December and June, and eggs take 2–4 weeks to hatch (Mieszkowska et al., 2009). They spawn both in inshore areas and on offshore banks (Stokesbury et al., 2017). The spawning occurs in the waters where depths can vary from tens (Smedbol and Wroblewski, 1997) to hundreds of meters (Brander, 1994; Morgan et al., 1997). The spawning period usually lasts less than three months (Brander, 1994; Chambers and Waiwood, 1996; Kjesbu et al., 1996). Even though spawning primarily occurs during the spring or winter, it also occurs during summer and autumn (ICES, 2005). Individuals with mature gonads are infrequently found outside the peak spawning periods (Zemeckis et al., 2014). In coastal regions, Atlantic cod spawn in a range of habitats such as rocky slopes (Meager et al., 2010), boulder outcrops (Dean et al., 2012), and patchy rock elevations (Marteinsdottir et al., 2000). As cod is a highly fecund fish species, with only a handful of offspring surviving to recruit to the fishery, spawning in the right place and at the right time is crucial for successful recruitment (Link and Sherwood, 2004). Recruitment refers to the process by which small, young fish transition to an older, larger life stage (Camp et al., 2020, p. 01).

Cod are omnivorous (animals that eat both plants and animals) demersal feeders (Link and Sherwood, 2004). Juvenile cod are specialized feeders (Grabowski and Grabowski, 2004), preferring small crustaceans, such as mysids, euphausiids, amphipods (Lilly and Fleming, 1981; Link and Sherwood, 2004) and small shrimps (Rose and O'Driscoll, 2002; Dawe et al., 2012; DFO, 2021). Medium-sized cod prefer to feed on larger crustaceans and small fish, in particular capelin, sand lance, herring, arctic cod, and other juvenile gadids (e.g., hakes). Large cod feed on crabs and medium-sized demersal and forage fish (Lilly and Fleming, 1981; Link and Sherwood, 2004), such as capelin and sand lance. Sometimes forage fish may be supplemented by squids or the juveniles of larger fish. In addition, their diet may include other taxa such as ctenophores, cnidarians, polycheates, gastropods, bivalves and echinoderms. However, these are rare in large quantities. Large amount of ctenophores and brittle stars in the gut content of cod is an indication of poor feeding condition. In general, it is more accurate to consider cod as opportunistic feeders that feed upon whatever is available in the prey field (Link and Sherwood, 2004).

1.2 History and synopsis of the recent status of cod fishery in the Northwest Atlantic and Atlantic Canada

The history of Northwest Atlantic fishery resources dates back to the 1490s and has evolved over the centuries. Initially, the groundfish fishery was exclusively dependent on cod due to its abundance. Later, the fishery developed to include other groundfish and eventually expanded to include all the fishing areas of the Northwest Atlantic. The efficiency of fish harvesting improved with the introduction of fishing gears such as cod traps and longlines in the late 1800s. This efficiency was further enhanced in the 1900s with the introduction of otter-trawlers in 1908 parallel to the industrialization (Lear, 1998).

In the Northwest Atlantic, the nominal catches of cod increased sharply during the 1960s, reaching a peak in 1968 at slightly over 1800 kilotonnes. However, catches decreased rapidly during the 1970s, dropping below 500 kilotonnes by 1977. An increase in catch (up to 750 kilotonnes) occurred after that until 1982, followed by minor fluctuations until 1989. Subsequently, catches rapidly decreased in the 1990s until 1995. Since then, catches have remained relatively steady, not exceeding 80 kilotonnes to date (Figure 1.4).

In Atlantic Canada, there was a substantial fishery for Atlantic cod and almost 400 kilotonnes were caught in 1990. However, a rapid decline in fishery landings occurred from 1990 to 1995, coinciding with the collapse of Atlantic cod populations in Canadian waters. There was no fishery catches greater than 50 kilotonnes thereafter, except in 1999 when the catch slightly exceeded 50 kilotonnes. The landings dropped below 15 kilotonnes by 2021 (Figure 1.5).

1.3 Atlantic cod in the SGB

1.3.1 Distribution and habitat

Newfoundland and Labrador populations of Atlantic Cod inhabit the inshore and offshore waters from the northern tip of Labrador to eastern Newfoundland, including the Grand Banks. Atlantic cod consists of four stocks on the Grand Banks and Labrador shelf: NAFO Divisions 2GH, 2J3KL, 3M, and 3NO (Figure C.4) (DFO, 2021). The cod stock in the NAFO Divisions 3NO is also referred to as SGB cod. During the summer, the juvenile cod tend to distribute over shallower areas of the bank, notably in the Southeast shoal area of 3N (Walsh et al., 1995; Lilly et al., 2000; Rideout et al., 2021). This is the nursery site for SGB cod (Walsh et al., 1995; NAFO, 2001). Older fish aggregate on the southwestern and southeastern slope areas (see Figure 2.1) when

winter cooling begins and distribute over the plateau of the bank during the summer (Lilly et al., 2000; Rideout et al., 2021).

1.3.2 Biology

Even though cod show a common life history pattern, considerable regional variations in their recruitment, growth rate, age of maturity, migration patterns, food and spawning time are apparent. Noticeably, population parameters (e.g., K; von Bertalanffy growth parameter) also vary among the stocks due to different temperature regimes (Brander, 1995; Rätz and Lloret, 2003).

Spawning

Historical reports had initially indicated that cod predominantly spawned in the slope areas of the SGB (Lilly, 2005). However, according to spring survey catches, Hutchings et al. (1993) reported that cod spawning is more prominent on plateaus compared to slopes. The precise locations of cod spawning are not yet fully understood. Consequently, further studies are crucial to demarcate these spawning areas, employing methods such as acoustic surveys to minimize disturbances compared to traditional trawl surveys (Lilly et al., 2000). However, the Southeast Shoal and the tail of the SGB (see Figure 2.1) have been identified as a crucial spawning sites for Atlantic cod in NAFO divisions 3NO (Walsh et al., 1995; NAFO, 2001; Drinkwater, 2005). Cod spawning on the Grand Bank begins in April, peaks in late May, and extends into June (Templeman, 1981; Lilly, 2005). The mean spawning date in 3NO is approximately one week earlier than in NAFO Division 3Ps and 3–4 weeks earlier than in NAFO Division 3L (Lilly, 2005).

Fecundity

May (1967), reported fecundity estimates, which represent the number of eggs produced by a mature fish, for Divisions 3NO cod, in relation to length and age. In Division 3N, fecundity estimates ranged from approximately 0.5 to 7 million eggs for cod aged 6 to 26 years. For Division 3O, these estimates varied between around 0.5 million and over 9 million eggs for cod aged 6 to 15 years. May (1967) also provided fecundity estimates based on length for fish aged 9 and 10. Fecundity for cod with lengths approximately ranging from 62 to 93 cm at age 9 ranged from 1 to approximately 3.2 million eggs. At age 10, the estimates were between 1.5 million and close to 5 million eggs.

Recruitment

Since the mid–1960s, there has been a stark decline in cod recruitment on the Southern Grand Bank (SGB), with relatively low recruits per spawner observed since the mid–1980s, as reported by Morgan et al. (2000) and Healey et al. (2003). These studies highlighted that recruitment has been poor while spawning stock biomass (SSB) has been poor, which is the ecological expectation for almost all stocks (i.e., Ricker, 1954). However, the stock exhibited significant productivity at moderately high SSBs during the 1960s, than at comparable levels during the 1980s. Similarly, it exhibited greater productivity at relatively low SSBs during the late 1970s compared to comparable levels during the early 1990s. Recruitment of SGB cod has been consistently poor for over three decades (e.g., Stansbury et al., 1998b,a; Rideout et al., 2021), and biomass is far below the SSB limit reference point, which is $B_{lim} = 60$ kilotonnes (see Rideout et al., 2021).

Growth and maturity

The mean age at 50% maturity (i.e., A_{50}) for combined male and female SGB cod was about 6 years (Trippel et al., 1997; Stansbury et al., 2001; COSEWIC, 2003), based on data from the 1970's and 1980's. For female cod, A_{50} ranged between 5.9 and 7.4 years for cohorts throughout the 1950's and 1980's. Between 1980 and the late 1990's, it declined from around 6.8 to 4.5 years (Healey et al., 2003; Rideout et al., 2021). During subsequent years A_{50} was variable, with an average of 5.5 years (see Figure 10 in Rideout et al., 2021). Furthermore, they reported the estimated mean catch weight-at-ages 3–12 for the period from 1959 to 2019 (see Table 5 in Rideout et al., 2021). The highest and lowest weights-at-age 3 observed in 1994 and 1982 from the fishery catches were 0.27 kg and 0.94 kg, respectively. For age 12, these values were 5.47 kg and 15.27 kg, respectively for the years 2017 and 2016. The variability of estimated mean catch weight-at-ages 3 and 12 from commercial sampling are illustrated in Figure 1.3.

For 3NO cod, Stansbury et al. (1998b) estimated mean lengths-at-age using sampling data from Canadian surveys conducted in the springs of 1972 to 1997. Mean lengths-at-age increased from the early 1970s to the early 1980s, followed by a slight decline. However, from the late 1980s to the late 1990s, little consistent change in mean lengths-at-age was observed. Furthermore, they provided estimates for the average weight and length at different ages for the fishery in 3NO during 1999 and 2000. In 1990, the average weight and length at age 1 were 0.10 kg and 22.99 cm, respectively, while at age 20, they were 19.22 kg and 126.81 cm. In 2000, these values increased to 0.2 kg and 29.37 cm at age 1, and 22.27 kg and 133 cm at age 20. From 1959 to 2020, DFO fall and spring surveys in NAFO Divisions 3NO collected age and length data from 0 to 23 years and 4 to 148 cm, respectively. The mean length-at-age ranged from 10.17 cm (for age 0) to 129.53 cm (for age 21) (see Figure 1.6).

Morgan et al. (2007) reported a significant effect of temperature on the growth

in length, when the temperature is included in the modified Von Bertalanffy growth model. However, the effect they observed was negative. This means the cod in 3NO growing less at higher temperatures.

Food and feeding

Capelin is a significant prey item for small and average-sized cod inhabiting the southernmost shoal of the SGB. These cod feed on redfish (Albikovskaya et al., 1991; González et al., 1998), flatfishes and even juvenile cod, a phenomenon commonly referred to as cannibalism. Additionally, benthic invertebrates such as crabs, molluscs and amphipods are also an important part of cod's diet in this area (Albikovskaya et al., 1991). González et al. (1998) found an extensive variety of prey items during stomach content analysis. In total, 76 prey items were discovered in the stomach contents of 3NO cod. However, only five prey items were dominant, collectively representing 74% of the total stomach content. Among the dominant prey groups, fish and crustaceans played significant roles, contributing 64% and 31%, respectively. Notable prey items included northern sand lance (40%), capelin (13%), and snow crab (11%). Mysids, which are small shrimp-like crustaceans, were also identified as important prey items in cod less than 20 cm in length. In contrast, cod 20–50 cm displayed preferences for feeding on crustaceans like hyperiids and northern shrimp, as well as fish such as capelin and northern sand lance.

Furthermore, González et al. (1998) found a notable correlation between feeding habits and habitat depth among all fish species studied, including cod. Specifically, the consumption of fish as prey decreased with increasing depth, representing approximately 59% of the diet up to a depth of 800 m. Conversely, there was an increase in the consumption of other prey groups within the depth range of 400 m to 1000 m. For cod, sand lance was the dominant prey item at depths less than 200 m, but it was surpassed by capelin at depths between 200 m and 400 m, where capelin exceeded twice the weight

percentage of sand lance in the prey content. Capelin dominance continued in the depth range of 400–600 m, with no recorded instances of sand lance as a prey item. Neither sand lance nor capelin were observed at depths between 600 m and 800 m. Moreover, capelin reemerged as the dominant prey item at depths between 800 m and 1000 m, with no recorded sand lance contribution. At depths greater than 1000 m, cod relied on other prey items (see Figure 7 in González et al., 1998). Additionally, González et al. (1998) indicated instances of competition between thorny skate and cod for the consumption of northern sand lance and snow crab. Moreover, they also compete, to some extent, with American plaice (Langton, 1982; González et al., 1998) and Greenland halibut in relation to capelin predation González et al. (1998). However, the notion of competition between marine fishes is heavily debated in the literature (e.g., Link and Auster, 2013).

1.3.3 History and present status of the cod fishery on the SGB

There was a substantial fishery for Atlantic cod (*Gadus morhua*) on the Southern Grand Bank (SGB) of Newfoundland for over 500 years. In 1967, catches peaked at 227000 tonnes but gradually decreased to 15000 tonnes by 1978. Catches increased in the 1980s and peaked at 51,000 t in 1986, followed by a decrease to around 11000 tonnes in 1993 (ICES, 2005; Rideout et al., 2021). In 1994, the total catch was 2702 tonnes, of which 47 tonnes was caught by Canadian fleets (Figure 1.7). That year the Total Allowable Catch (TAC; the maximum quantity of fish that a fishery is permitted to harvest within a designated season or year.) was set at 6000 tonnes, but in February of that year a fishing moratorium was declared and all directed fishing was entirely restricted within and outside of the NAFO regulatory area (Rideout et al., 2021). Therefore, since 1994, cod are caught as a by-catch from the other commercial fisheries.

1.3.4 Summary of data and assessments for SGB cod

Two sources of data are available for SGB cod in NAFO divisions 3NO: annual research surveys and fisheries landings.

Surveys and survey data

Both the Department of Fisheries and Oceans Canada (DFO) and Spain conduct annual bottom trawl surveys in NAFO Divisions 3NO. DFO's surveys have been conducted in Divisions 3N and 3O since 1971 and 1973, respectively. There were no surveys in Division 3N in 1983 and Division 3O in 1974 and 1983. The spring survey in 2020 and the surveys in 2021 were not conducted due to the COVID-19 pandemic (Rideout et al., 2021). The spring survey in 2022 was also not conducted. DFO's spring surveys take place from April to June and follow a stratified-random sampling approach (Doubleday, 1981). Stratification is based on depth, and prior to 1991, surveys covered depths up to a maximum of 367 meters (200 fathoms). However, the survey depth was extended in 1991 to a maximum of 732 meters (400 fathoms). The research vessel (RV) *A.T. CAMERON* was used for surveys from 1971 to 1982. Since 1984, surveys have been conducted using the RV *WILFRED TEMPLEMAN* or its sister ship RV *ALFRED NEEDLER*. In cases where mechanical issues arise with RV *WILFRED TEMPLEMAN*, the RV *TELEOST* is occasionally deployed to ensure the completion of the spring surveys (Rideout et al., 2021).

DFO conducts fall surveys from September to December. In 1990, DFO initiated fall surveys in 3NO using the RV *WILFRED TEMPLEMAN* for strata with depths less than 732 meters, continuing until 2008. However, starting in 1995, DFO utilized the RV *TELEOST* to sample strata with depths greater than 732 meters, reaching a maximum depth of 1463 meters (800 fathoms). The coverage in greater depths was not consistent. As a result, in 1996, RV *ALFRED NEEDLER* conducted surveys in

strata less than 732 meters. In the fall of 2009, the survey was carried out using the RV *ALFRED NEEDLER*, while strata greater than 732 meters in Division 3N were partially covered by *TELEOST*. Mechanical issues with the vessel led to the incomplete fall survey in 2014. However, from 2018 to 2020, fall surveys were successfully completed. Initially, all surveys used the *Engel* 145 net trawl type. However, in 1995, the *Engel* 145 net trawl was replaced by the *Campelen* 1800 shrimp trawl with rockhopper footgear (Rideout et al., 2021). The *Campelen* trawl is more effective at catching small cod and slightly less effective for large cod compared to the *Engel* 145 net trawl (Warren, 1996; Warren et al., 1996; Rideout et al., 2021).

DFO has developed an R package, "Rstrap" (Healey et al., 2020) for the analysis of observations obtained from DFO multi-species surveys. The package has been integrated with the data collected during the annual surveys. The current version 1.14 includes data up to 2020. The annual survey data covers the Fall season from 1990 to 2020, Spring surveys from 1984 to 2019, and Juvenile surveys from 1989 to 1994. DFO survey data includes a wide range of biological measurements, including fish length, body weight (whole and gutted), girth, gonad weight, stomach fullness, maturity, age, sex, and parasites. In addition, data has also been included with survey information, including season (i.e., fall, spring), and other information such as survey gear (i.e., either *Campelen* or *Engel*), survey strata, fish depth, and trip information, such as day, month and year of the survey. In general, during DFO surveys the maximum and minimum lengths recorded were 5 cm and 148 cm, respectively. For age, the minimum and maximum records were 0 and 23 years, respectively.

Spain has consistently conducted surveys during the spring–summer period (i.e., May–June) from 1995 to 2022, with the exception of 2020 (Garrido et al., 2023). Spanish surveys also collect similar data to DFO surveys. However, the Spanish surveys are geographically restricted to the areas outside the Canadian Exclusive Economic Zone (EEZ), specifically the tail of the SGB (see Figure 2.1). They used commercial vessel

Playa de Menduíña with a net trawl type *Pedreira* for the surveys from 1995–2000, followed by RV *Vizconde de Eza* with the *Campelen* trawl since 2001 (Garrido et al., 2023). During these surveys, the maximum and minimum recorded cod lengths were 6 cm and 132 cm respectively. For age, the minimum and the maximum values were 1 and 20 years, respectively (González-Troncoso et al., 2012; Garrido et al., 2023).

Fisheries landing data

Landing data for 3NO cod is accessible from 1953 to 2020. Notably, a fishing moratorium was imposed on 3NO cod in February 1994, leading to the absence of reported landings from directed fishing activities thereafter. Consequently, post-1994 landing data is reported primarily as by-catch during other directed commercial fisheries. This data is further categorized, with separate reporting for Canadian fleets and other nations, including Spain, Russia (USSR), and Portugal (see Figure 1.7). The majority of the landings are attributed to the otter trawl fishery, although there are also some catches reported from the longline fishery (see Rideout et al., 2021).

In recent years, the commercial sampling of cod by-catch from Division 3NO has been poor, which can significantly impact future catch-at-age estimations (Rideout et al., 2021). For the years 2018 and 2019, commercial sampling data were available for the Canadian otter trawl fishery (Healey and Parrill, 2019; Rogers and Simpson, 2020; Rideout et al., 2021). Commercial sampling data were also available from the 130 mm Spanish otter trawl fishery, with the exception of the 280 mm Spanish otter trawl fishery (González-Costas et al., 2019, 2020; Rideout et al., 2021). In 2018, sampling data were available from the Portuguese 130 mm otter trawl fisheries; however, no data were available from the 280 mm trawl fishery, and there was a complete absence of sampling data for 2019. Additionally, no sampling data from the Russian commercial fishery were available for either 2018 or 2019 (Fomin and Pochtar, 2019, 2020; Rideout et al., 2021).

This complicates the estimation of catch-at-age (e.g., Rideout et al., 2021). In 2020, no commercial sampling data of cod by-catch were available from any country(Rideout et al., 2021). Consequently, the data for 2018, 2019, and 2020 are provisional.

3NO cod stock assessments

I summarize the scientific assessments presented at the annual scientific meetings of the regional fisheries management bodies: the International Commission for Northwest Atlantic Fisheries (ICNAF) and the Northwest Atlantic Fisheries Organization (NAFO). First I provide a brief outline of these regional fisheries management bodies before reviewing the assessments.

In 1950, ICNAF was officially formed after ratification by contracting parties (i.e., participating countries), including Canada (including Newfoundland), Iceland, the United Kingdom (UK), and the USA. ICNAF's mission was to investigate, protect, and conserve the fisheries of the Northwest Atlantic to enable the sustainable harvest of maximum yields. In 1976, the USA and Canada declared their intention to extend their fishing zones to the limit of 200 nautical miles. Consequently, in 1977, ICNAF's contracting parties came up with a new arrangement for multinational fisheries management in the Northwest Atlantic. This led to the establishment of NAFO in January 1979, officially dissolving ICNAF on December 31, 1979. NAFO has since continued its regional fisheries management activities in the Northwest Atlantic (Anderson, 1998).

I utilized the NAFO online library archive (www.nafo.int/Publications) to explore and compile this concise review of 3NO cod assessments. The ICNAF research document by Pinhorn and Wells (1973) was the oldest research document available about the assessment of 3NO cod. They used virtual population analysis for the period spanning from 1959–1970 with length and age data from Sampling Yearbooks and age-length keys from the Newfoundland research vessel surveys to supplement or replace commercial

age-length keys for certain years. Their results indicated an overall increase in stock abundance (see Figure 1.8).

Bishop (1977) estimated biomass trends using four different approaches and compared them to Spanish Pair Trawl catch-per-unit-effort (CPUE, tonnes/hour) values during 1971–1975. These estimates indicated that biomass remained at decreased levels compared to late 1960. Consequently, ICNAF set the total allowable catch (TAC) at 15000 tonnes for 1978 to facilitate the rebuilding of the sock. Assessments continued in 1978 and 1979. Bishop and Wells (1978, 1979) updated the abundance estimates, similar to Bishop (1977), but, they additionally introduced a general production model. The assessment concluded that in 1977, the stock was depleted to a level insufficient to sustain a catch equilibrium at 2/3 of the effort for Maximum Sustainable Yield (MSY; the maximum fishery yield that stock can sustain).

Gavaris (1979) implemented a generalized stock production model Fox (1975) using standardized catch and effort data from Spanish pair trawlers. The production model estimated a MSY of 104768 tonnes. The yield at 2/3 of the effort for MSY was approximately 85000 tonnes.

However, Vazquez and Larraneta (1980) were skeptical regarding the previous conclusions about the depletion of the 3NO cod because of fishing. Referring to the Figure 3 in Gavaris (1979), they pointed out that there was no reasonable evidence to support the claim of overfishing. They further elaborated that the results of production model in Gavaris (1979) lacked realism. Their assessment emphasized that overfishing was not be the sole reason for the depletion of 3NO cod, and the low CPUE could be attributed to its association with periods of low recruitment. They also recommended a TAC of 68500 tonnes for 1980. Furthermore, they suggested that 2/3 of MAY was around 65000 tonnes rather than 85000 tonnes postulated by Gavaris (1979).

Chekhova and Postolaky (1981) performed an assessment using the data from a

trawl survey conducted in 1980. They used the catchability coefficients determined by Chumakov and Serebrov (1978) to assess the abundance and biomass. By considering the number of cod in a catch (n) and the catchability coefficient (K), the total number of fish caught per trawling hour in the area of fished was estimated. The assessment estimated an increase in the abundance and biomass of SGB cod compared to 1978–79. Subsequent assessments for 3NO cod were continued annually, using similar methodologies with updated data.

Gavaris (1988) introduced an adaptive framework ($ADAPT$) for population size estimation, which involves minimizing the discrepancy between observed variables and the values predicted as functions of population parameters (see Gavaris, 1988, for full model description). Subsequently, Baird and Bishop (1989) implemented $ADAPT$ with research vessel data for 3NO cod. They derived population abundance estimates at ages 3–12 and 3+, and fishing mortality rates at ages 3–12. Notably, their analysis revealed that the total abundance estimates of age 3+ (i.e., 42 millions fish) derived from $ADAPT$ was 7% higher than those from their 1988 assessment (see Baird and Bishop, 1988).

Different from previous assessments, Bulatova (1990) assessed the 3NO cod based on the data collected during an acoustic survey conducted in 1989. Their findings indicated a gradual decline in abundance from 1983–1988 due to poor recruitment.

However, the invention of $ADAPT$ was revolutionary. Following the the assessment by Baird and Bishop (1989), a majority of subsequent assessments for 3NO cod relied on $ADAPT$. Remarkably, since the 2000's, assessments of this stock have exclusively depended on $ADAPT$, and this model formulation remained unchanged for over two decades (Rideout et al., 2021; Cadigan et al., 2022a). However, considering the recommendations made in the 2018 assessment (see Rideout et al., 2018, 2021) attempted

to explore an alternative *ADAPT* formulation. However, the inclusion of Spanish survey data resulted poorer model fit, as indicated by a higher mean square error and an increase in the relative error for estimates of catchability. Additionally, they made number of attempts to incorporate a plus group age into the assessment model, but these efforts were unsuccessful.

Major weaknesses identified for the 3NO cod *ADAPT* model formulation are: 1) it does not include a plus group, 2) it assumes catch-at-age is known without error despite the poor quality of catch information that is frequently emphasized in recent assessments (e.g., Rideout et al., 2021), 3) the model assumes $M = 0.2$, while NAFO (2021) recommended exploring other non-stationary options, 4) it does not use indices from an EU-Spain survey on the tail of the Grand Bank in the NAFO Regulatory Area (NRA). However, all of these issues were addressed in a state-space stock assessment model (SSAM) for SGB cod developed by Cadigan et al. (2022a) as an alternative to the *ADAPT* VPA (Virtual Population Analysis) model currently used for this stock. The SSAM considered the same assessment period (1959–2020) as Rideout et al. (2021). The SSAM found that since 1990, SSB estimates were largely similar to *ADAPT* estimates. In contrast, there were larger differences during 1960-1900 (see Figure 17 in Cadigan et al., 2022a). They concluded that these differences were due to to differences in the M assumptions, the inclusion or exclusion of a plus group, and different estimates for fish weights-at-age. For 2020, the biomass estimates were 7279 tonnes (*ADAPT*) and 5757 tonnes (SSAM). However, these values still remain far below the limit reference point (B_{lim} = 60000 tonnes; González-Costas and González-Troncoso, 2013), indicating no signs of recovery since the cod collapse in the earl 1990's and even after implementing a fishing moratorium in 1994.

1.4 Fish length-weight relationship

Length and weight measurements are fundamental data collected in fisheries surveys, that provide the basis for defining metrics of fish condition, which assess the weight of a fish relative to what is expected given its length. This expectation is often established using the conventional Length-Weight Relationship (LWR), originally introduced by Keys (1928), in the form of $W(l) = al^b$ or its logarithmic representation, $\log\{W(l)\} = \log(a) + b\log(l)$. In this equation, $W(l)$ represents the weight as a function of length l, a is the condition coefficient parameter, and b is the allometric coefficient.

LWRs play a vital role in fisheries research and management. They are utilized to estimate total stock biomass, facilitate the conversion of growth in length to growth in weight within stock assessment models, and enable comparisons of various life history characteristics among fish species (Jellyman et al., 2013). Furthermore, LWRs are instrumental in estimating the number of fish from the total weight caught (Cadigan et al., 2022b), a fundamental input for many stock assessment models. As a result, the accurate estimation of LWRs is crucial for obtaining precise estimates of other derived quantities, including stock size and reference points.

1.5 Fish condition index

The condition index is often used to assess the general well-being of fish populations (Bolger and Connolly, 1989; Ridanovic et al., 2015; Latour et al., 2017). Moreover, it is intricately connected to critical aspects of fish biology, including survival, reproduction (Ridanovic et al., 2015; Mu et al., 2021; Haberle et al., 2023), and maturity (Ridanovic et al., 2015). Fish growth and condition are indicative of energy reserves within the body, which, in turn, profoundly influence population productivity by impacting survival and reproduction dynamics (Lloret and Planes, 2003; Morgan et al., 2018). Poor

condition among fish individuals can lead to reduced productivity, manifested as slow growth and limited recruitment potential (Lloret and Planes, 2003). Fish with poor condition may also face higher natural mortality rates (M) due to heightened vulnerability to diseases and predation, along with a diminished ability to capture mobile prey (Dutil et al., 1999; Dutil and Lambert, 2000; Rose and O'Driscoll, 2002). In contrast, fish exhibiting improved growth and condition contribute to enhanced population productivity (Rätz and Lloret, 2003), characterized by increased survival (Dutil et al., 2006; Casini et al., 2016) and higher reproductive rates (Rideout and Rose, 2006; Rideout and Morgan, 2010b). It is worth noting that a significant portion of inter-annual and long-term variability in fish production is attributed to recruitment (Rätz and Lloret, 2003), with good condition in fish individuals holding the potential for favorable recruitment outcomes (Rätz and Lloret, 2003; Marshall et al., 2000). Furthermore, Haberle et al. (2023) proposed that fish condition can serve as an indicator of stock size relative to the carrying capacity in food-limited populations.

1.6 Natural mortality

In fisheries science, accurately quantifying the total number of fish deaths within a population is a complex task that cannot be directly observed (Lee et al., 2011). Consequently, indirect methods are employed to estimate natural mortality rates (M) (Xiao, 2001; Lee et al., 2011). Direct estimation of M poses considerable challenges, particularly for exploited fish stocks (Lee et al., 2011; Punt et al., 2021b; Björnsson et al., 2022). As a result, M is often assumed to be a constant value, such as $M = 0.2$, across time, age, and sex (Lee et al., 2011; Casini et al., 2016; Björnsson et al., 2022).

However, Lee et al. (2011) demonstrated that it is possible to estimate M in stock assessment models when appropriate data are available. Their profile likelihood analyses underscored the necessity of informative length or age composition data for reliable M

estimation. More recently, a component of M has been linked to variations in the proportion of Atlantic cod (*Gadus morhua*) in very poor condition. Casini et al. (2016) estimated a condition-based M (M_K) for Eastern Baltic cod, which was added to the constant M (i.e., $M = 0.2$) to obtain a condition-corrected M, denoted as $M_{K_{corrected}} = 0.2 + M_K$. For Northern cod, Regular et al. (2022) found a positive correlation between an M_K index and independent M estimates derived from an integrated assessment model. Additionally, Björnsson et al. (2022) estimated the annual condition-based M (M_C) using factors such as the condition factor and liver condition of Icelandic cod. They proposed that M could be expressed as the sum of the condition-based M and length-based M (M_L), i.e., $M = M_C + M_L$. An index of condition is used to model time-varying M in the state-space assessment model HYBRID (see Varkey et al., 2022), developed for the neighbouring stock of 3NO cod (i.e., cod stock in NAFO Division 3Ps). This model combines features from both the State-space Assessment Model (SAM) by Nielsen and Berg (2014) and the State-Space Assessment Model for 3Ps (Cod3PsSSAM) by Cadigan (2023b).

1.7 Spatiotemporal statistical modeling

Spatiotemporal statistical models have gained widespread popularity across diverse scientific disciplines due to their ability to elucidate and predict spatially explicit processes that evolve over time. These models serve a multitude of purposes, including: 1) prediction in space (e.g., interpolation): They enable accurate predictions of phenomena at unobserved spatial locations by leveraging the information from observed data points; 2) prediction in time (forecasting): Spatiotemporal models are instrumental in forecasting future developments in dynamic processes, allowing for informed decision-making and planning; 3) assimilation of observations with deterministic models: They facilitate the

integration of observational data with deterministic models, enhancing our understanding of complex spatiotemporal systems; and 4) inference on parameters: Spatiotemporal modeling allows for the estimation of key parameters that describe various components of the spatiotemporal process, providing valuable insights into underlying mechanisms (Wikle, 2015).

Spatiotemporal statistical modeling encompasses two primary approaches: the descriptive approach and the dynamic approach. The descriptive approach characterizes the spatiotemporal process with regard to its mean function and covariance function. This approach often relies on an important statistical characteristic of dependent data; that is, in space and time, nearby observations tend to be more alike than those far apart. The dynamic spatiotemporal modeling approach examine how a spatial process changes over time (Wikle et al., 2019).

The role of autocorrelation in spatiotemporal statistical modeling is significant. "The term 'autocorrrelation' refers to the degree of correlation of a variable and itself ('auto')" (Dale and Fortin, 2014, p. 9). In spatiotemporal statistical modeling there are two types of autocorrelation: spatial and temporal. "Given a set S containing n geographical units, spatial autocorrelation (SA) refers to the relationship between some variable observed in each of the n localities and a measure of geographical proximity defined for all $n(n-1)$ pairs chosen from S" (Hubert et al., 1981, p. 224). The magnitude of the SA is inversely proportional to spatial distance, spatial correlation decreases when the spatial distance increases and vice versa (Dale and Fortin, 2014). The relationship between successive values (i.e., lags) of the same variable is simply referred to as temporal autocorrelation (TA). This is also called serial correlation (Abdulhafedh, 2017).

SA seeks to identify correlations in all geographic directions, making the study more complex and specialized. In contrast, temporal autocorrelation primarily focuses on a one-way direction. However, when studying both SA and TA, it is essential to identify

outliers, spatial and temporal trends, degrees of association, statistical significance, and appropriate models. Nevertheless, they are calculated and understood differently. Therefore, compared to TA, SA is more complex and multifaceted (Getis, 2008).

1.8 State-space models (SSMs) in fisheries stock assessment

Models that allow both process and observation errors are generally referred to as SSMs (Aeberhard et al., 2018). These models combine stochastic assumptions about both observed quantities and unobserved states deriving a dynamic system (Aanes et al., 2007; Gudmundsson and Gunnlaugsson, 2012). The SSM framework was first introduced by Kalman (1960) and Kalman and Bucy (1961). This was initially applied in engineering, focusing on online computations, where real-time data required efficient implementation of iterative predictions and updates (Aeberhard et al., 2018). However, SSM's are now commonly used in analyzing ecological time-series data (Newman et al., 2014; Auger-Méthé et al., 2021). For instance, SSM's are often used to model population dynamics (Newman et al., 2014) and in particular, for fisheries stock assessment, SSMs were introduced by Sullivan (1992) and Gudmundsson (1994). Thus, in fisheries stock assessment, SSMs allow inclusion of the process error in population dynamics and the observation error in the data used to estimate the model parameters (Aeberhard et al., 2018), making the modeling process more flexible and reliable. In particular, it is useful in fisheries management in which future prediction of stock size is a significant component.

With the development of Automatic Differentiation Model Builder (ADMB), a statistical application that used automatic differentiation using C^{++} classes and a native template language (Fournier et al., 2012) followed by Template Model Builder (TMB),

an R package that implements automatic differentiation using C^{++} templates (Kristensen et al., 2016), SSMs received much more attention (e.g., Nielsen and Berg, 2014; Cadigan, 2015) as they enabled efficient implementation of highly nonlinear models with a large number of parameters. These recent advancements made SSMs fully operational and frequently used in stock assessment and fisheries management (Aeberhard et al., 2018) to provide tactical advise.

1.9 Thesis objectives

The principle objective of this thesis is to develop a spatiotemporal condition model for SGB cod and utilize it to derive starvation mortality indices to include in a state-space stock assessment model (SSAM) for SGB cod. The specific objectives of the study are to,

1. integrate data from fall and spring surveys to describe how condition changes over time (years and seasons) and space.
2. develop estimates of annual condition for the stock as a whole.
3. estimate the annual proportion of cod in severe condition and unlikely to survive in the short-term.
4. estimate age-based starvation mortality rates from length-based ones.
5. integrate age-based starvation mortality rates with the SSAM in Cadigan et al. (2022a).

1.10 Outline of the thesis

Chapter 2 is the core of the thesis that introduces a novel spatiotemporal model of condition for Atlantic cod on the SGB (i.e., NAFO Divisions 3NO), using DFO's annual research survey data. Chapter 3 describes how the spatiotemporal model can be utilized to derive a length-specific starvation mortality index. Chapter 4 describes a stochastic growth model to estimate the probability distribution of length at age and how that can be used to convert length-specific starvation mortality rates into age-specific starvation mortality rates. The purpose of the Chapter 5 is to update the SSAM developed by Cadigan et al. (2022a) by integrating age-specific starvation mortality rates derived in Chapter 4. Finally, in Chapter 6, I conclude the research and provide recommendations for future work, followed by bibliography and appendices.

1.11 Figures

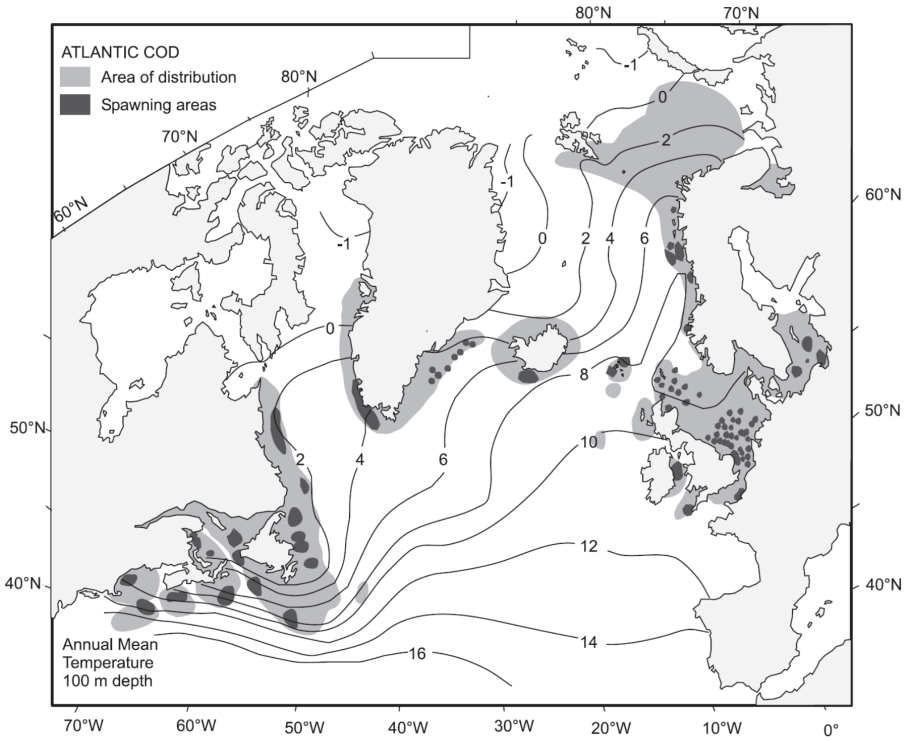

Figure 1.1: Spatial distribution of Atlantic cod stocks (shaded), their spawning areas (darkly shaded) and the annual mean temperature at 100 m depth in the North Atlantic. Figure courtesy of Sundby (2000).

.

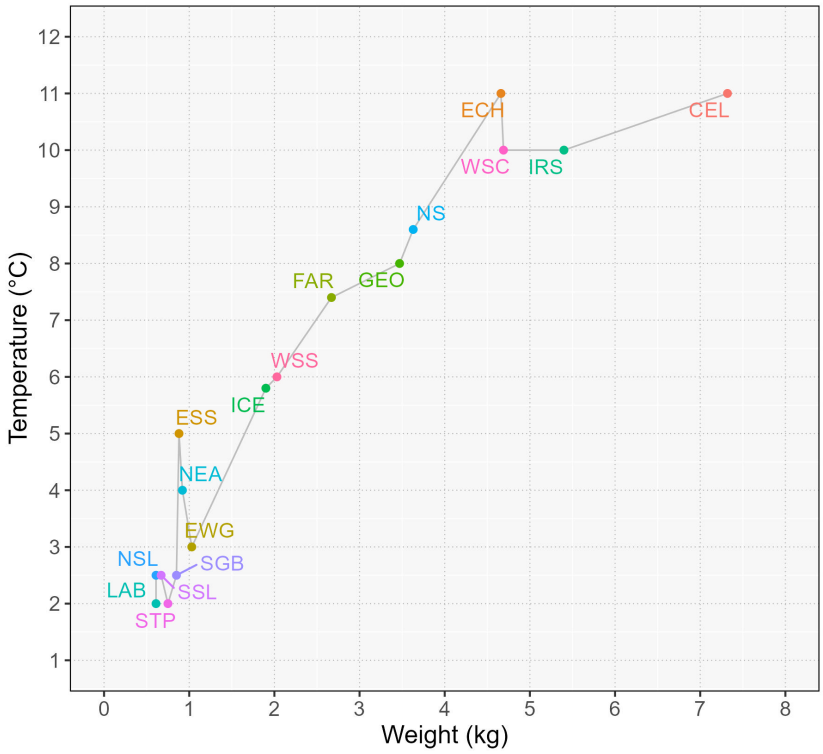

Figure 1.2: Variation in weight-at-age 4 for cod from various regions around the North Atlantic with respect to temperature. Abbreviations: STP - St. Pierre Bank; LAB - Labrador/ Grand Bank; NSL - Northern Gulf of St. Lawrence; SSL - Southern Gulf of St. Lawrence; SGB - Southern Grand Bank; ESS - Eastern Scotian shelf; NEA - Northeast Arctic; EWG - East & West Greenland; ICE - Iceland; WSS - Western Scotian shelf; FAR - Faroe; GEO - Georges Bank; NS - North Sea; ECH - Eastern channel; WSC - West Scotland; IRS - Irsh Sea; CEL - Celtic Sea. Data source: Brander (1995).

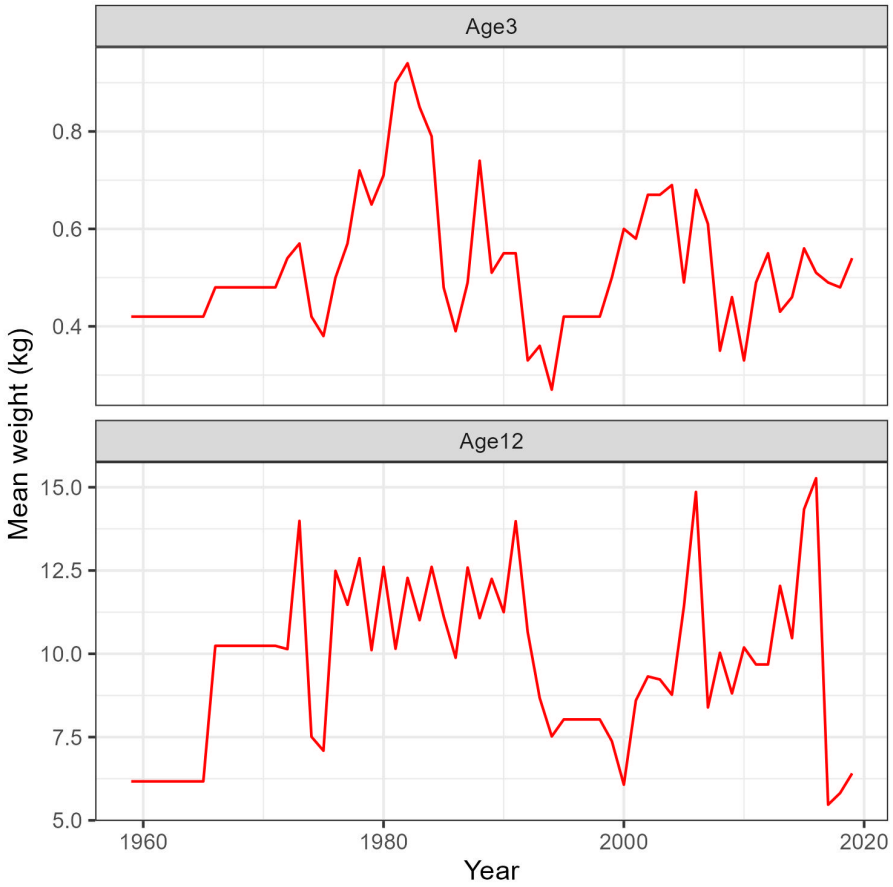

Figure 1.3: Estimated mean catch weight-at-age (ages 3 and 12) for 3NO cod, 1959–2019. Data source: Rideout et al. (2021).

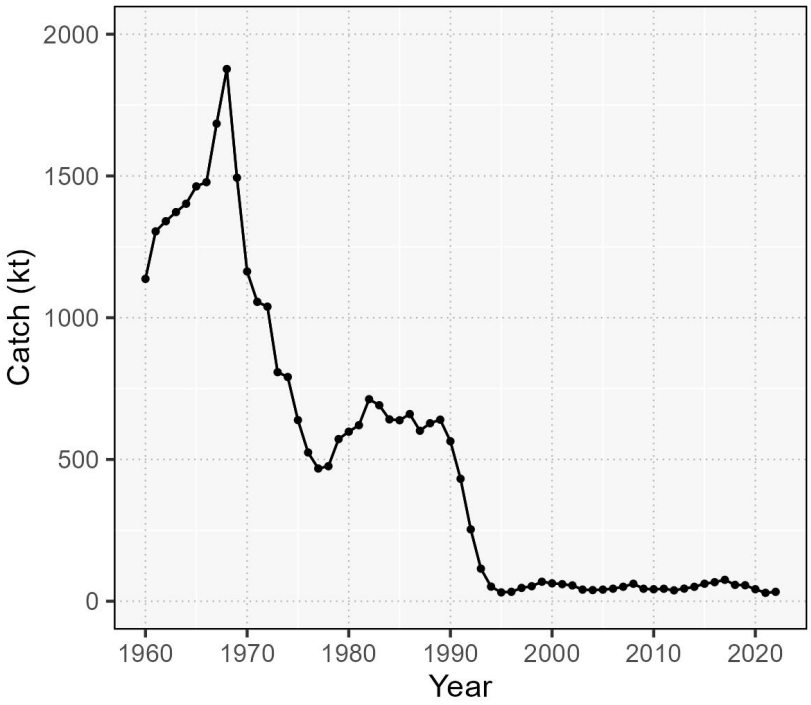

Figure 1.4: Nominal catches of Atlantic cod in the Northwest Atlantic, 1960–2022. Data source: NAFO, STATLANT 21A.

.

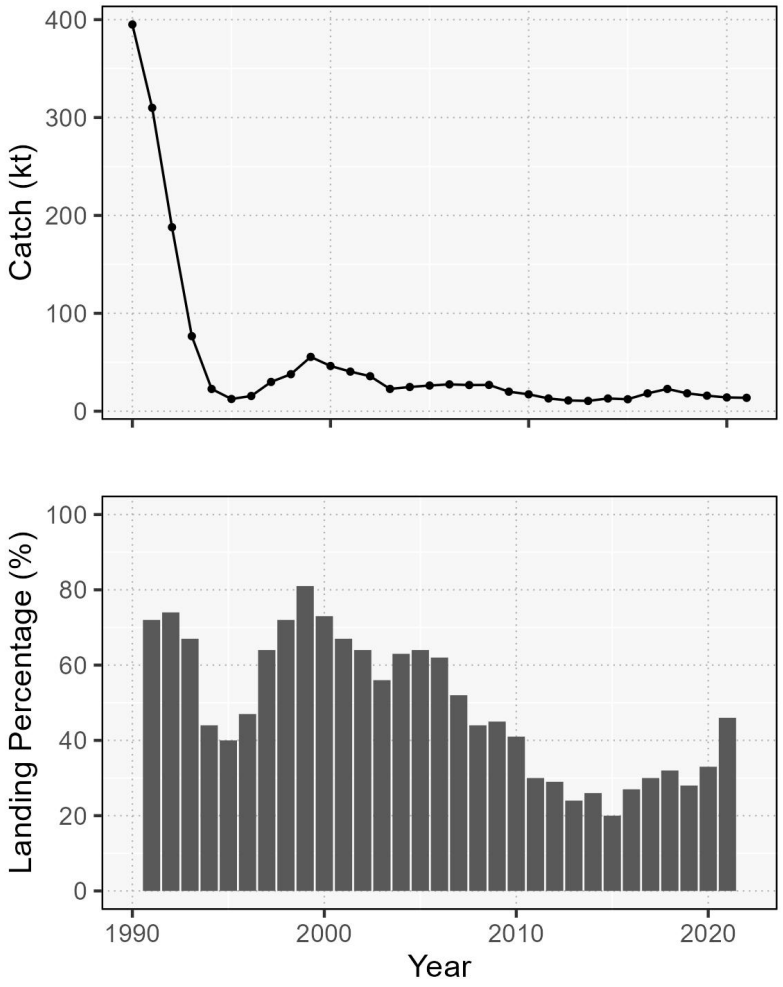

Figure 1.5: Top Panel: Time series (1990–2021) of commercial landings (i.e., catch in tonnes) of Atlantic cod in Atlantic Canada (i.e, the total of landings from Nova Scotia, New Brunswick, Prince Edward Island, Quebec, and Newfoundland). Bottom panel: Percentage of total landings from Northwest Atlantic that were taken by Atlantic Canadian fleets. Data source: DFO, Canada.

.

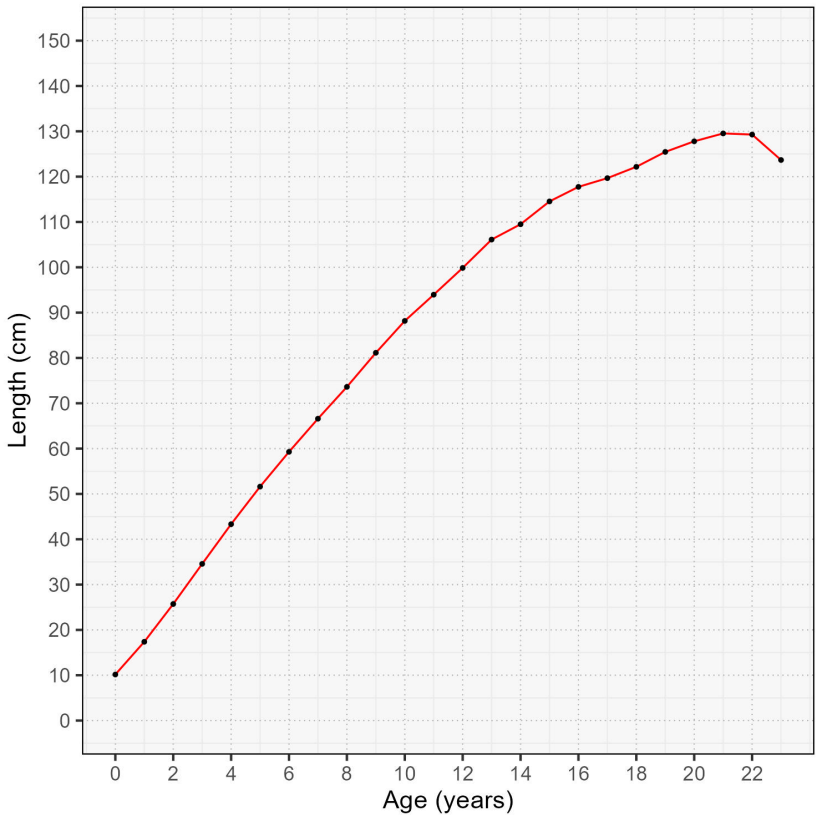

Figure 1.6: 3NO cod average length-at-age values calculated using DFO fall and spring survey data from 1959–2020.

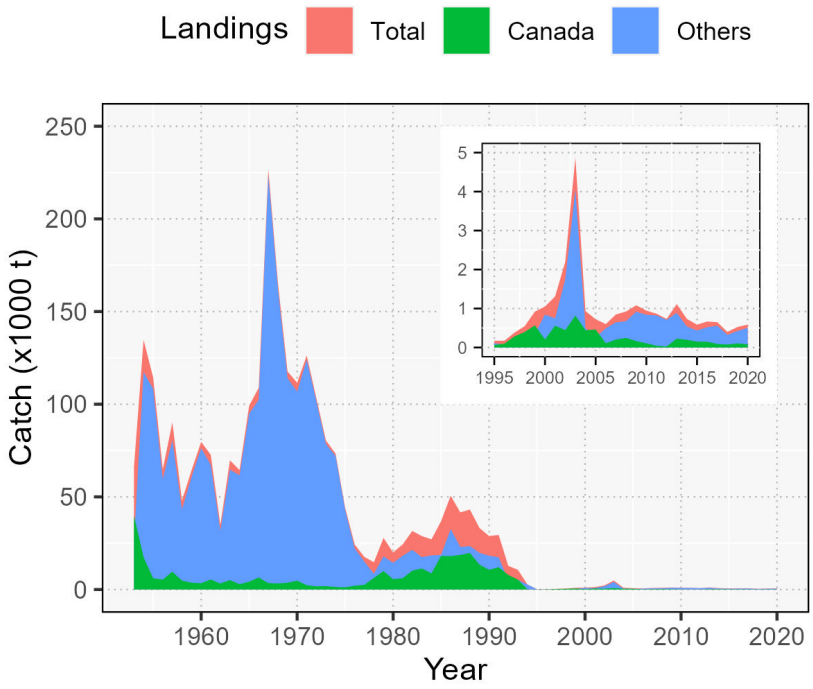

Figure 1.7: Atlantic cod fishery landings (in tonnes) reported by the fleets of Canadian and other countries for the Divisions 3NO. Data source: DFO, Canada.

Figure 1.8: Estimates of total number of cod caught per year and age-groups 4–12+ and 7–10+ for ICNAF Divisions 3NO (i.e., SGB) during 1959–1970. Data source: Pinhorn and Wells (1973).

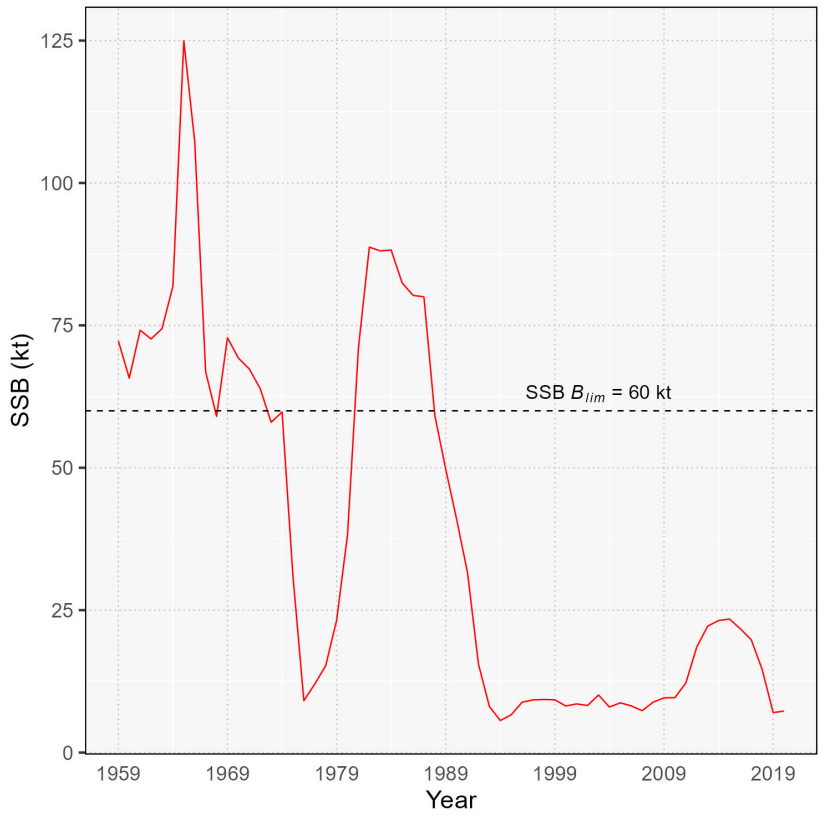

Figure 1.9: *ADAPT* estimates of SSB during 1959–2020. Dashed line represents the SSB limit reference point. Data source: Rideout et al. (2021).

Chapter 2

Spatiotemporal condition model for SGB cod

The purpose of this chapter is to describe a novel spatiotemporal model of condition for Atlantic cod on the SGB.

2.1 Rationale

Historically, there was a substantial fishery for SGB cod for over 500 years (Lear, 1998). However, cod on the SGB of Newfoundland have been at low levels for nearly three decades since the inception of the fishing moratorium in 1994. The most recent assessment also estimated the stock was only about 12% of the limit reference point (see Rideout et al., 2021, and Figure 1.9). Linked to the lack of recovery are reports of periods of very low productivity for SGB cod (e.g., Morgan et al., 2014b) and low fish condition relative to some other cod stocks in the North Atlantic (Rätz and Lloret, 2003).

Previous studies have found an association between the poor condition of cod and population decline (e.g., Lambert and Dutil, 1997; Marshall et al., 2000; Bundy and Fanning, 2005). For instance, this may have contributed to the decline in northern

cod, particularly in the northern areas (Morgan et al., 2018). Additionally, other studies have suggested that poor growth and/or condition could have contributed to the lack of recovery of northern cod (Rose and O'Driscoll, 2002; Sherwood et al., 2007; Buren et al., 2014; Mullowney and Rose, 2014). Regular et al. (2022) concluded that starvation-induced mortality is an important component of northern cod natural mortality. Morgan et al. (2010) found that temperature is an important factor for SGB cod condition and reproduction. This study revealed significant inter-annual variations in relative gutted body condition and liver condition for SGB cod, but trends were not consistent among two types of condition (see Figure 3 in Morgan et al., 2010). Interestingly, they found the highest gutted body condition at warm temperatures, consistent with the findings of Rätz and Lloret (2003). In contrast, they found liver condition was highest at low temperatures. However, they did not investigate spatial or size differences in body condition.

As I previously mentioned in Chapter 1, fish with poor body condition can experience elevated M due to increased vulnerability to diseases and predation, as well as reduced ability to capture mobile prey. These factors ultimately impact population productivity by impacting survival and reproduction dynamics. Therefore, modeling and investigating the spatial and temporal changes in condition of SGB cod can provide a basis for developing a starvation mortality index. Importantly, this index may provide important information of variation in M, which can be included in stock assessment models, such as age-based SSAM's.

2.2 Research approach

Similar to Thorson (2015) and Cadigan et al. (2022b), I use a spatiotemporal LWR model to derive a population-level condition metric. The model in Cadigan et al. (2022b)

was

$$\log(W_i) = A_{g_i t_i} + B_{g_i t_i l_i} \log(l_i) + \Delta_{d_i l_i} + \varepsilon_{wi}, \quad \varepsilon_{wi} \overset{iid}{\sim} N(0, \sigma_w^2). \tag{2.1}$$

The random variable W_i represented the weight of the i'th fish sampled at spatial location g_i in year t_i, day d_i, and length bin l_i. Note that different fish in the same strata and year share the same A and B parameters. The model assumed the slope B_{gtl} varied over length, space, and time, and the condition parameter A_{gt} varied across space and time. The survey timing effect was Δ_{dl}, where d was the Julian date. ε_{wi} is the measurement error. In this model, condition may vary spatially and temporally, both within- and between-years, because of changes in prey availability, among other reasons.

In this thesis, I extend the models of Thorson (2015) and Cadigan et al. (2022b) for SGB cod. Here, the main innovation is an approach to model cyclical seasonal changes in gutted-weight condition. Different from Cadigan et al. (2022b), a single b fixed-effect slope parameter is used instead of B_{gtl}, while the A effect is dynamic and varies over length, space, and time. The rationale for this change is that in preliminary models, a high correlation in estimates of A_{gt} and B_{gtl} in Eqn. (2.1) was found, which complicated the interpretation of these effects. However, by using a constant b parameter, spatiotemporal and length changes in A_{gtl} can be directly interpreted as spatiotemporal changes in condition. In contrast to Cadigan et al. (2022b) but similar to Regular et al. (2022), month is used as the seasonal (s) temporal resolution of the spatiotemporal model for the survey timing effect, Δ_{sl} (see Section 2.3.3).

2.3 Methods

2.3.1 Study area

The study area, SGB, and adjacent areas are illustrated in Figure 2.1. The SGB is a large offshore bank (Lilly, 2005) located to the south and east of the island of Newfoundland (Lilly, 2005; DFO, 2007). It is separated from Newfoundland by the Avalon Channel (Lilly, 2005). The continental slope along the SGB is notably steep, with depths exceeding 1000 meters over a relatively short distance. Importantly, the tail of the SGB extends beyond the Canadian 200 nautical mile Exclusive Economic Zone (EEZ) (DFO, 2007). More information can be found in Section 1.3.

2.3.2 Data

Total length and gutted-weight measurements of cod collected during Fisheries and Oceans Canada's (DFO) annual spring and fall bottom surveys in NAFO Divisions 3NO (i.e., SGB) from 1984 to 2018 were utilized. All surveys were conducted using a stratified random sampling design (Doubleday, 1981). DFO provided shapefiles delineating strata boundaries, which are illustrated in Figure C.1. Bathymetry data were sourced from the National Oceanic and Atmospheric Administration (NOAA) server using the R package "marmap" (Pante and Simon-Bouhet, 2013). The digital data were in the WGS84 map projection. For this analysis, gutted-weight data of cod measuring $\geq$ 15 cm in length were employed. Weight data for sizes $<$ 15 cm were deemed unreliable due to numerous outliers and were therefore excluded from the dataset. A summary of the survey data processed for the analyses is presented in Table B.1.

2.3.3 Statistical model

All the mathematical notations are summarized in Table B.3.

Let W_i be a random variable representing the fish weight for the i'th observation in year t_i, stratum g_i, and for a length l_i fish sampled. The spatiotemporal statistical model I considered, for individuals $i = 1, \ldots, n$, is

$$\log(W_{g_i,t_i,l_i}) = A_{g_i,t_i,l_{3i}} + \Delta_{s_i,l_{3i}} + b\log(l_i) + \varepsilon_{wi}, \quad \varepsilon_{wi} \overset{iid}{\sim} N(0, \sigma_w^2), \tag{2.2}$$

where *iid* means independent and identically distributed. In Eqn. (2.2), the intercept A_{g,t,l_3} varies across strata g, years t, and lengths l_3 in 3 cm length bins. The survey month (s) effect Δ_{sl_3} is also assumed to be length-dependent. These length effects can account for nonlinearity in the $\log(W)$ versus $\log(L)$ relationship. To improve the model run times, 3 cm length bins were used for the seasonal (month) and spatiotemporal effects. The slope b (i.e., the allometric coefficient) was assumed to be constant for all l, t, g, and s. It was assumed $t = 1, \ldots, T$ are the years, $g = 1, \ldots, G$ are the strata, $l = 1, \ldots, L$ indicate the 1 cm length bins, $l_3 = 1, \ldots, L_3$ indicate the 3 cm length bins, and $s = 1, \ldots, S$ are the months. The intercept, A_{g,t,l_3} was modeled as a sum of main effects: Δ_g for spatial location g, Δ_t for time t, and Δ_{l_3} for length l_3. The effects Δ_{gt} for strata-time, Δ_{gl_3} for strata-length, and Δ_{tl_3} for time-length were included in the model as second-order interaction effects (i.e., random effects). These random effects are correlated across strata, years, and lengths, which is described as follows.

The stochastic model I used for A_{g,t,l_3} is

$$A_{g,t,l_3} = a + \Delta_g + \Delta_t + \Delta_{l_3} + \Delta_{gt} + \Delta_{gl_3} + \Delta_{tl_3}, \tag{2.3}$$

Similar to Cadigan et al. (2022b), the sets of temporal effects $\{\Delta_t;\ t = 1, \ldots, T\}$ and the length effects $\{\Delta_{l_3}; l_3 = 1, \ldots, L_3\}$ are modelled as AR(1) autoregressive Gaussian

stochastic processes in time and length, with zero means and autocorrelations $\varphi_{\mathcal{T}}$ and $\varphi_{\mathcal{L}_3}$ and standard deviations $\sigma_{\mathcal{T}}$ and $\sigma_{\mathcal{L}_3}$, respectively (see Eqn. 2.4 and 2.5).

$$\Delta_t = \varphi_{\mathcal{T}}\Delta_{t-1} + \varepsilon_t \quad (\text{i.e., } \Delta_t \sim AR1\ (0, \sigma^2_{\mathcal{T}})) \tag{2.4}$$

$$\Delta_{l_3} = \varphi_{\mathcal{L}_3}\Delta_{l_3-1} + \varepsilon_{l_3} \quad (\text{i.e., } \Delta_{l_3} \sim AR1\ (0, \sigma^2_{\mathcal{L}_3})). \tag{2.5}$$

Including third-order interactions between g, t, and l was computationally very slow and this was not pursued.

The spatiotemporal interaction effects $\{\Delta_{gt};\ \ g = 1, \ldots, G,\ \ t = 1, \ldots, T\}$ had a mean zero multivariate normal (MVN) distribution with a covariance matrix that is Kronecker products of a spatial GMRF covariance matrix (with $q_{\mathcal{GT}}$ and $\omega_{\mathcal{GT}}$ parameters) and an AR(1) covariance matrix (with $\varphi_{\mathcal{GT}}$ autocorrelation parameter; see Eqn. 2.6). Similar to Δ_{gt}, the set of spatial-length interaction effects $\{\Delta_{gl_3};\ \ g = 1, \ldots, G,$ $l_3 = 1, \ldots, L_3\}$ had a MVN distribution with mean zero and a $GRMF \times AR(1)$ covariance matrix with $q_{\mathcal{GL}_3}$, $\omega_{\mathcal{GL}_3}$ and $\varphi_{\mathcal{GL}_3}$ (see Eqn. 2.7) parameters.

$$\Delta_{gt} = \varphi_{\mathcal{GT}}\Delta_{g,t-1} + \varepsilon_{gt} \quad (\text{i.e., } \Delta_{gt} \text{ in } t \sim GMRF \quad \& \quad \Delta_{gt} \text{ in } g \sim AR1(0,1)) \tag{2.6}$$

$$\Delta_{gl_3} = \varphi_{\mathcal{GL}_3}\Delta_{g,l_3-1} + \varepsilon_{gl_3} \quad (\text{i.e., } \Delta_{gl_3} \text{ in } l_3 \sim GMRF \quad \& \quad \Delta_{gl_3} \text{ in } g \sim AR1(0,1)) \tag{2.7}$$

The set of temporal-length interactions $\{\Delta_{tl_3};\ \ t = 1, \ldots, T,\ \ l_3 = 1, \ldots, L_3\}$ had a mean zero MVN distribution with a covariance matrix that was a Kronecker product of two AR(1) covariance matrices, with $\varphi_{\mathcal{T}^*\mathcal{L}_3}$, $\varphi_{\mathcal{T}\mathcal{L}_3^*}$ and $\sigma_{\mathcal{T}\mathcal{L}_3}$ parameters, where $\sigma_{\mathcal{T}\mathcal{L}_3}$ is the

standard deviation (see Eqn. 2.8).

$$\Delta_{tl_3} - \varphi_{\mathcal{T}^*\mathcal{L}_3}\Delta_{t-1,l_3} = \varphi_{\mathcal{T}\mathcal{L}^*{}_3}(\Delta_{t,l_3-1} - \varphi_{\mathcal{T}*\mathcal{L}_3}\Delta_{t-1,l_3-1}) + \varepsilon_{tl_3} \tag{2.8}$$
$$\text{(i.e., } \Delta_{tl_3} \text{ in } t \sim AR1(0, \sigma_{\mathcal{T}\mathcal{L}_3)} \quad \& \quad \Delta_{tl_3} \text{ in } l_3 \sim AR1(0, \sigma_{\mathcal{T}\mathcal{L}_3})$$

The set of seasonal (month)-length interaction effects $\{\Delta_{sl_3};\ \ s = 1, \ldots, S, l_3 = 1, \ldots, L_3\}$ is modeled somewhat similar to the Δ_{tl_3}'s; that is, the Δ_{sl_3}'s had a mean zero MVN distribution with a covariance matrix that was a Kronecker product of an AR(1) covariance matrix (with $\varphi_{\mathcal{S}\mathcal{L}_3^*}$ autocorrelation parameter) for length and a seasonal AR(1) covariance matrix (with $\varphi_{\mathcal{S}^*\mathcal{L}_3}$ autocorrelation parameter) for month. The standard deviation of Δ_{sl_3} was assigned with parameter $\sigma_{\mathcal{S}\mathcal{L}_3}$ (see Eqn. 2.9).

$$\Delta_{sl_3} - \varphi_{\mathcal{S}^*\mathcal{L}_3}\Delta_{s-1,l_3} = \varphi_{\mathcal{S}\mathcal{L}_3^*}(\Delta_{s,l_3-1} - \varphi_{\mathcal{S}^*\mathcal{L}_3}\Delta_{s-1,l_3-1}) + \varepsilon_{sl_3} \tag{2.9}$$
$$\text{(i.e., } \Delta_{sl_3} \text{ in } s \sim AR(1)(0, \sigma_{\mathcal{S}\mathcal{L}_3)} \ \ \& \ \ \Delta_{sl_3} \text{ in } l_3 \sim AR(1)\mathcal{N}(\mu, \Sigma_s)$$

The covariance matrix for the seasonal AR(1) process is

$$\Sigma_s(\varphi) = \frac{1}{1-\varphi^2}\begin{pmatrix} 1 & \varphi & \ldots & \varphi^5 & \varphi^6 & \varphi^5 & \ldots & \varphi^2 & \varphi \\ \varphi & 1 & \ldots & \varphi^4 & \varphi^5 & \varphi^6 & \ldots & \varphi^3 & \varphi^2 \\ \vdots & \ddots & \ddots & \vdots & \vdots & \vdots & \ddots & \vdots & \vdots \\ \varphi^5 & \varphi^4 & \ldots & 1 & \varphi & \varphi^2 & \ldots & \varphi^6 & \varphi^5 \\ \varphi^6 & \varphi^5 & \ldots & \varphi & 1 & \varphi & \ldots & \varphi^5 & \varphi^6 \\ \varphi^5 & \varphi^6 & \ldots & \varphi^2 & \varphi & 1 & \ldots & \varphi^4 & \varphi^5 \\ \vdots & \vdots & \ddots & \vdots & \vdots & \vdots & \ddots & \vdots & \vdots \\ \varphi^2 & \varphi^3 & \ldots & \varphi^6 & \varphi^5 & \varphi^4 & \ldots & 1 & \varphi \\ \varphi & \varphi^2 & \ldots & \varphi^5 & \varphi^6 & \varphi^5 & \ldots & \varphi & 1 \end{pmatrix}. \tag{2.10}$$

This is a symmetric and positive definite matrix with the same correlation between

January–February and December–January, etc. This process can account for cyclic seasonal changes in condition from higher values in the summer and fall following improved feeding conditions, to lower values in the winter and spring, presumably when prey are more scarce. However, seasonal variation may also be affected by a combination of temperature related metabolic effects, overlap with prey, and energetic investment in reproductive organs. This seasonal process is assumed to be the same each year.

The covariance matrices for the spatial fields (e.g., Δ_{gt}, Δ_{gl_3}) in Eqn. (2.3) were based on GMRF's (e.g., Rue and Held, 2005). The elements of precision matrices Ω were

$$\Omega_{gg'} = q \begin{cases} -h_{gg'} \left(\dfrac{1}{d_{gg'}} \right)^{\tau} & \text{if } g \neq g', \\ \omega + \sum_{g' \neq g} h_{gg'} \left(\dfrac{1}{d_{gg'}} \right)^{\tau} & \text{if } g = g', \end{cases} \tag{2.11}$$

where $h_{gg'} = 1$ if strata g and g' are neighbours, and is 0 otherwise, $d_{gg'}$ was the distance between the centroids of strata g and g'. The positive parameters q and ω were estimated separately for each Δ and subscripts were used similar to the Δ's to indicate this. I used irregular spatial units (i.e., strata), so I also used the distance between strata centroids to model spatial correlation. An extra power parameter τ was included to improve its flexibility in modeling irregular spatial strata, and a common value was assumed for all Δ's.

The parameter q scales the precision matrix, so that q^{-1} is an overall measure of the level of the covariance matrix. Interpreting the spatial correlation parameter ω can be challenging. To aid in understanding this parameter, I plotted the elements of the correlation matrices against the distance between centroids of the strata. The decorrelation formula used by Zheng et al. (2020b) was fitted, $corr(d) = \exp\{-(d/D)^{\delta}\}$, which is a model to describe how the correlation declines as a function of the distance d between two strata, based on the parameters D (i.e., the decorrelation distance)

and δ (i.e., the speed of decorrelation). Estimating the values of D and δ allows for the calculation of the average distance at which the spatial correlation reaches 0.5, denoted as $\bar{d}_{0.5}$. This measure offers a straightforward way to assess the extent of spatial correlation.

In preliminary analyses I found that σ_w^2 in Eqn. 2.12 depended on fish length; in particular, when the length was small then the residual variation was much larger. However, for larger sized fish the residual variance was approximately constant. This was accounted for using a non-linear variance model,

$$\sigma_w^2(l) = c + \exp\left\{d - e\log(l)\right\}, \tag{2.12}$$

where c is a positive parameter, and d and e are real-valued parameters to estimate.

To derive annual average stock weight-at-length, it is needed to average estimated weights across all strata each year, and weight by abundance (λ_{gtl}),

$$\bar{w}_{tl} = \frac{\sum_g \lambda_{gtl} \times w_{gtl}}{\sum_g \lambda_{gtl}}. \tag{2.13}$$

However, estimating the λ_{gtl} for all strata, years, and lengths is complex because there are missing strata in some years, and no surveys in some years. Therefore, for simplicity, similar to Cadigan et al. (2022b), a strata-size weighted average was employed,

$$\bar{w}_{tl} = \frac{\sum_g S_g \times w_{gtl}}{\sum_g S_g}, \tag{2.14}$$

where S_g is the size (i.e., area) of stratum g. Eqn. (2.14) is easier to implement but it is only suitable for stocks that have an approximately homogeneous distribution over space.

The Template Model Builder (TMB; Kristensen et al., 2016) package within R (R

Core Team, 2022) was used to implement the models. The R function "nlminb" was used to find the maximum likelihood estimates.

2.3.4 Model selection

Model selection was performed to identify and retain effects that significantly explained variability in the data. The Akaike Information Criterion (AIC) and Bayesian Information Criterion (BIC) were used, along with residuals and mean squared residuals (MSE) to compare model predictions. AIC evaluates the accuracy of the predictions, while BIC measures the goodness of fit (Sober, 2002). Both criteria were used as it is not clear which criterion performs better. The model was run for eleven different combinations of the main effects (i.e., Δ_g, Δ_t and Δ_{l_3}) and interaction effects (i.e., Δ_{gt}, Δ_{gl_3}, Δ_{tl_3}, and Δ_{sl_3}) to yield eleven distinct models (see Table 2.1), from which the best one was selected.

2.4 Results

2.4.1 Spatiotemporal condition model for 3NO cod

All the tables and figures referred to in the text below are separately presented in the Sections, 2.6 and 2.7 respectively.

Model selection results are presented in Table 2.1. The full model (see Eqn. 2.2), which included all main effects (Δ_g, Δ_t and Δ_{l_3}) and interactions (Δ_{gt}, Δ_{gl_3}, Δ_{tl_3}), did not provide the best fit as measured by AIC and BIC. The best fitting model included only the interaction effects, including the survey timing (season) and length interaction effects (Δ_{sl_3}). This was selected as the final model formulation (see M02 in Table 2.1). Consequently, the intercept, A_{g_i,t_i,l_i} of the final model is sum of the interaction effects.

Thus, the full version of the final spatiotemporal model is

$$\log(W_{g_i,t_i,l_i}) = A_{g_i,t_i,l_{3i}} + \Delta_{s_i,l_{3i}} + b\log(l_i) + \varepsilon_{wi}, \quad \varepsilon_{wi} \overset{iid}{\sim} N(0,\sigma_w^2),$$

where

$$A_{g_i,t_i,l_{3i}} = a + \Delta_{g_i t_i} + \Delta_{g_i l_{3i}} + \Delta_{t_i l_{3i}}. \tag{2.15}$$

The parameter estimates for the final model are presented in Table 2.2. The estimates of a and b were 4.7×10^{-6} and 3.119, respectively.

2.4.2 Interaction effects of spatiotemporal model

Spatiotemporal interaction effect (Δ_{gt})

The estimates of the spatiotemporal effects Δ_{gt} ranged between -0.05 and 0.05 (Figure 2.2), with low spatial correlation. The average distance at which the correlation reached 0.5 ($\bar{d}_{0.5\mathcal{GT}}$; detailed in Table 2.2 and Figure 2.3) was only 0.69 km. The estimate of the temporal correlation parameter, $\varphi_{\mathcal{GT}} = 0.173$, was also low. Many of these effects were estimated to be close to zero, which is also indicated by the low value of $\sqrt{q_{\mathcal{GT}}^{-1}}$ as shown in Table 2.2.

Spatial strata-length interaction effect (Δ_{gl_3})

The spatial strata-length interactions Δ_{gl_3} were usually larger in absolute value than the spatiotemporal effects, a fact that is also evident from the greater value of $\sqrt{q_{\mathcal{GL}_3}^{-1}}$ compared to $\sqrt{q_{\mathcal{GT}}^{-1}}$ as presented in Table 2.2. The length correlation estimate ($\varphi_{\mathcal{GL}_3} = 0.950$; Table 2.2 and Figure 2.3) indicates that Δ_{gl_3} were similar for fish of similar sizes. There was a higher spatial correlation observed in Δ_{gl_3} in comparison to Δ_{gt}, with an

average distance of 44 km at which the correlation reached 0.5 (i.e., $\bar{d}_{0.5gl_3} = 44$ km). Summary statistics for spatial strata are presented in Table B.2.

Temporal length interaction effect (Δ_{tl_3})

The temporal length interaction effects (Figure 2.5) exhibited a magnitude similar to that of the Δ_{gl_3} effects. This similarity is evidenced by the comparable values of $\sigma^2_{\mathcal{TL}3}$ and $\sqrt{q^{-1}_{\mathcal{GL}3}}$ provided in Table 2.2. These effects displayed a high level of length correlation ($\varphi_{\mathcal{TL}^*_3} = 0.93$ in Table 2.2). There was usually high between-year consistency in these estimates, but more abrupt changes in 1990–1991 and 2013–2014, which is why the temporal correlation estimate ($\varphi_{\mathcal{T}^*\mathcal{L}_3} = 0.70$) was lower. This indicates more abrupt changes in condition in those years. Figure 2.5 also indicates poorer condition overall for fish between 45–75 cm and larger fish over 120 cm, although the sample sizes at the larger sizes were low as indicated in Figure 2.6.

Seasonal length interaction effect (Δ_{sl_3})

The seasonal effects are shown in Figure 2.7. The main trend is a decrease in fish condition from January to April and May, followed by an increase that continues until September. Smaller increases occur during the period from September to December. Similar to the temporal length interaction effects displayed in Figure 2.5, the seasonal effects also indicate poorer condition overall for fish between 45–75 cm and larger fish over 120 cm. The length correlation in the seasonal effects was high ($\varphi_{\mathcal{TL}^*_3} = 0.93$ in Table 2.2) and the month correlation was somewhat lower ($\varphi_{\mathcal{S}^*\mathcal{L}_3} = 0.79$).

2.4.3 Variance model

The estimates of the error variance model (Eqn. 2.12) indicate that the variation was approximately constant at fish sizes of about 30 cm and higher, but the error variation

was higher for smaller fish (see Figure. 2.8).

2.4.4 Temporal variability in mean gutted-weight

The spatiotemporal model was used to predict mean gutted-weight for SGB cod for every length bin, month, strata, and year. The Eqn. (2.14) was used to summarize the temporal patterns as illustrated in Figure 2.9. The results indicate that weight is lower in the spring (e.g., May) than the fall (e.g., October), particularly for fish between 40–80 cm. Larger fish experienced an abrupt decrease in weight in 1990, and after several years weight improved. This pattern was more gradual for smaller-sized fish. At larger sizes, weight also decreased after 2013 but this did not appear to happen to the same extent for fish between 40–60 cm.

Annual average spatial and seasonal patterns of the log condition coefficient parameter ($\bar{A}_{gls}$) values are illustrated in Figure 2.10. The overall pattern is low spatial variability in cod weight, both in the spring and fall. Figure 2.11 demonstrates a good fit of the spatiotemporal model to the data (also see Figures 2.12 - 2.14). The patterns presented in Figure 2.9 are less obvious in Figure 2.11. However, the observed trends in Figure 2.11 are also influenced by noise from measurement error and spatiotemporal variability in sampling locations (e.g., Figure 2.15 and C.2), which is accounted for in Figure 2.9.

2.5 Discussion

I developed a novel spatiotemporal model to examine variations in fish condition over time (year and season), space (i.e., spatial strata), and size (i.e., fish length). The spatiotemporal condition model incorporates random effects to account for interactions among length, space, time, and season (i.e., survey months). This modeling approach

was employed to address issues related to sampling gaps and changes in the locations where fish were weighed. The spatiotemporal interaction effects of the model (i.e., Δ_{gt}) had low variability and low temporal and spatial correlation. Many of the predicted spatiotemporal interactions were very close to zero. These interaction effects were relatively low compared to the spatial length interaction effects (i.e., Δ_{gl_3}), which had higher variability and more spatial correlation. For Atlantic cod on the Icelandic shelf, Pardoe et al. (2008) found little variation in mean relative body condition, while the hepatosomatic index was identified as a dynamic indicator of condition. Their study revealed that condition can have an important spatial component. Thus, they highlighted the significance of considering the spatial aspect, especially for stocks living under heterogeneous environmental conditions. Moreover, their study emphasized the importance of identifying a suitable index for condition and determining the most appropriate spatial resolution. The temporal length interaction effects (Δ_{tl_3}) were of similar magnitude compared to the Δ_{gl_3} effects. In general, Δ_{tl_3} had a relatively high between-year consistency, with only a few exceptions in some years (see Figure 2.5). The random interaction effects between year-length and month-length (i.e., Δ_{tl_3} and i.e., Δ_{sl_3}) together indicated poorer condition overall for fish between 45–75 cm and larger fish over 120 cm, although the sample sizes at the larger sizes were low. The spatiotemporal model fit to the data reasonably well. By quantifying the correlations in the weight-length intercept by space, year, season, and length, we can use the model to predict the weight for any length fish in each survey strata, month, and year.

I used gutted-weight and total length of Atlantic cod in SGB to model the cod condition, which extended the models in Thorson (2015) and Cadigan et al. (2022b). However, the spatiotemporal model preserves the fundamentals of the conventional LWR first introduced by Keys (1928) (see section 1.4). Therefore, it can easily be utilized to estimate mean total weights-at-length over the stock area. Importantly, these estimates can be used as inputs for certain stock assessment models. Changes in the

sample locations year to year affect the comparability of the condition information, and we use our model to standardize condition for the entire stock. In this thesis, I did not focus much on the spatial variations in weights, which seemed low from the model results. However, I illustrated the temporal variability (annual and seasonal) in the model-predicted and observed area-weighted (strata average) gutted weights for April and October (see Figure 2.9). This figure illustrates differences in condition between the spring (i.e., April) and the fall (i.e., October), but also years with poor condition for the stock as a whole. An improvement for future research will be to use a stock density-weighted average to aggregate spatial results for the whole stock, rather than the area-weighted average that I used in this thesis. I did not have spatial density-at-length estimates available for my research.

I employed a novel procedure to model the seasonal effect, utilizing a modified AR(1) process (see Eqn. 2.10). This adjustment ensures that January and December maintain the same correlation as other consecutive months. Thus, this process can account for cyclic seasonal changes in body condition. It is important to note that in this modeling approach, I assumed that the seasonal effects remained consistent across all years. This is why we estimate the same annual trends in relative condition between the spring and fall. However, this assumption may not entirely reflect reality. I examined residuals versus month for each year and did not find evidence of lack of fit for the assumption of the same seasonal effect each year.

Our results indicated substantial annual variation in gutted-weight relative condition, with low values during 1991-1993. These findings are consistent with the results in (Morgan et al., 2010), who analyzed spring survey conditions only. Stares et al. (2007) did not find significant differences between SGB cod condition between 1993–1995 and 2002–2004 (see Table 5 in Stares et al., 2007), which is somewhat consistent with our results that indicated only small increases in condition between these two time periods, depending on the length of the fish (see also Figure 9 in Taggart et al., 1994). I also

found that SGB cod were in poorer condition in the spring compared to the fall, which is a seasonal cycle commonly reported for north Atlantic cod stocks (e.g., Regular et al., 2022; Taggart et al., 1994).

The a (condition coefficient parameter) and b (allometric growth coefficient parameter) estimates of the spatiotemporal model are reported in section 2.4. The allometric growth coefficient estimated is close to the value reported ($b = 3.088$) by Healey et al. (2013) and the value reported ($b = 3.174$) by Cadigan et al. (2022b) for Atlantic cod in NAFO Division 3Ps. The value of a in Healey et al. (2013) was 5.4×10^{-6}, which is similar to the value estimated by the model. Walsh and Hiscock (2005) estimated $b = 2.86$ for cod in the inshore of 3Ps, which is less than the value estimated by the model, and their estimate $a = 13 \times 10^{-6}$ was greater. These variations may be attributed to the influence of spatial and temporal components, as demonstrated by previous studies such as Pardoe et al. (2008), Thorson (2015), and Cadigan et al. (2022b). Re-estimating these parameters (Cadigan et al., 2022b), would enhance the accuracy of LWR estimations, especially in studies where the role of spatial and temporal components is significant.

The estimation of spatial correlations was based on the centroid distance between spatial strata, following a similar approach to Cadigan et al. (2022b). In their work, Cadigan et al. (2022b) suggested the potential use of depth information to calculate 3-dimensional centroid distances of the strata. However, there are complications in weighting vertical and horizontal distances when incorporating depth information. This is an aspect to consider in potential future extensions of the model. Additionally, Pardoe et al. (2008) found that the impact of depth on mean relative condition can vary depending on the region.

The primary objective of this chapter was to develop a novel spatiotemporal condition model, aiming to utilize it to derive starvation-induced natural mortality index (i.e., starvation mortality index) for SGB cod. The approach I used for deriving the

starvation mortality index is elaborated in Chapter 3.

2.6 Tables

Table 2.1: Model comparisons using: 1) Akaike information criterion (AIC), 2) bayesian information criteria (BIC), and 3) root mean squared error (RMSE). The total number of observations is 26,660, and the minimum AIC and BIC values and RMSE are -55 169.32, -5 5021.89, and 0.08, respectively. MLL is the marginal loglikelihood and k is the number of model parameters. Models are numbered in the first column. Δ effects are defined in Table B.3.

	Model with							MLL	k	Δ AIC	Δ BIC	Δ MSE	Δ RMSE
	Δ_g	Δ_t	Δ_l	Δ_{gt}	Δ_{gl}	Δ_{tl}	Δ_{sl}						
M01	+	+	+	+	+	+	+	27602.66	24	12.00	61.15	0.000000	0.000000
M02				+	+	+	+	27602.66	18	0.00	0.00	0.000000	0.000000
M03				+	+	+		25662.47	15	3874.39	3849.82	0.000821	0.004717
M04				+	+		+	27475.88	15	247.56	222.99	0.000169	0.000993
M05				+		+	+	27518.87	15	161.58	137.01	0.000104	0.000611
M06				+			+	27393.35	12	406.62	357.48	0.000275	0.001609
M07					+	+	+	27341.50	15	516.32	491.74	0.000384	0.002240
M08					+		+	26907.65	12	1378.02	1328.88	0.000753	0.004335
M09						+	+	26703.65	11	1784.02	1726.68	0.000829	0.004760
M10							+	20750.28	7	13682.77	13592.67	0.006457	0.032049
M11								-47051.22	4	149279.75	149165.08	2.663730	1.549576

Table 2.2: Parameter estimates and standard errors (SE) for model 2 (see M02 in Table. 2.1). Parameters are defined in Table. B.3.

Parameter	Category	Estimate	SE
$\varphi_{\mathcal{GT}}$	correlation	0.173	0.079
$\varphi_{\mathcal{GL}_3}$	correlation	0.950	0.014
$\varphi_{\mathcal{T}^*\mathcal{L}_3}$	correlation	0.696	0.089
$\varphi_{\mathcal{T}\mathcal{L}_3^*}$	correlation	0.925	0.020
$\varphi_{\mathcal{S}^*\mathcal{L}_3}$	correlation	0.785	0.081
$\varphi_{\mathcal{S}\mathcal{L}_3^*}$	correlation	0.978	0.010
$\sqrt{q_{\mathcal{GT}}^{-1}}$	Standard Deviation	0.004	0.007
$\sqrt{q_{\mathcal{GL}_3}^{-1}}$	Standard Deviation	0.027	0.004
$\sigma^2_{\mathcal{TL}_3}$	variance	0.023	0.003
$\sigma^2_{\mathcal{SL}_3}$	variance	0.021	0.004
$\omega_{\mathcal{GT}}$	other	1.430	0.899
$\omega_{\mathcal{GL}_3}$	other	0.077	0.056
$\bar{d}_{0.5\mathcal{GT}}$	other	0.687	–
$\bar{d}_{0.5\mathcal{GL}_3}$	other	43.764	–
a	other	-12.270	0.060
b	other	3.119	0.014
c	other	0.080	0.000
d	other	14,179	0.812
e	other	5.997	0.285
τ	other	0.005	0.174

2.7 Figures

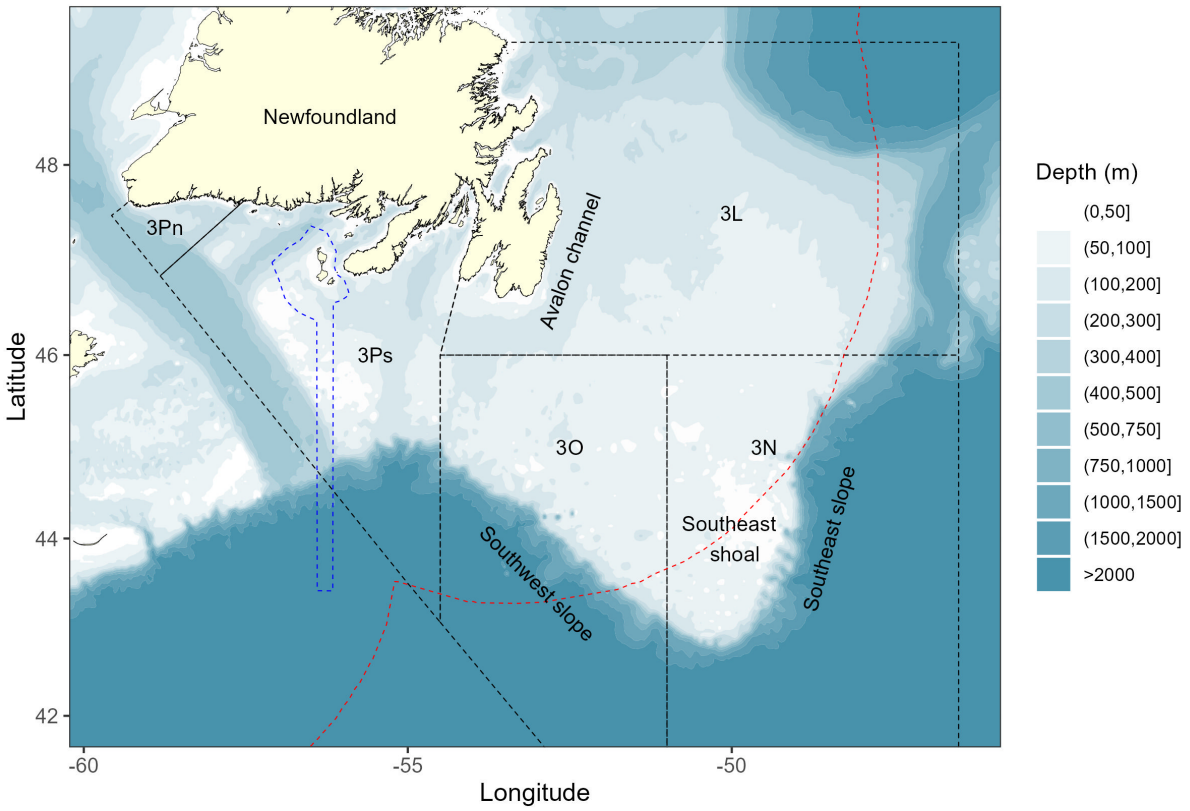

Figure 2.1: Southern Grand Bank and adjacent areas. The red dashed line indicates the boundary of Canadian 200 nautical mile Exclusive Economic Zone (EEZ). SGB is enclosed by the boundaries of NAFO Divisions 3NO.

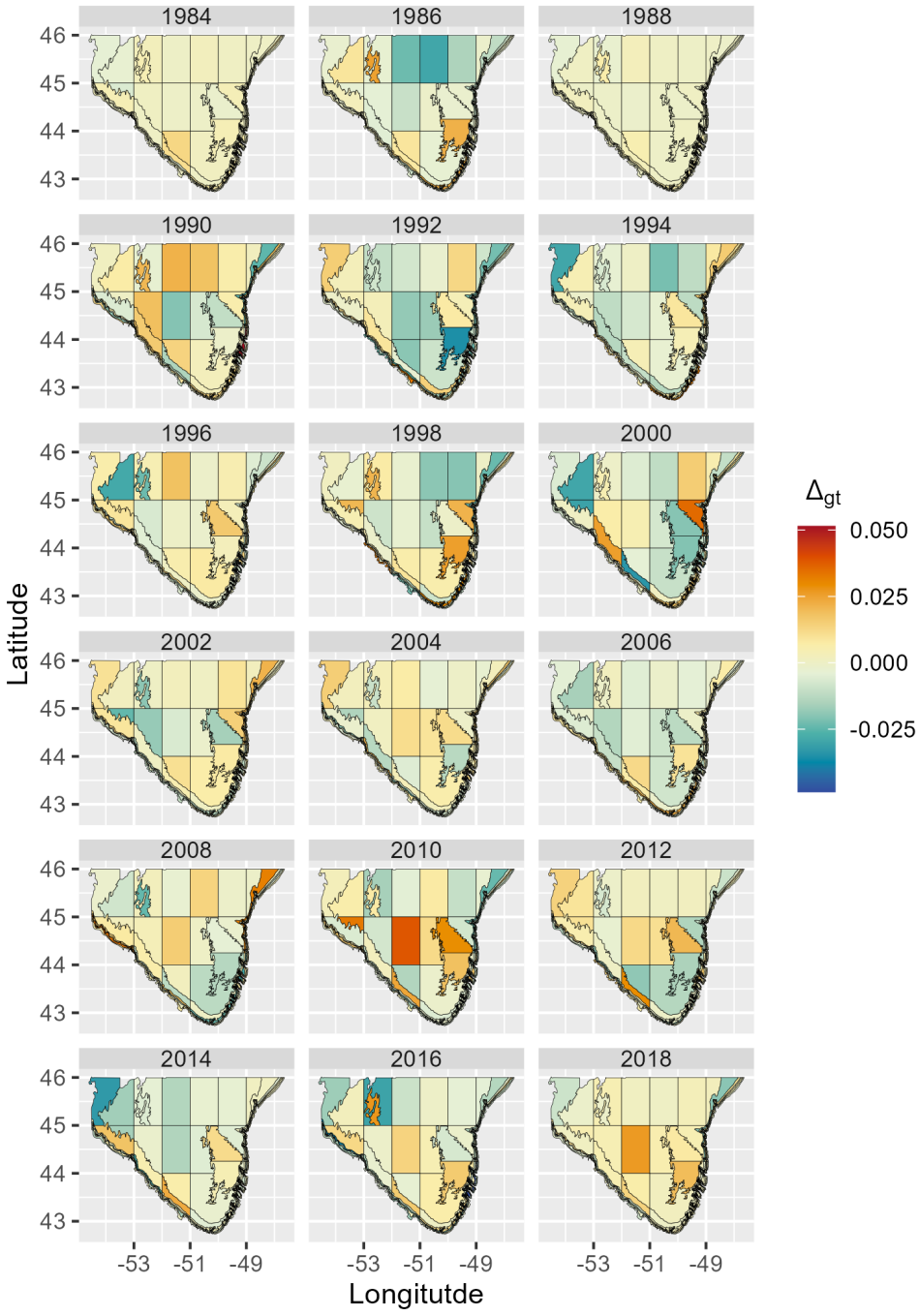

Figure 2.2: Variation in the mean strata-time interaction effects (Δ_{gt}) over years and across strata. The analysis accounted for 35 years, 1984–2018, however, spatiotemporal maps are produced every second year to simplify the visualization and interpretation.

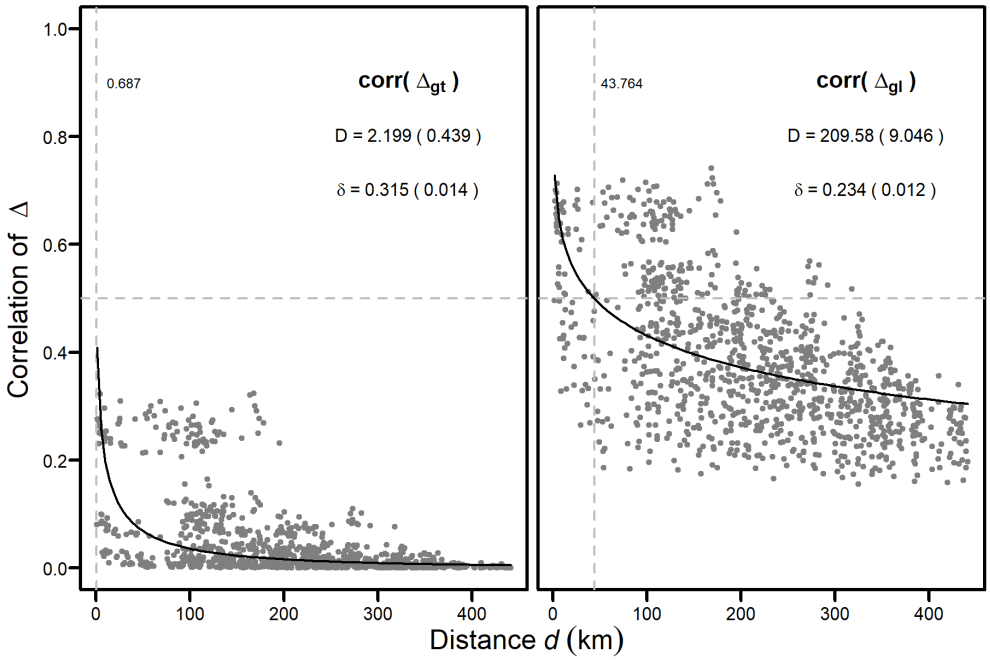

Figure 2.3: Variation in spatial correlations with respect to centroid distance of strata. Black curves are the fitted lines of the correlation and distance data to the formula, $corr_{\Delta} = \exp\{-(d/D)^{\delta}\}$, where D is the distance between centroids of two strata and δ is a parameter. The vertical grey dashed lines are at fitted average distance that the spatial correlation was 0.5.

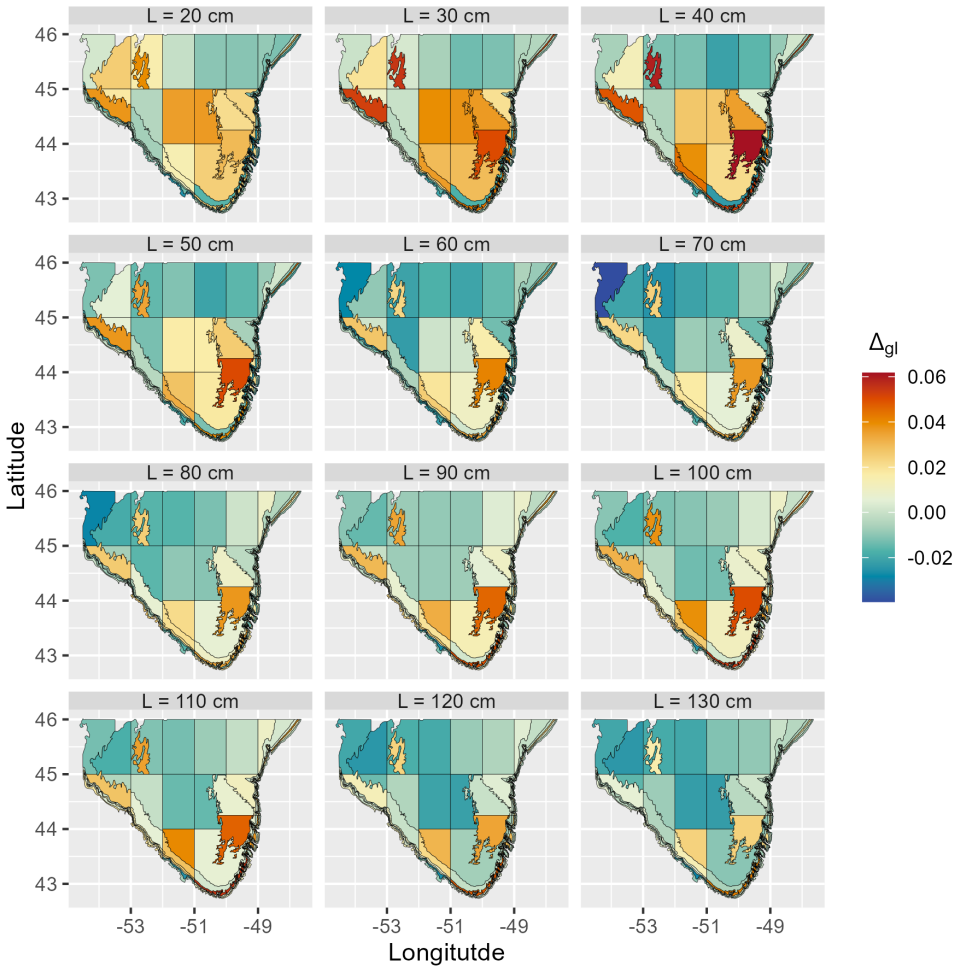

Figure 2.4: Variation in the mean strata-length interaction effects (Δ_{gl_3}) over spatial strata. Each panel is for a selected length class.

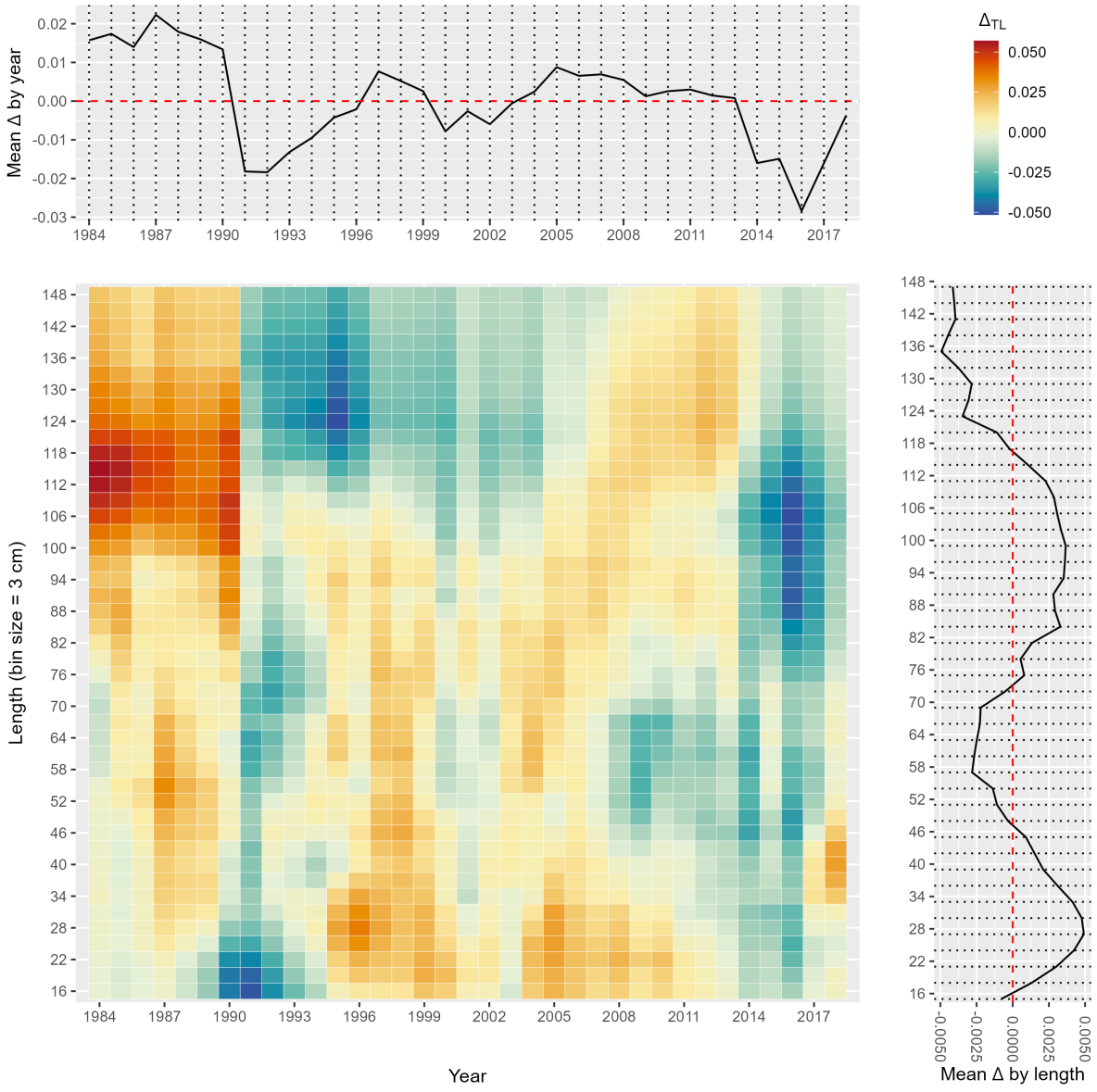

Figure 2.5: Variation in the mean time-length interaction effect (Δ_{tl_3}). Variability of mean Δ over years and lengths are annotated at the top and right of the main plot, respectively. Dashed lines indicate the series average.

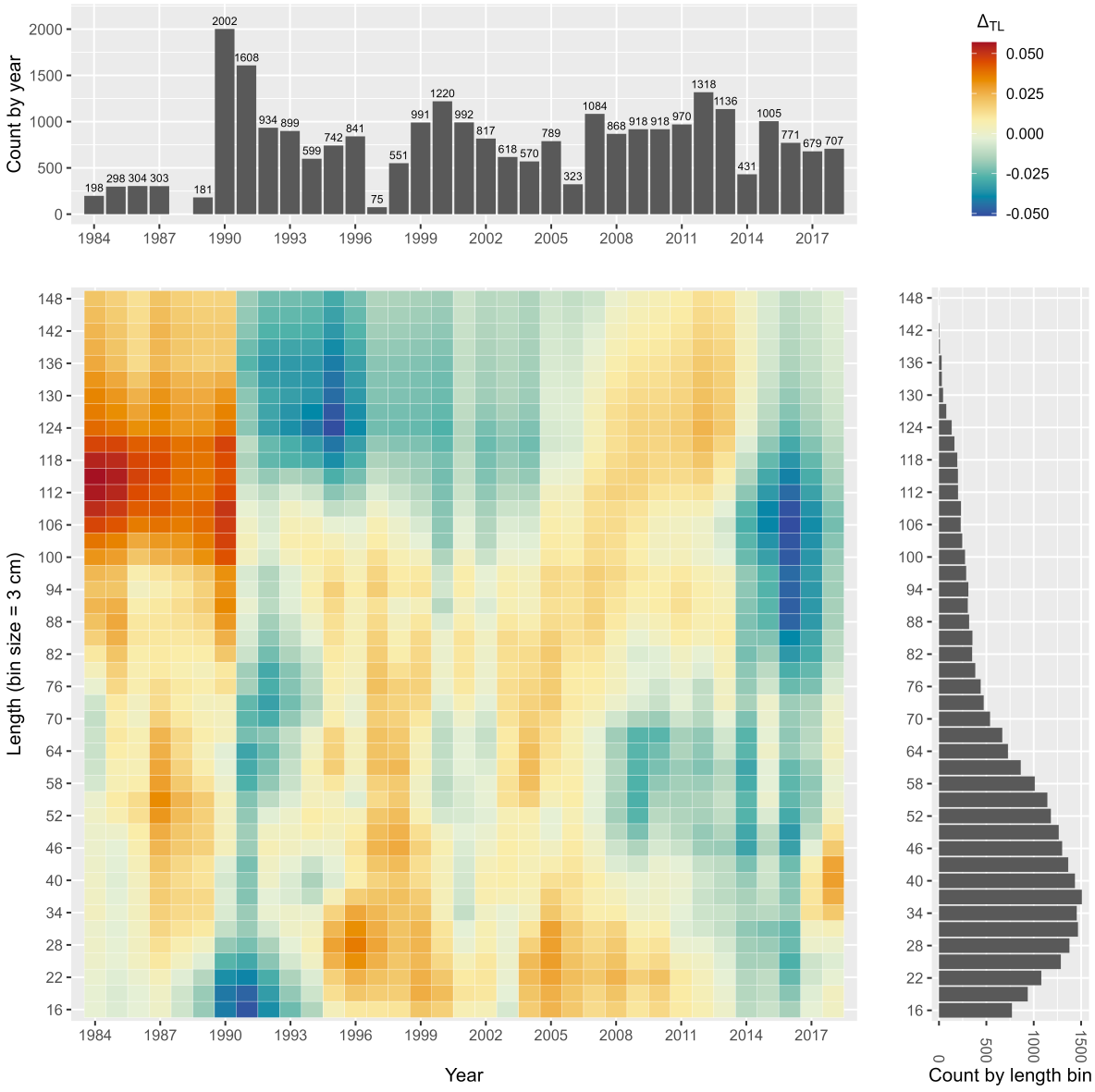

Figure 2.6: Variation in the mean time-length interaction effect (Δ_{tl_3}). Sample sizes for years and lengths are annotated at the top and right of the main plot, respectively.

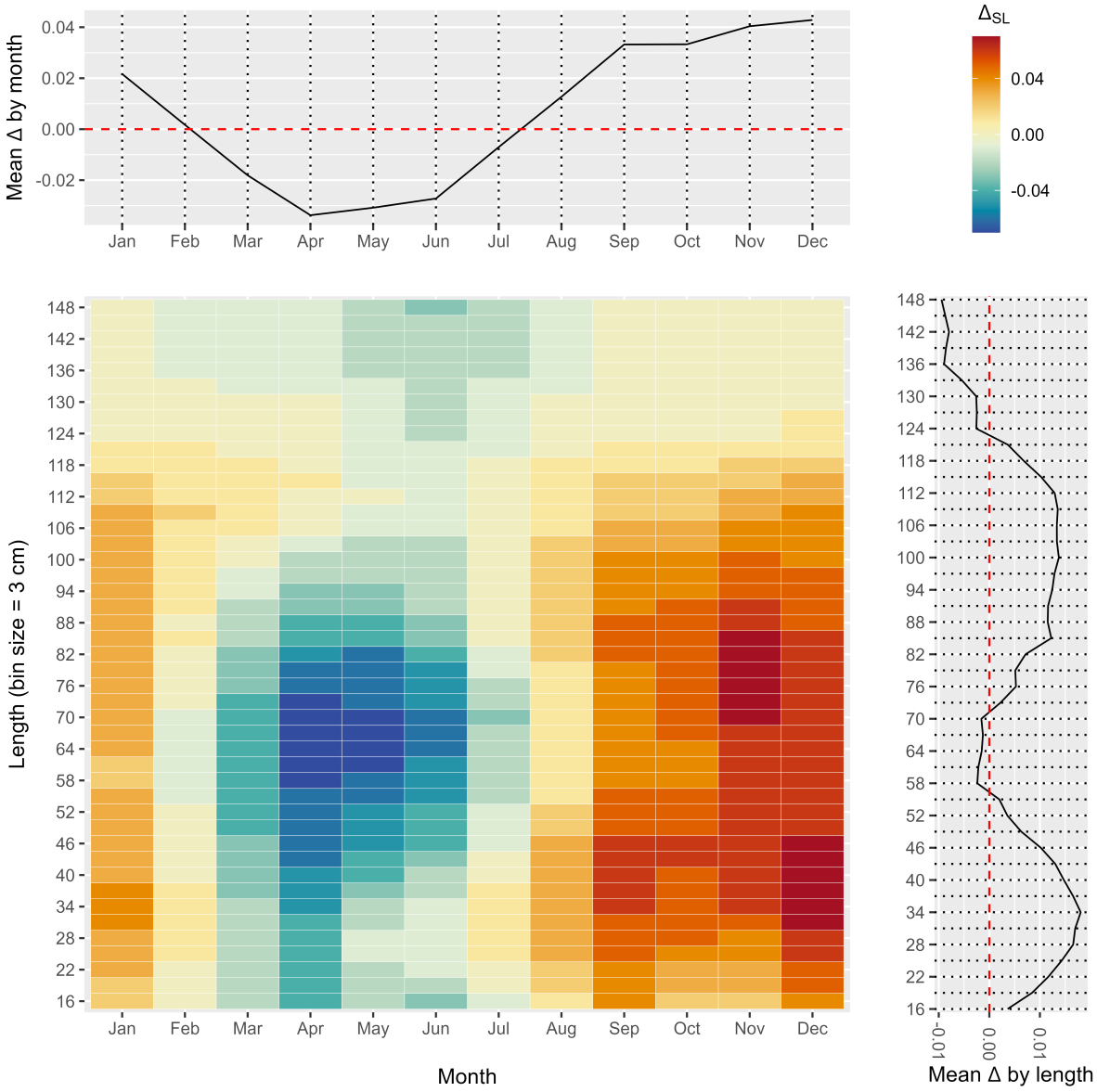

Figure 2.7: Season (month) and length interaction effect (Δ_{sl_3}) from model M02 (see Tables 1 and 2). Colors indicate the size of the effect, which is described in the legend at the top-right. Variability of mean Δ over seasons and lengths are annotated as marginal summaries at the top and right of the main plot, respectively. Dashed lines indicate the series average.

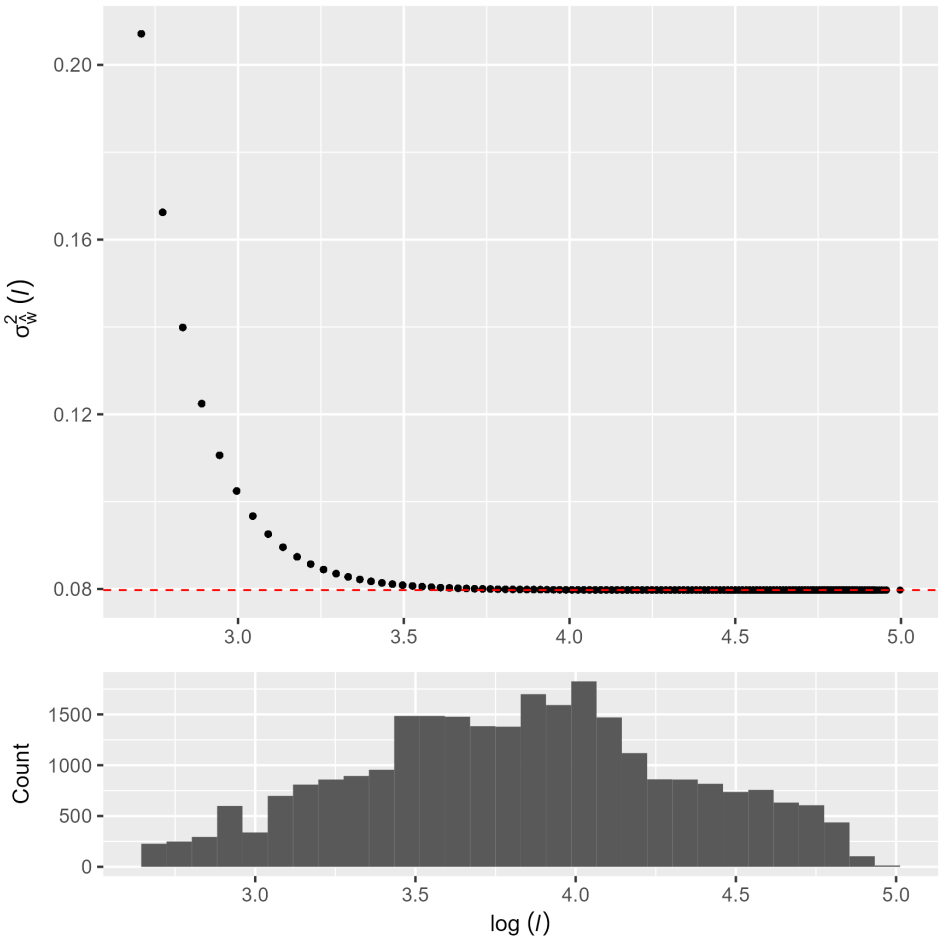

Figure 2.8: The non-linear variance model (see Eqn. 2.12) used for the residuals of the spatiotemporal weight-length model (top panel). The frequency of log-lengths are shown in the bottom panel.

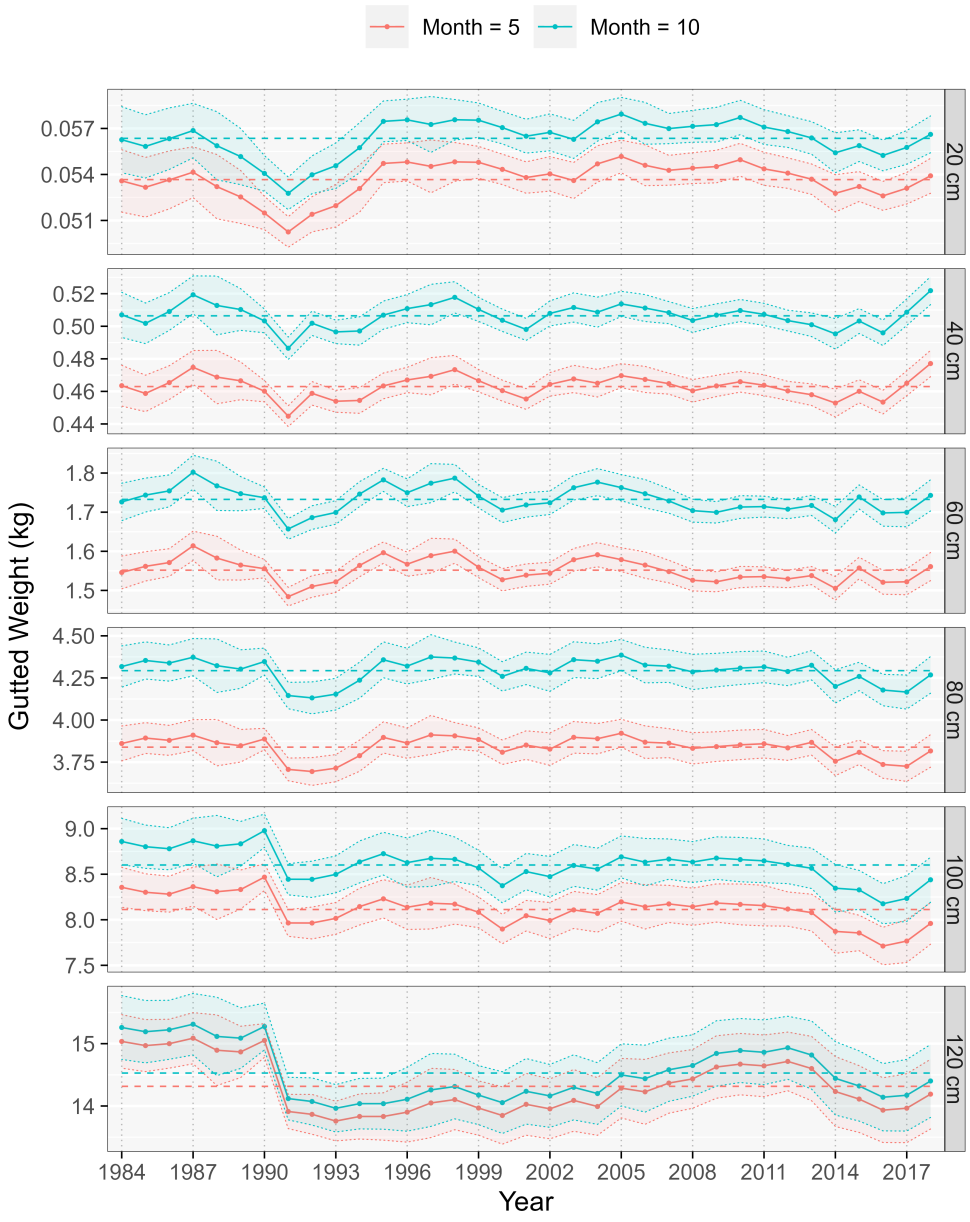

Figure 2.9: Time-series of area-weighted mean gutted-weights of 3NO cod (kg; defined in Eqn. 2.14) in the spring (orange line) and fall (green line). Month 5 is May and Month 10 is October. Shaded regions indicate 95 % confidence intervals. Each panel represents a different sized cod. Horizontal dashed lines indicate the series averages.

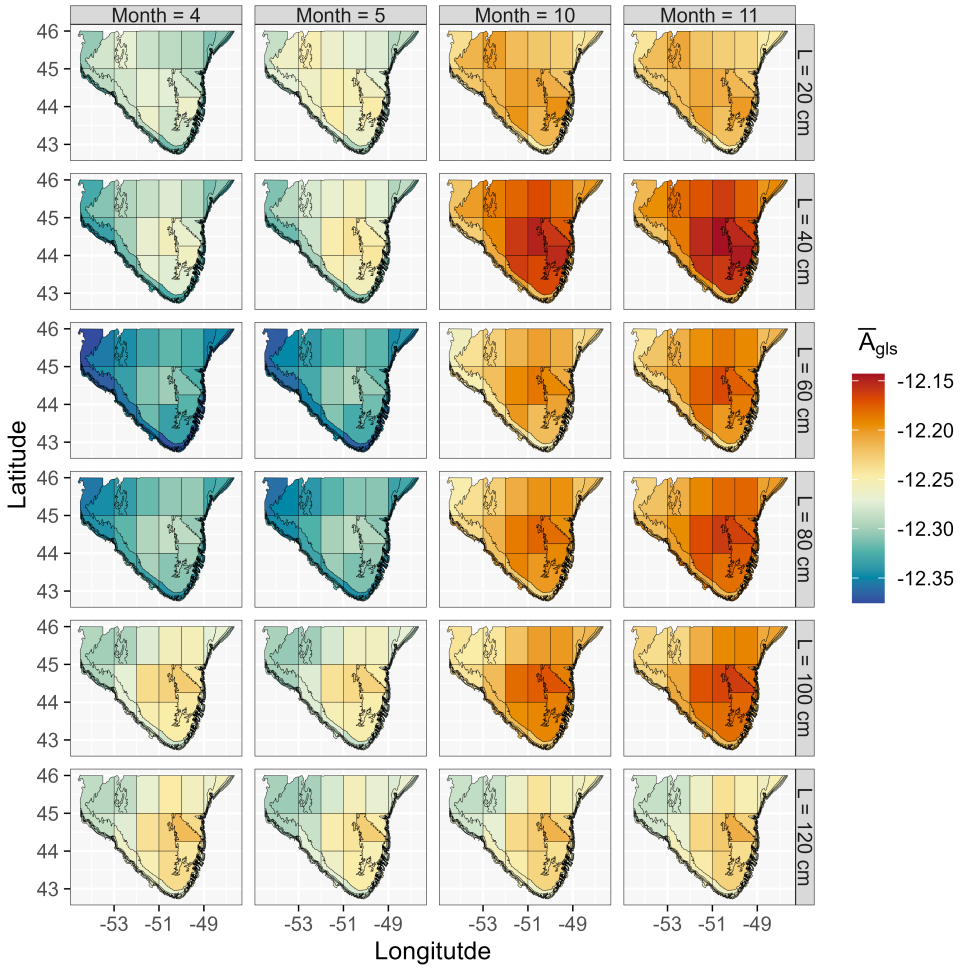

Figure 2.10: Annual average values of the log condition coefficient parameter ($\bar{A}_{gls} = T^{-1} \sum_{t=1}^{T} A_{gtls}$), illustrated for four choices of month (i.e., spring and fall; figure columns) and a wide range of fish lengths (rows).

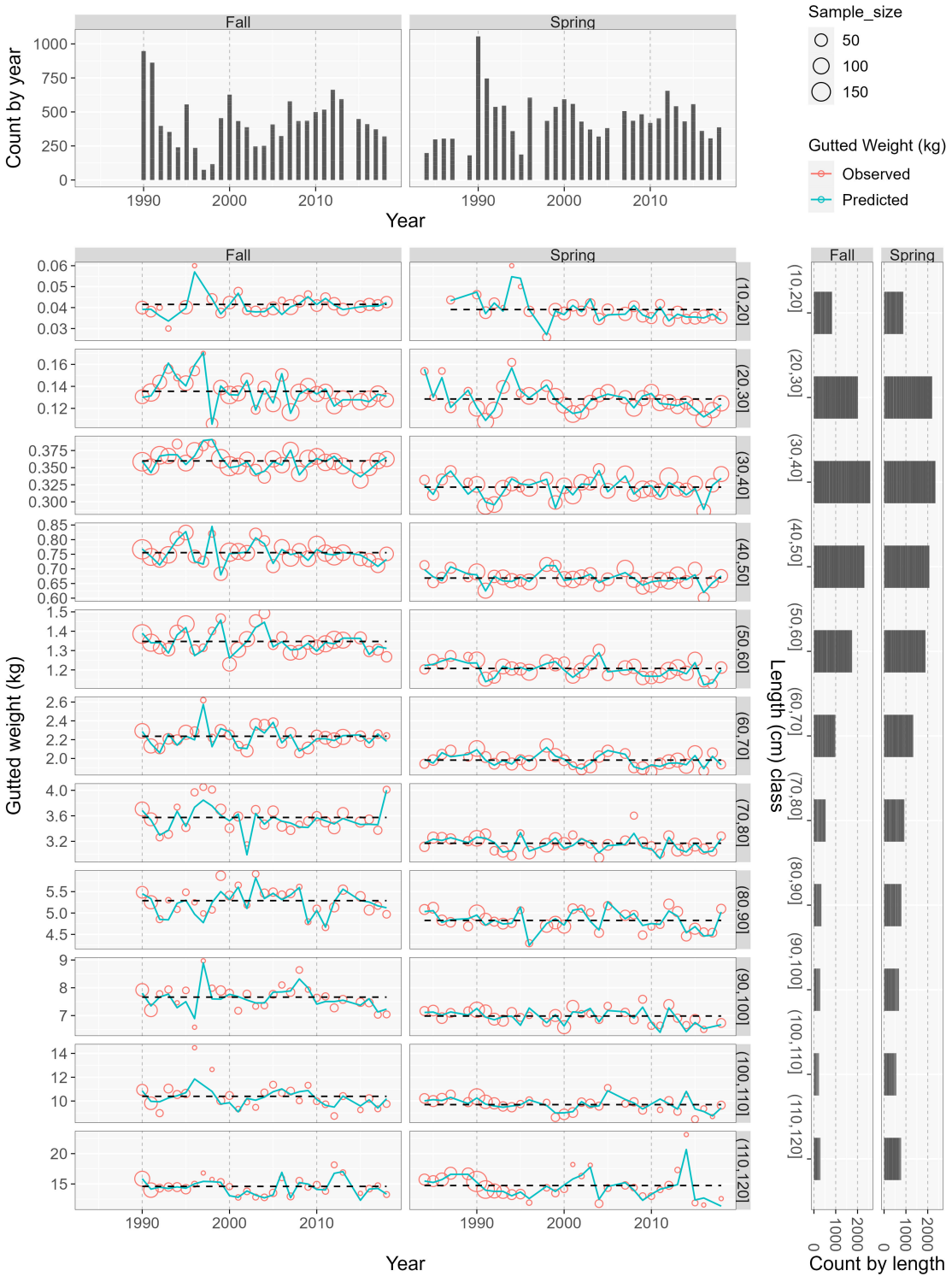

Figure 2.11: Time-series of seasonal (columns) sample-average predicted (line) and observed (circle) gutted-weight of 3NO cod from the spatiotemporal weight-at-length model. The circles are proportional to sample sizes. Each row represents a 10 cm length range. Horizontal dashed lines indicate the series average. The annual number of gutted-weight samples are annotated at the top and the number of samples per length range is annotated at the right.

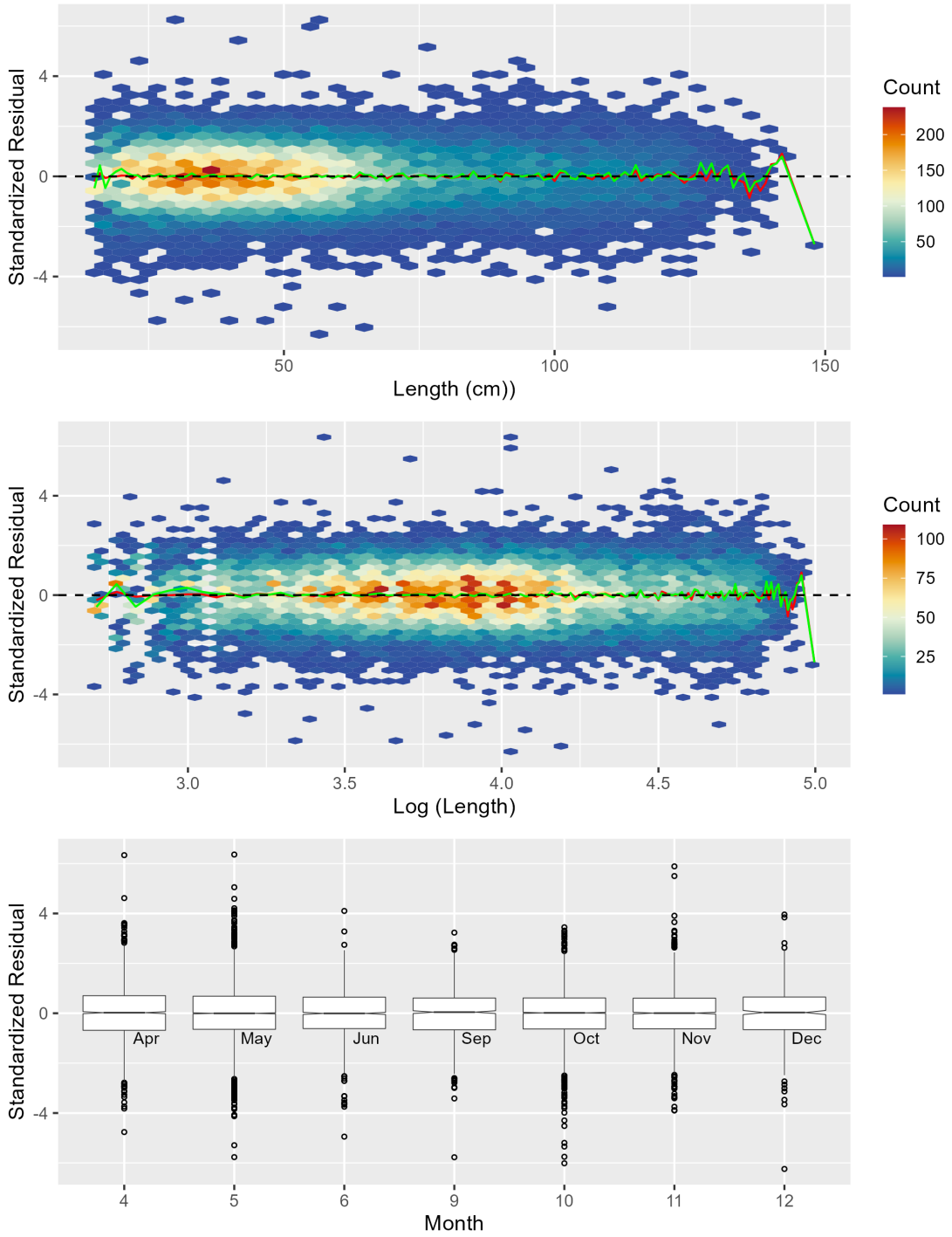

Figure 2.12: Standardized residuals of the model M02 over length and seasons (months). The red and green lines in the top and middle panels indicate the means and medians of standardized residuals, respectively.

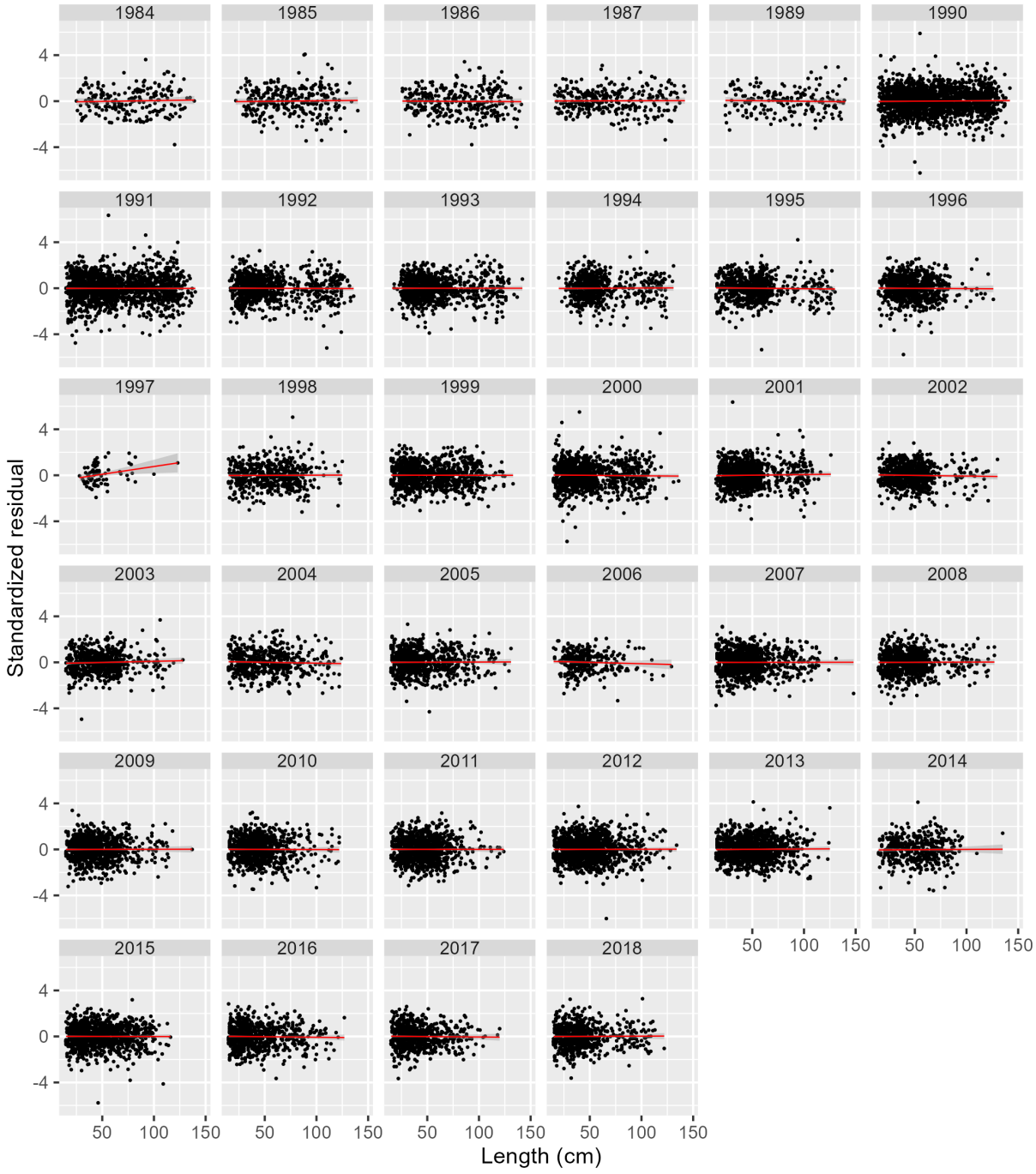

Figure 2.13: Standardized residual of model versus length. Red lines indicate the linear models (i.e., trend lines) of standardized residuals. The gray shaded regions indicate 95% confidence intervals.

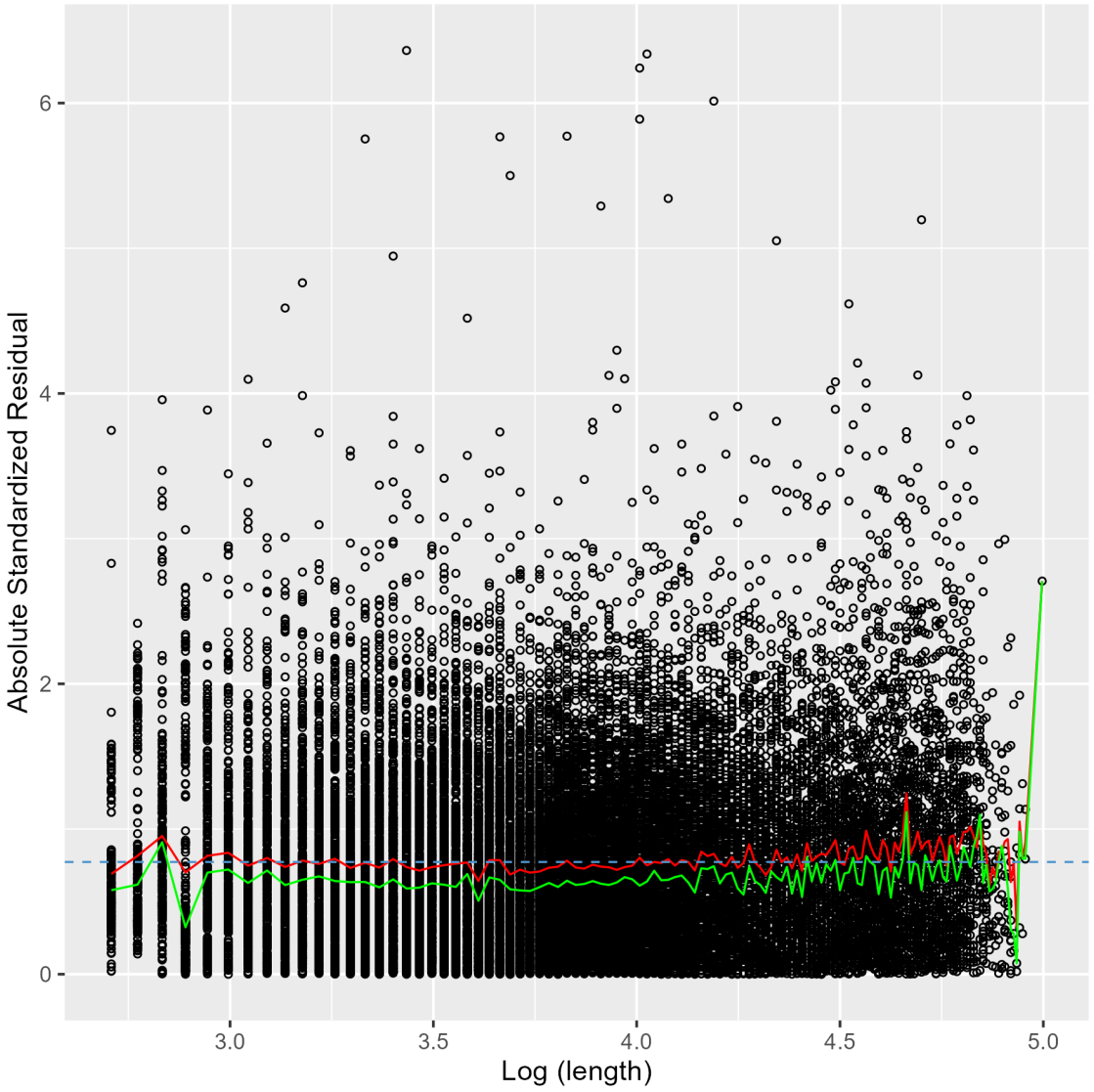

Figure 2.14: Absolute standardized residuals vs. log-length for model M02. The red and green lines indicate the means and medians at log-lengths, and the blue line indicates the overall mean of the absolute standardized residuals.

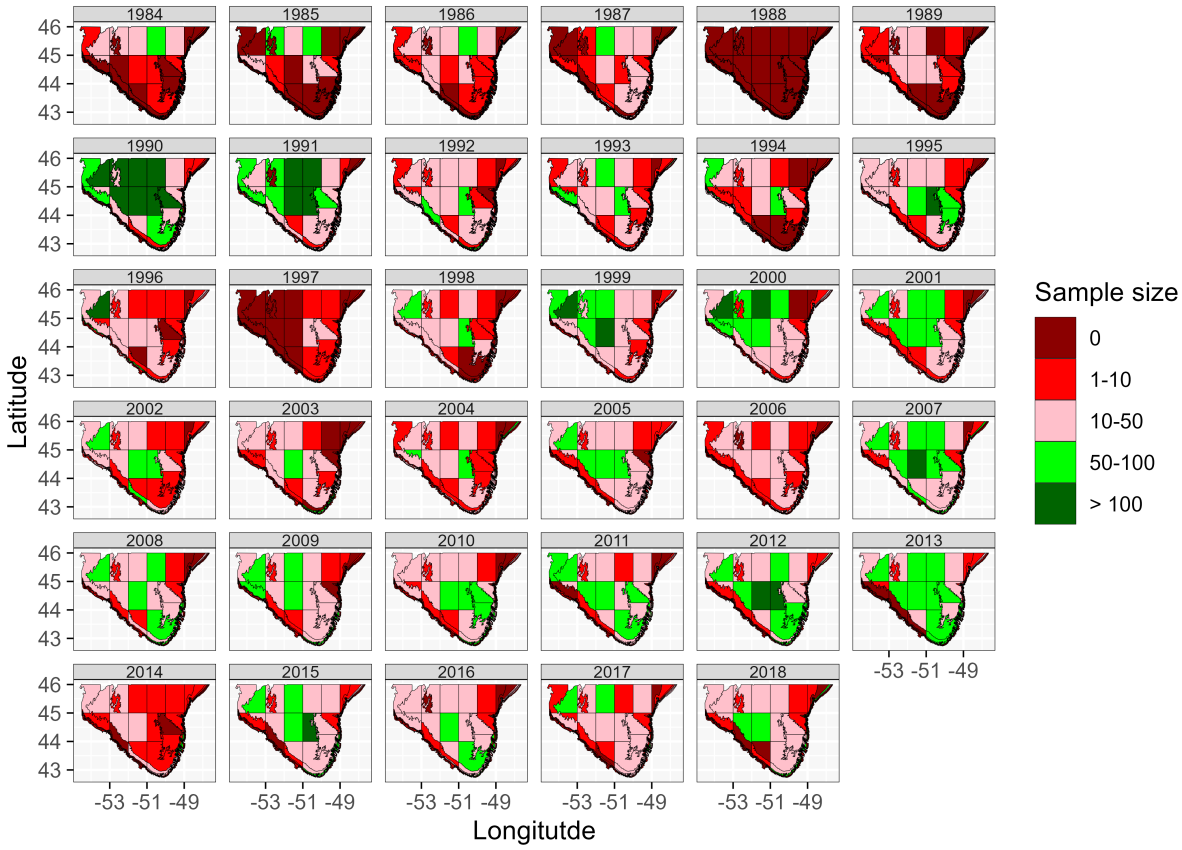

Figure 2.15: Spatiotemporal variability in sampling locations (i.e., strata).

Chapter 3

Starvation mortality index for SGB cod

This chapter focuses on the application of the spatiotemporal condition model developed in Chapter 2 to derive a novel starvation mortality index. It describes the rationale, the approach, the methodology used, the findings, and the significance of this index within the context of my thesis objectives.

3.1 Rationale

The mortality of fish due to natural processes (i.e., natural mortality, M) such as starvation, predation and senescence is difficult to observe and quantify (Lee et al., 2011; Vincent and Pilling, 2023). While direct estimation of M is feasible through tag-recapture experiments, it is constrained by the high costs associated with tagging programs (Höffle and Planque, 2023). Consequently, indirect methods are commonly employed to estimate M (Xiao, 2001; Lee et al., 2011; Punt et al., 2021a; Vincent and Pilling, 2023), assuming M remains constant over space, time, and age Punt et al. (2021a); Vincent and Pilling (2023). However, it is widely recognized that M likely varies with age, sex, and time (Punt et al., 2021a; Cadigan et al., 2022b; Hamel et al., 2023). In the spatiotemporal condition model I developed for SGB cod (see Chapter 2),

I assumed the condition parameter (i.e., slope, A_{g,t,l_3}) varied across spatial strata, years and length along with seasonal (months) effects (see Eqn. 2.2). Therefore, the use of this information to establish an indirect method for deriving a starvation M index, which I refer to as M_K, is potentially important. Such an index can be utilized in a stock assessment model to give better estimates of time– and age–varying M (e.g., Casini et al., 2016; Varkey et al., 2022), potentially improving the reliability of assessment model estimates of stock size and fishery harvest rates. This is important for SGB cod, where the potential for change in M is a concern (Cadigan et al., 2022a), which we describe in Chapter 5 in more detail.

3.2 Research approach

For many species, interpretations of changes in body condition should be done carefully, as they vary over annual cycles and between individuals (Cren, 1951; Lambert and Dutil, 1997; Rikardsen et al., 2006; Regular et al., 2022). Consequently, starvation mortality rates can display seasonal patterns and there can be wide differences in condition among fish in the population at any time. Only fish in really poor condition are at risk of dying due to starvation. Therefore, the mean body condition of fish in a population may not directly correlate with starvation mortality; instead, starvation mortality rates can be inferred from the proportion of fish that fall below a certain critical threshold Dutil and Lambert (2000); Geissinger et al. (2021); Regular et al. (2022).

Estimating annual M_K for the entire stock requires aggregating results across space and throughout the year. For SGB cod, research surveys conducted in the spring and fall provide information about seasonal changes in condition, but the survey fish weight data are not random samples from the stock, and standardization is required. The spatiotemporal model is used to account for these issues. Like Casini et al. (2016), the probability that a fish is in critical condition is estimated and, assuming fish in critical

condition will soon die, it is translated into spatiotemporal estimates of the starvation-induced M. Eventually, the goal is to use condition indices to estimate trends in a component of M. The methodology used is elaborated in Section 3.3.

3.3 Methods

3.3.1 Modeling starvation mortality index

The weight-length relationship for a length l fish in stratum g, year t, and month s (Eqn. 2.2), can also be written as

$$\log(w_{g,t,l,s,i}) = A_{g,t,l_3,s} + b\log(l_i) + \varepsilon_{BI,i} + \varepsilon_{ME,i}, \tag{3.1}$$

where

$$A_{g,t,l_3,s} = a + \Delta_{gt} + \Delta_{gl_3} + \Delta_{tl_3} + \Delta_{sl_3}. \tag{3.2}$$

ε_{BI} is between individual variability in weight-at-length within a stratum, and ε_{ME} is the log-weight measurement error. It is assumed that ε_{ME} is close to zero for large fish and that $\varepsilon_{BI} \sim N(0, \sigma^2_{BI})$ and $\sigma^2_{BI} \approx 0.08$ (see Figure 2.8). We have no empirical estimates of the measurement error variance for weight, but we assume this is small relative to the total weight of larger fish. The "true" log-weight of an individual fish i is $A_{g,t,l,s} + b\log(l_i) + \varepsilon_{BI,i}$. The expected log-weight of a length l fish, averaged over all strata, years, and months, is $a + b\log(l)$. In Chapter 2 we used model selection to remove unnecessary terms in Eqn. 2.3, and found the main effects could be dropped but all second-order interaction terms were important in Eqn. 3.2 (i.e., M02 in Table 2.1).

The relative condition is the weight of an individual relative to the average weight

of the same size. The log of relative condition is $K_{g,t,l_3,s,i} = A_{g,t,l_3,s} - a + \varepsilon_{BI,i}$. The probability of being less than a critical value, K_{crit}, is

$$Pr(K_{g,t,l_3,s,i} < K_{crit}) = P_{g,t,l_3,s} = \Phi\left(\frac{K_{crit} - A_{g,t,l_3,s} + a}{\sigma_{BI}}\right), \tag{3.3}$$

where $\Phi(z)$ is the cumulative distribution function of a standard normal random variable. The probability of critical condition can be estimated,

$$\hat{P}_{g,t,l_3,s} = \Phi\left(\frac{K_{crit} - \hat{A}_{g,t,l_3,s} + \hat{a}}{\hat{\sigma}_{BI}}\right). \tag{3.4}$$

I used a residual-based $K_{crit} = 0.18$, which was also used by Regular et al. (2022) for Northern cod starvation mortality. Hence, the survival probability for the entire year is

$$P_{g,t,l_3} = Pr\left(K_{g,t,l_3,s,i} > K_{crit},\ s = 1..., 12\right) = \prod_{s=1}^{12}(1 - P_{g,t,l_3,s}). \tag{3.5}$$

If $M_{K,g,t,l_3,s}$ is the monthly mortality rate due to poor condition, defined via the survival probability, $\exp\left(-M_{K,g,t,l_3,s}\right)$, then

$$M_{K,g,t,l_3,s} = -log(1 - P_{g,t,l_3,s}) \tag{3.6}$$

and the annual total is

$$M_{K,g,t,l_3} = \sum_{s=1}^{12} M_{K,g,t,l_3,s}. \tag{3.7}$$

Thus, M_{K,g,t,l_3} can be estimated using Eqn. (3.7).

M_{K,g,t,l_3} is the annual mortality rate due to poor condition for a length l fish in stratum g and year t. For stock assessment that needs to be aggregated for the entire stock. Ideally this should be a strata abundance (i.e., number-at-length, N_{g,t,l_3}) weighted average, and to estimate the stock level M_K, the N_{g,t,l_3} should be estimated. While

it is possible to use average survey catch-at-length and assume it is proportional to $N_{g,t,l}$, not all strata are sampled each year. A spatiotemporal model can be developed for survey catches to estimate spatial abundance-at-length for all strata, but this is beyond the scope of this thesis. Hence, for simplicity, I assumed a spatially homogeneous stock distribution to facilitate aggregation using stratum areas (S_g). I consider this assumption further in the discussion. Hence, Eqn. (3.8) is used to estimate length-based condition mortality rates each year,

$$\hat{M}_{K,t,l_3} = \frac{\sum_{g=1}^{G} S_g \hat{M}_{K,g,t,l_3}}{\sum_{g=1}^{G} S_g} \tag{3.8}$$

Alternatively, the survival probabilities P_{g,t,l_3} can be aggregated using the same procedure used in Eqn. (3.8). Thus, the stratum-average survival probability can be obtained using,

$$\hat{P}_{t,l_3} = \frac{\sum_{g=1}^{G} S_g \hat{P}_{g,t,l_3}}{\sum_{g=1}^{G} S_g}, \tag{3.9}$$

and therefore, the length-specific annual mortality rates can also be calculated as

$$\hat{M}^{*}_{K,t,l_3} = -log(1 - \hat{P}_{t,l_3}). \tag{3.10}$$

This can be used as an alternative method to calculate M_K's. I calculated the M_K's using both methods and compared the results from both methods to examine the sensitivity for deriving the final M_K values for SGB cod.

3.4 Results

3.4.1 Estimates of starvation mortality index (M_K)

Estimates of annual condition $\hat{M}_{K,t,l_3}$ by length-bin (Figure 3.1) were aggregated over months using Eqn. (3.7), and then aggregated over strata using Eqn. (3.8). The latter step is justified by the low spatial variation in condition (i.e., Figure 2.10). The values of $\hat{M}_{K,t,l}$ ranged between 0.01 and 0.96, and the overall mean M_K over length and years was 0.2. M_K was elevated in 1991–1993 and 2016, particularly for cod between 55 and 80 cm. For example, in 1991, the M_K was 0.96 at size class 64 cm. M_K was also high in 1991–1995 for cod larger than 120 cm. However, cod of these sizes are relatively rare. Time-series of M_K for each length bin, including confidence intervals, are shown in Figure 3.2. I compared these M_K values to the values calculated using the alternative method (i.e., using equations 3.9 and 3.10). Notably, the M_K values calculated via the first method were almost identical to those obtained through the alternative method (see Figures 3.3 and 3.4).

3.5 Discussion

The spatiotemporal condition model was used to estimate a starvation mortality index (i.e., M_K) by year, spatial strata, length, and month (i.e., season), for cod on the SGB. It was assumed that the death of a cod due to starvation occurs within a month (30 days) of critically poor condition, following the same assumption made by Regular et al. (2022) for indexing starvation mortality of Northern cod. The primary conclusions drawn from this analysis are: M_K is 1) higher in the spring than the fall, 2) higher for cod between 55 and 80 cm, and cod greater than 120 cm, and 3) higher during 1991–1993 when the stock experienced a significant decline, but was also high in 2016.

Cod between 55–80 cm feed on forage fish such as capelin and sand lance more than smaller cod that are too small to prey on these forage fish, or very large cod that can feed on many fish species in additional to forage fish. Later in this chapter, I describe how temporal changes in the abundance of forage fish may have influenced M for cod between 55–80 cm.

Total mortality (Z) in exploited fish stocks is the sum of natural mortality (M) and fishing mortality (F): $Z = M + F$. Therefore, the accuracy of estimating fishing mortality (F) depends on obtaining precise estimates of natural mortality (M) (e.g., Höffle and Planque, 2023). While M is one of the most crucial parameters for fish stock assessment models, its estimation is challenging. More often M is simply assumed to be 0.2 or some value considered to be appropriate for the species. However, recent advancements have introduced both direct and indirect methods for estimating M (Hamel et al., 2023). Direct estimation of M is possible using tag-recapture experiments, but it is limited by the high cost of tagging programs (Höffle and Planque, 2023). Therefore, indirect methods are often used to estimate M. The spatiotemporal model I developed was used to derive length-specific M_K for SGB cod. This may offer a promising alternative to direct estimation methods.

As detailed in Section 3.3.1, I tested two methods to calculate final M_K index. However, results indicated that there was no significant difference among the M_K values calculated using both methods. Therefore, either of the two methods is valid for calculating the final M_K values. Figure 3.1 is based on the first method (i.e., Eqn.'s 3.7) and 3.8). Similar to the recommendation in Chapter 2, an improvement for future research will be to use a stock density-weighted average to aggregate spatial M estimates for the whole stock, rather than the area-weighted average that I used in this thesis. I did not have spatial density-at-length estimates available for my research.

Starvation can be directly impacted by a lack or limited accesses to food, which

causes body mass to reduce due to utilization of available energy reserves (Bar, 2014; Regular et al., 2022). For Northern cod, Regular et al. (2022) found that variations in starvation-induced mortality correlate with the relative biomass of key prey species, capelin and shrimp. Sand lance (*Ammodytes dubius*) and capelin (*Mallotus villosus*) are considered significant prey items for cod on the Grand Bank (Lilly and Fleming, 1981). The relative importance of these forage species has likely varied through time, however, results from the spring bottom-trawl surveys in this area between 1984 and 1986 showed that sand lance's contribution for cod diet was rather significant compared to capelin (Lilly and Meron, 1986). The high abundance of sand lance during this period may have contributed to the low estimates of M_K (see Figure 3.1). This period was, however, followed by a collapse of the cod stock in the early 1990s, which aligns with an increase in the estimates of M_K. This coincides with the disappearance of the Southeast Shoal (see Figure 2.1) stock of capelin (Fomin, 2021) and a broader collapse of the demersal fish community (Pedersen et al., 2017). While it is unknown whether the sand lance population collapsed alongside the rest of the community, capelin have not shown any signs of recovery (Fomin, 2021) and a novel diet-based model indicates that the sand lance population has oscillated without increase since 1995 (Robertson et al., 2022). Interestingly, periods when sand lance estimates were above average (see Figure 9 in Robertson et al., 2022) roughly correspond to local minima of M_K estimates (1998, $\sim$ 2005, $\sim$ 2011). If these patterns are more than correlations, results suggest that a lack of sustained growth in the local forage fish populations may be hampering the recovery of SGB cod.

The dependence of SGB cod on sand lance and/or capelin may have also varied with size, location, and season. For instance, Lilly and Fleming (1981) reported that cod between 35–90 cm in length mainly feed on capelin in the Avalon channel, while sand lance was the dominant prey for cod between 50–69 cm length in the Eastern Grand Bank. Thus, this may contribute to variability in condition over time and space with respect

to prey abundance. Changes in the condition of Northern cod have been observed over time corresponding to the trends in capelin availability (Rose and O'Driscoll, 2002; Morgan et al., 2018; Regular et al., 2022). This could be a reason for the spatial and temporal (including seasonal) variability of condition, which is observed for 3NO cod (see Figures 2.4, 2.2, 2.5, and 2.7).

Physiological impacts due to environmental changes (e.g., water temperature) can also influence fish condition and growth (Portner and Knust, 2007). For instance, reduced condition was reported for Atlantic cod when the bottom temperature decreased (Krohn et al., 1997; Sandeman et al., 2008). Cadigan et al. (2022b) suggested that the productivity of the ecosystem, reflected by the availability of prey, can be affected by environmental phenomena. For instance, based on the observations on stomach fullness of Atlantic cod in eastern Grand Bank, Lilly and Fleming (1981) reported that sand lance predation in 1967 was even higher in the length range of 50–69 cm compared to 1966, that presumably reflected the fluctuation of sand lance abundance due to the effect of Labrador current in those years. Therefore, this may ultimately impact on cod diet, and hence the cod condition. Cod are highly mobile fish and likely seek optimal temperatures within smaller geographic regions. Moreover, while temperature is a crucial factor, other environmental variables, such as prey availability, habitat characteristics, and oceanographic conditions, could also play a significant role in shaping cod distribution. If these factors are relatively consistent across spatial regions, they might mask the potential influence of temperature on distribution. These could be possible reasons why we did not observe significant spatial differences in condition.

Condition is found to be an important metric which influences or correlates with a number of life parameters. It is linked with energetic processes, and potentially provide significant information about the productivity and the reproductive potential of stock (Pardoe et al., 2008). Moreover, as previously mentioned in Chapter 1, poor condition may result in increased rates of natural mortality through greater vulnerability

to disease, predation, and reduced capability to catch mobile prey (Dutil et al., 1999; Dutil and Lambert, 2000; Rose and O'Driscoll, 2002; Dutil et al., 2006). Thus, patterns generated by length as a function of gutted-weight provided the basis for estimating a component of natural mortality index (i.e., starvation mortality index). Therefore, this index can be used in stock assessment, along the lines of Casini et al. (2016). Cadigan et al. (2022a) have proposed an age-based state-space stock assessment model for 3NO cod. Thus, the next step is to investigate how to integrate these length-based estimates of M_K into that age-based assessment model. This is investigated and reported in Chapter 4 and 5, respectively.

3.6 Figures

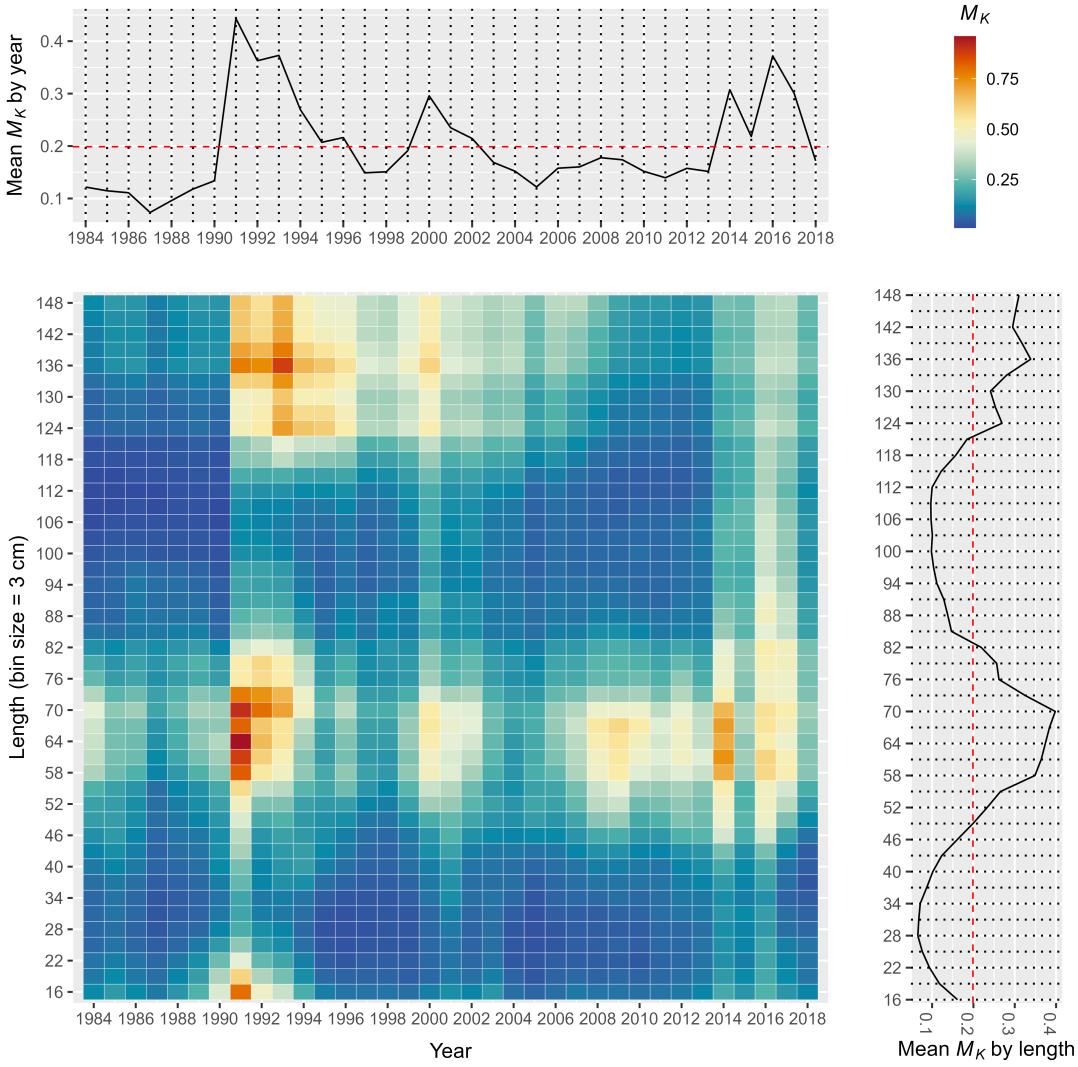

Figure 3.1: Starvation mortality index (i.e., M_K) for each year and length (bin size = 3 cm). M_K was averaged across strata. Colors indicate the magnitude of M_K as indicated in the top right-hand legend. Raw average M_K over years and lengths is annotated as marginal summaries at the top and right, respectively. Dashed lines in the marginal plots indicate the series average.

Figure 3.2: Length bin-wise (bin size = 3 cm; panels) variability of M_K index. The red dashed lines indicate the mean M_K index. Shaded regions indicate 95% confidence intervals.

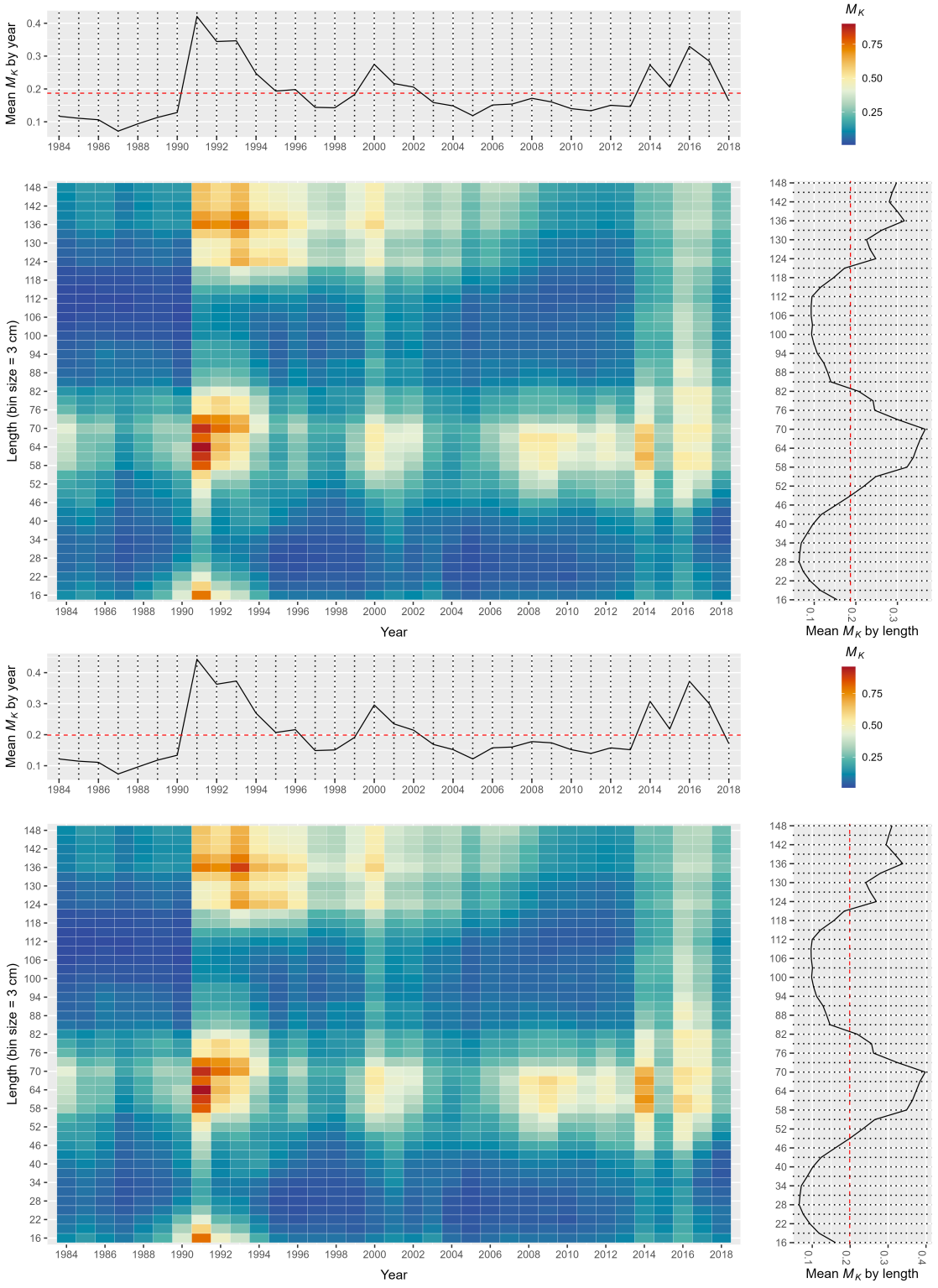

Figure 3.3: Comparison for M_K values calculated from two methods. The top panel shows the M_K values calculated using the second method (see Eqn. 3.10), and the bottom panel shows the M_K values calculated using the first method (see Eqn. 3.8)

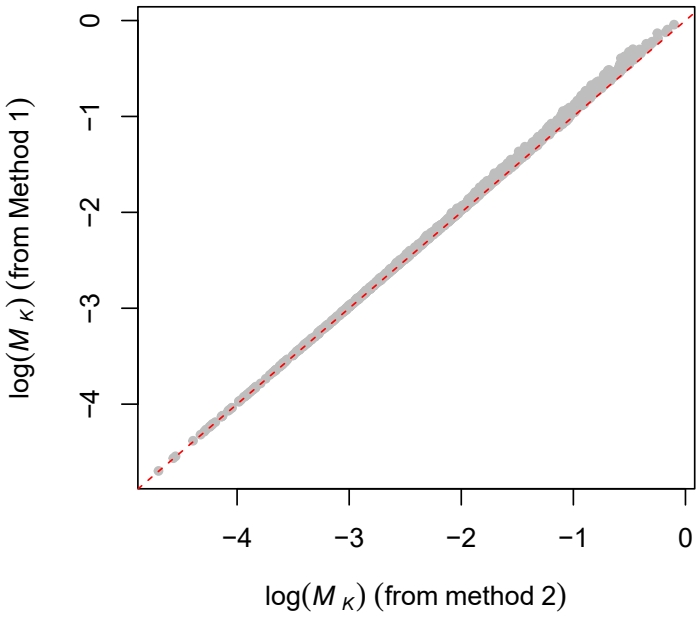

Figure 3.4: Representation for $\log(M_K)$ values, the second method vs. first method. Grey colour points represent M_K values, and red dashed line indicates the regression line.

Chapter 4

A Stochastic Growth Model to Estimate an Age-based Starvation Mortality Index from the Length-based Index, to Include in Age-based State-space Stock Assessment Model (SSAM)

The purpose of this chapter is to outline a methodology for converting the length-based starvation mortality index, which I refer to as $M_{KI,l,y}$, derived in Chapter 3, into an age-based index, which I denote as $M_{KI,a,y}$.

4.1 Introduction

Direct inclusion of a length-based mortality index in an age-based State-space Stock Assessment Model (SSAM) is not possible. Therefore, an appropriate methodology is required to convert the length-based starvation mortality index (i.e., $M_{KI,l,y}$) derived in Chapter 3 into an age-based starvation mortality index (i.e., $M_{KI,a,y}$). These age-based values will then be incorporated into a SSAM in Chapter 5.

The process of converting length-based starvation mortality index into an age-based

starvation mortality index involves two key steps:

1. Growth model: create a stochastic growth model to estimate the probability distribution of length at each age.

2. Calculate $M_{KI,a,y}$: use the estimated distribution of length at each age to convert $M_{K,l,y}$ into $M_{KI,a,y}$.

I use a stochastic growth model based on the mixed-effects growth model developed by Cadigan and Rideout (2022) for 3NO cod. Their model for mean length at age a in year y ($\bar{L}_{ay}$) is

$$\log\left(\bar{L}_{ay}\right) = \beta_a + \delta_y + \delta_c + \delta_{ay} + \varepsilon_{ay} = \mu_{ay} + \varepsilon_{ay}, \tag{4.1}$$

where $\mu_{a,y} = E\left\{\log\left(\bar{L}_{ay}\right)\right\} = \beta_a + \delta_y + \delta_c + \delta_{a,y}$. The log-length model is a linear function of an age-effect (β_a), a year-effect (δ_y), a cohort-effect (δ_c), an age-year interaction (δ_{ay}), and a measurement error term (ε_{ay}). I customize this model appropriately to estimate the length-at-age values and utilize it to calculate an age-based starvation mortality index. The methodology and the associated assumptions are detailed in Section 4.2.

4.2 Methods

4.2.1 Data

The "Rstrap" (Healey et al., 2020, an R package specifically developed for the analysis of observations obtained from DFO multi-species surveys) version 1.14 (Date: 2020–08–05) was used to extract fall and spring survey data for the years 1984–2018. The extracted data includes age and mean length-at-age (in cm) observations, along with the corresponding survey year (see Figure 4.1), number of age-length measurements,

the survey (i.e., either Campelen or Engel), and the season (i.e., either fall or spring). These data were utilized to fit a growth model using TMB.

4.2.2 Growth model

In the log length model $\log\left(\bar{L}_{ay}\right) = \beta_a + \delta_y + \delta_c + \delta_{ay} + \varepsilon_{ay} = \mu_{ay} + \varepsilon_{ay}$, β_a age-effects were modeled to increase monotonically with age, as described in Cadigan and Rideout (2022). The random effects, δ_y and δ_c, were assumed to have mean zero Gaussian distributions with AR(1) time-series covariances (Eqn.'s 4.2 and 4.3).

$$\delta_y = \varphi_{\mathcal{Y}}\delta_{y-1} + \varepsilon_y \quad \delta_y \sim AR(1)\ (0, \sigma_{\mathcal{Y}}) \tag{4.2}$$

$$\delta_c = \varphi_{\mathcal{C}}\delta_{c-1} + \varepsilon_c \quad \delta_c \sim AR(1)\ (0, \sigma_{\mathcal{C}}), \tag{4.3}$$

where $\varphi_{\mathcal{Y}}$ and $\varphi_{\mathcal{C}}$ are autocorrelation parameters, and ε_y and ε_c are residual error terms. The δ_{ay} are also Gaussian random effects with separable AR(1) correlation by age and year with autocorrelation parameters, $\varphi_{\mathcal{A}^*\mathcal{Y}}$ and $\varphi_{\mathcal{A}\mathcal{Y}^*}$, and a residual error term ε_{ay} (see Eqn.'s 4.4.

$$\delta_{a,y} - \varphi_{\mathcal{A}^*\mathcal{Y}}\delta_{a-1,y} = \varphi_{\mathcal{A}\mathcal{Y}^*}(\delta_{a,y-1} - \varphi_{\mathcal{A}^*\mathcal{Y}}\delta_{a-1,y-1}) + \varepsilon_{ay} \tag{4.4}$$

Cadigan and Rideout (2022) simply assumed that the standard deviation $SD\left\{\log\left(L_{ay}\right)\right\}$ is constant, which implies that the coefficient of variation (CV) of L_{ay} is constant. However, residuals analyses in Cadigan and Rideout (2022) suggested that the CV was not constant. To produce a better model of the distribution of size-at-age, I assumed that

$$\sigma_{ay} = SD\left\{\log\left(L_{ay}\right)\right\} = \exp\left(\tau_0 - \tau_1\mu_{ay}\right), \tag{4.5}$$

where τ_0 and τ_1 are parameters to estimate. If $\tau_1 > 0$ then σ_{ay} is a decreasing function of μ_{ay}, and σ_{ay} will also be a decreasing function of a if μ_{ay} is an increasing function of a, which will usually be the case. Of course if $\tau_1 = 0$ then Eqn. (4.5) is the same assumption as used by Cadigan and Rideout (2022).

Modeling individual growth data is complicated for many reasons (e.g., see Zheng et al., 2020a), but an important reason is that the DFO surveys use length-stratified age sampling, which produces a biased sample of length and age from the survey catches. For simplicity I only analyzed the bias-corrected mean length-at-age estimates ($\bar{L}_{ay}$; e.g., Echave et al., 2012) and sample sizes (i.e., $n_{a,y}$) provided by Rstrap. If the age samples were randomly selected from all catches then $SD\left\{\log\left(\bar{L}_{ay}\right)\right\} \approx \sigma_{ay}/n_{a,y}^{1/2}$. However, it is unlikely that these samples are completely random, so I introduced a parameter $\phi \leq 1$ to model the effective sample size. Finally, I approximated the standard deviation of the estimates of the log of mean length-at-age ($\bar{L}_a$) using

$$SD\left\{\log\left(\bar{L}_{ay}\right)\right\} = \sigma_{ay}/n_{ay}^{\phi/2}, \tag{4.6}$$

where σ_{ay} is based on Eqn. 4.5.

In Chapter 3, the length-based starvation mortality index was estimated using 3 cm length bins, with mid-points ranging from 16, 19, ..., 148 cm, a total of 45 length bins. I denote these bins as $B_{16}, B_{19}, ..., B_{148}$, with lower and upper limits $B_{l,lo} = l - 1.5$ and $B_{l,hi} = l + 1.5$, $l = 16, 18, ..., 148$. To convert $M_{KI,l,y}$ to $M_{KI,a,y}$, the probability that an age a fish is in each length bin, $P_{l|ay} = Prob(L_{ay} \in B_l)$, for $l = 16, 19, ..., 148$ was calculated for each year. Note that $P_{l|ay}$ is also equal to $Prob\left\{\log(L_{ay}) \in \log(B_l)\right\}$.

Defining $z_{lay,lo} = \{\log(B_{l,lo}) - \mu_{ay}\}/\sigma_{ay}$ and $z_{lay,hi} = \{\log(B_{l,hi}) - \mu_{ay}\}/\sigma_{ay}$, then

$$P_{l|ay} = \begin{cases} \Phi(z_{lay,hi}), & l = 16, \\ \Phi(z_{lay,hi}) - \Phi(z_{lay,lo}), & 19 \leq l \leq 145,\ y = 1, ..., Y, \\ 1 - \Phi(z_{lay,lo}), & l = 148, \end{cases} \tag{4.7}$$

where $\Phi(x)$ is the cumulative distribution function of a standard normal random variable. Eqn. (4.7) defines the stochastic growth model I use. Note that the growth model in (Cadigan and Rideout, 2022, i.e., Eqn. 4.1) only had age-effects, with fractional ages for the spring and fall surveys. Some interpolation is required to use this model to predict size at other times of the year. However, I used length-at-age in the spring for μ_{ay} when computing $P_{l|ay}$ because I use this to combine starvation mortality estimates, and in chapter 2 I demonstrated that this mostly represented mortality in the spring.

4.2.3 Calculate age-based starvation mortality index

I used the following equation to convert the length-based starvation mortality index ($M_{KI,l,y}$) to an age-based starvation mortality index ($M_{KI,a,y}$),

$$M_{KI,a,y} = \sum_{l=16}^{148} M_{KI,l,y} \times P_{l|ay}. \tag{4.8}$$

For each age, $M_{KI,a,y}$ is a weighted average of $M_{KI,16,y}, M_{KI,19,y}, ..., M_{KI,148,y}$ since $\sum_{l=16}^{148} P_{l|ay} = 1$. I used ages from 1 to 23 to convert the length-based starvation mortality indices; however, the SSAM has a plus group at age 10. I used a steady-state age distribution approximation similar to Cadigan and Rideout (2022) to average the starvation mortality indices at ages 10–23, to match the plus group at age 10 in the

SSAM. The steady-state age distribution is based on a total mortality rate $Z = 0.4$.

$$\bar{M}_{KI,10+,y} = \frac{\sum_{i=0}^{13} M_{KI,i+10,y} \exp(-0.4i)}{\sum_{i=0}^{13} \exp(-0.4i)}. \tag{4.9}$$

In Chapter 3, the M_{KI} values were derived using the data from 1984–2018. Thus, the age-converted starvation mortality rates ($M_{KI,a,y}$'s) were also estimated for that specific period. However, the SGB cod SSAM model years are from 1959–2020. Therefore, I used the average M_{KI}'s at each age during 2016–2018 for the values in 2019–2020. To fill in values for the years 1959–1983, I used the averages from 1984–1988. These are the values to be used in the SSAM described in Section 5.3.2).

4.3 Results

4.3.1 Model effects

Estimates of the effects in Eqn. (4.1) are illustrated in Figures 4.2 and 4.3. As expected, the age effects emerge as the most significant source of variability in these growth data. Cohort effects are more prominent than year effects and the age × year interaction effects. While Figure 4.3 does not provide the size of the effects, the lower values of $\sigma_{\mathcal{AY}}$ and $\sigma_{\mathcal{Y}}$ compared to $\sigma_{\mathcal{C}}$ in Table 4.1 indicate that the predicted values for both the δ_{ay}'s and the δ_y's are usually smaller than those for δ_c's. The τ_1 parameter is significantly greater than zero, suggesting that variation in length-at-age does not exhibit a constant CV. This declines rapidly as a function of mean length (see Figure 4.4). The estimate of ϕ is approximately exp(-0.44) $\approx$ 0.64, which indicates that the effective age sample sizes are substantially less than the number of samples, especially when the number of samples is large.

4.3.2 Length-at-age estimates

The model fit the sampled average lengths well (Figure 4.5), specifically at the ages 2–7 when sample sizes were higher (see Figures 4.1 and C.3). However, even at these ages, there were occasional years with anomalous means that the model could not fit accurately. Notably, there were no patterns in the model residuals (Figure 4.6). Although the average absolute residual is usually less than 1.0, indicating potential over-estimation of the variance of length-at-age, there is no trend with age or the mean. This is an improvement compared to the weight-at-age model presented by Cadigan and Rideout (2022), where the variation decreased with age.

4.3.3 Age-based starvation mortality index ($M_{KI,a,y}$)

The values of $M_{KI,a,y}$ are illustrated in Figure 4.7. The $M_{KI,a,y}$ estimates ranged between 0.03 and 0.74. They were elevated in 1991–1993, but also high in 2014 and 2016–17. Notably, these higher values were consistently observed at ages 6–8 years. Interestingly, the mean $M_{KI,a,y}$ across age and years remained close to 0.2 (i.e., $\bar{M}_{KI,a,y}$ = 0.18).

4.4 Discussion

I customized the mixed-effects growth model developed by Cadigan and Rideout (2022) for the purpose of estimating the distribution of length-at-age for SGB cod. The methodology I used to model the variance of length-at-age differs from the model in Cadigan and Rideout (2022). They simply assumed the standard deviation $SD\left\{log\left(L_{ay}\right)\right\}$ is constant, which implies that the coefficient of variation (CV) of L_{ay} is constant. This is a common assumption in growth studies (e.g., Perreault et al., 2020). However, Figure 8 in Cadigan and Rideout (2022) indicated that the variance decreased with age.

In preliminary analyses I found the same result for SGB cod. Therefore, I focused on this during the analysis because my objective is to model the distribution of length-at-age, which involves both the mean and variance of length. The focus of Cadigan and Rideout (2022) was only to model the means of the distribution of length-at-age. Using extensive individual growth data for American plaice, Zheng et al. (2020a) also found that the CV was not constant; they found that $SD(L_{ay})$ increased with mean length, and at larger lengths it was a concave function that converged to a constant. This implies that the CV was decreasing function of the mean. This is consistent with the CV of length, and the SD of log-length, decreasing with age, which was the pattern for SGB cod in our preliminary analyses. Hence, I modelled the $SD(L_{ay})$ as presented in Eqn.'s 4.5 and 4.6.

Use of Von Bertalanffy (VonB) growth model with modifications often involves mathematical assumptions about the body growth of fish (e.g., Cadigan, 2016; Cadigan and Konrad, 2016) but the mixed models do not. Fitting raw data from length-stratified age samples (LSAS) to the VonB growth model is also often complicated because the sampling design has to be accounted for (e.g., see Perreault et al., 2020), but the realized sampling design can be complex and change annually and by NAFO Divisions. Note that LSAS's are a biased sample of the population distribution of length-at-age, and not accounting for the sampling design will produce biased estimates of mean length-at-age and VonB parameters. Therefore, in stock assessment a bias-corrected mean length-at-age (BCLA's) are estimated (e.g., Perreault et al., 2020). This estimation is commonly performed using

$$\bar{L}_a = \frac{\sum_k N_k \left(n_{a,k}/n_k\right) l_k}{\sum_k N_k \left(n_{a,k}/n_k\right)}, \tag{4.10}$$

where l_k is the midpoint of length bin k, $n_{a,k}$ is the number of age a fish in length bin k, and N_k is the total number of fish sampled in length bin k in the first sampling phase. The R package "Rstrap" has been included with length data in the form of BCLA and I used them to formulate mixed effect model.

The ages of cod in the fall and spring surveys ranged from 0 to 23 years old. However, the number of survivors in the catch or stock at older ages is low (Cadigan, 2023a). I used a plus group of age 10+ for the $M_{KI,a,y}$ calculations (see Eqn. 4.9), to match the plus group age in the SSAM of Cadigan and Rideout (2022). Furthermore, a steady-state-age-distribution approximation based on Z value of 0.4 was assumed for this plus group $M_{KI,a,y}$ calculation, consistent with the value used in Cadigan (2023a) for 3Ps cod. Other values of Z could be assumed; however, reasonable values will not change results substantially. For example, I used $Z = 0.6$ and the age 10+ M's changed within -10% to 15%, and the average change for all years was only 0.06%.

The age-based starvation mortality indices (i.e., $M_{KI,a,y}$) that I calculated here are utilized in Chapter 5 to include in a SSAM.

4.5 Tables

Table 4.1: Estimates (EST) and standard errors (SE) for the covariance parameters of the stochastic growth model (Eqn. 4.1). Variances are marginal, for the equilibrium distribution of the time-series processes. Correlations are lag 1. A * indicates a bounded estimate

Parameter	Link	EST	SE
$\sigma_{\mathcal{Y}}$	log	-3.790	0.290
$\sigma_{\mathcal{C}}$	log	-3.235	0.182
$\sigma_{\mathcal{AY}}$	log	-3.669	0.159
$\varphi_{\mathcal{Y}}$	logit	0.237	1.143
$\varphi_{\mathcal{C}}$	logit	0.301	0.640
$\varphi_{\mathcal{A}^*\mathcal{Y}}$	logit	-10.0^*	-
$\varphi_{\mathcal{AY}^*}$	logit	0.933	0.625
τ_0	identity	0.454	0.272
τ_1	identity	0.620	0.059
ϕ	log	-0.440	0.091

4.6 Figures

Figure 4.1: Mean length-at-age from the fall and spring surveys. Panels are for age. Colors are defined at the top. The bubble centers indicate length and the bubble areas are proportional to sample size. Horizontal lines indicate series averages.

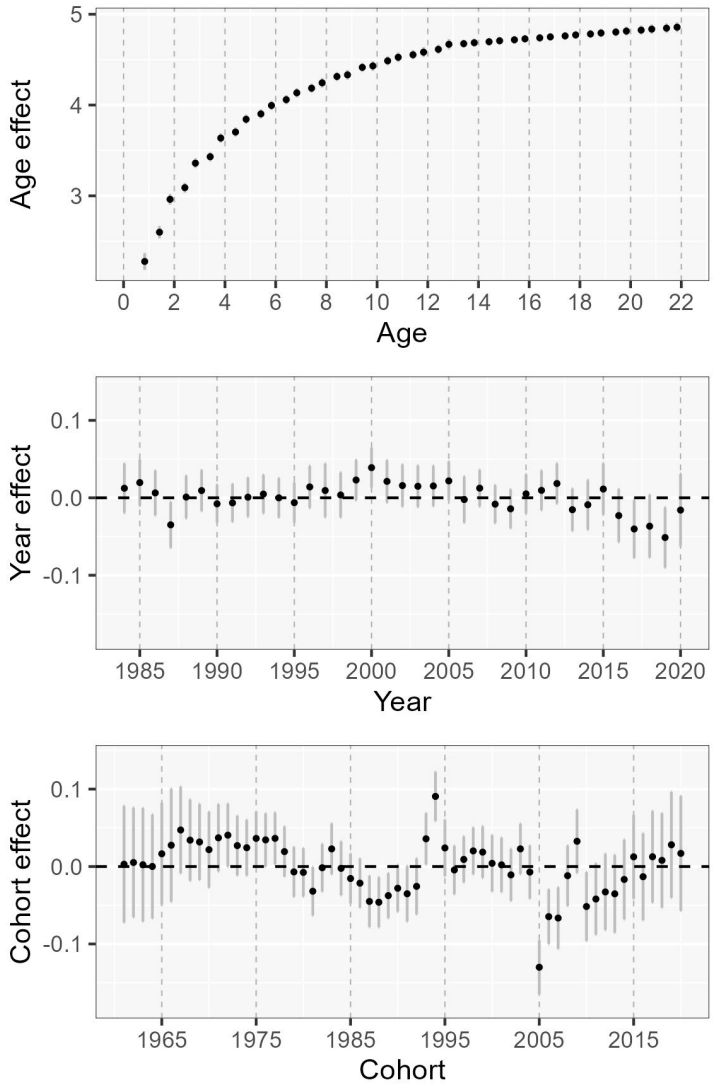

Figure 4.2: Estimates of the main effects in the length-at-age model. Vertical line segments indicate 95% confidence intervals.

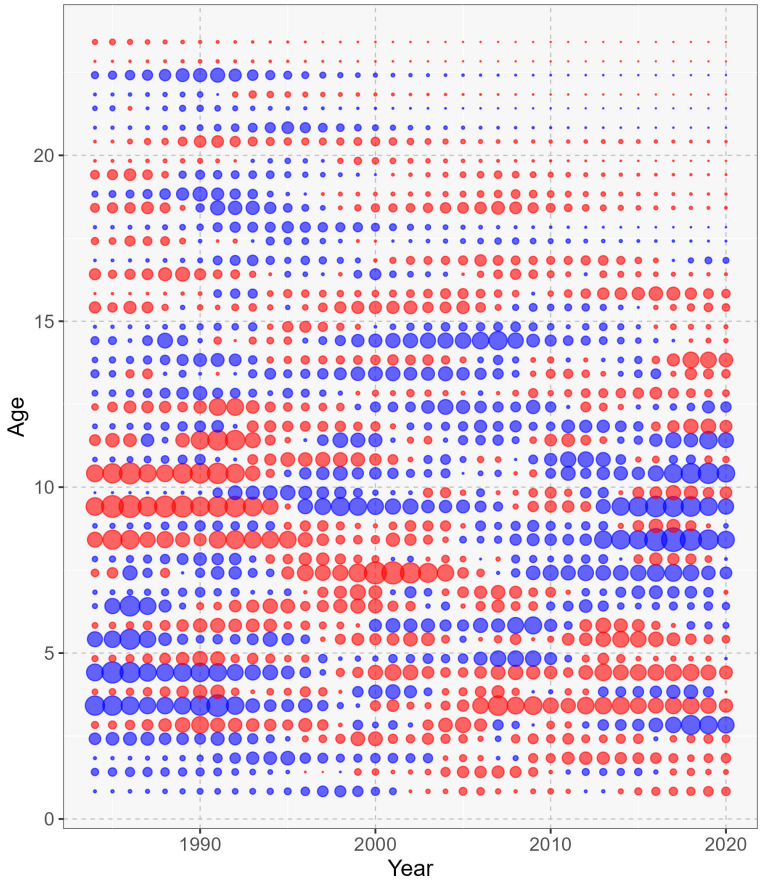

Figure 4.3: Estimates of the age × year interactions effects. The area of the circles indicates the absolute value of the effect, and the color indicates the sign (red +; blue -).

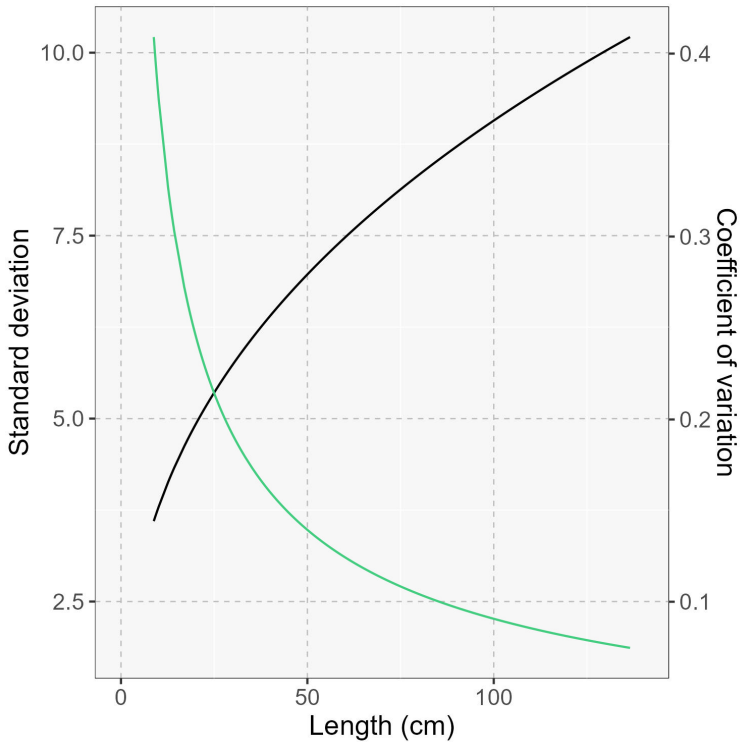

Figure 4.4: Standard deviation (black curve) and coefficient of variation (green) of length as a function of the mean.

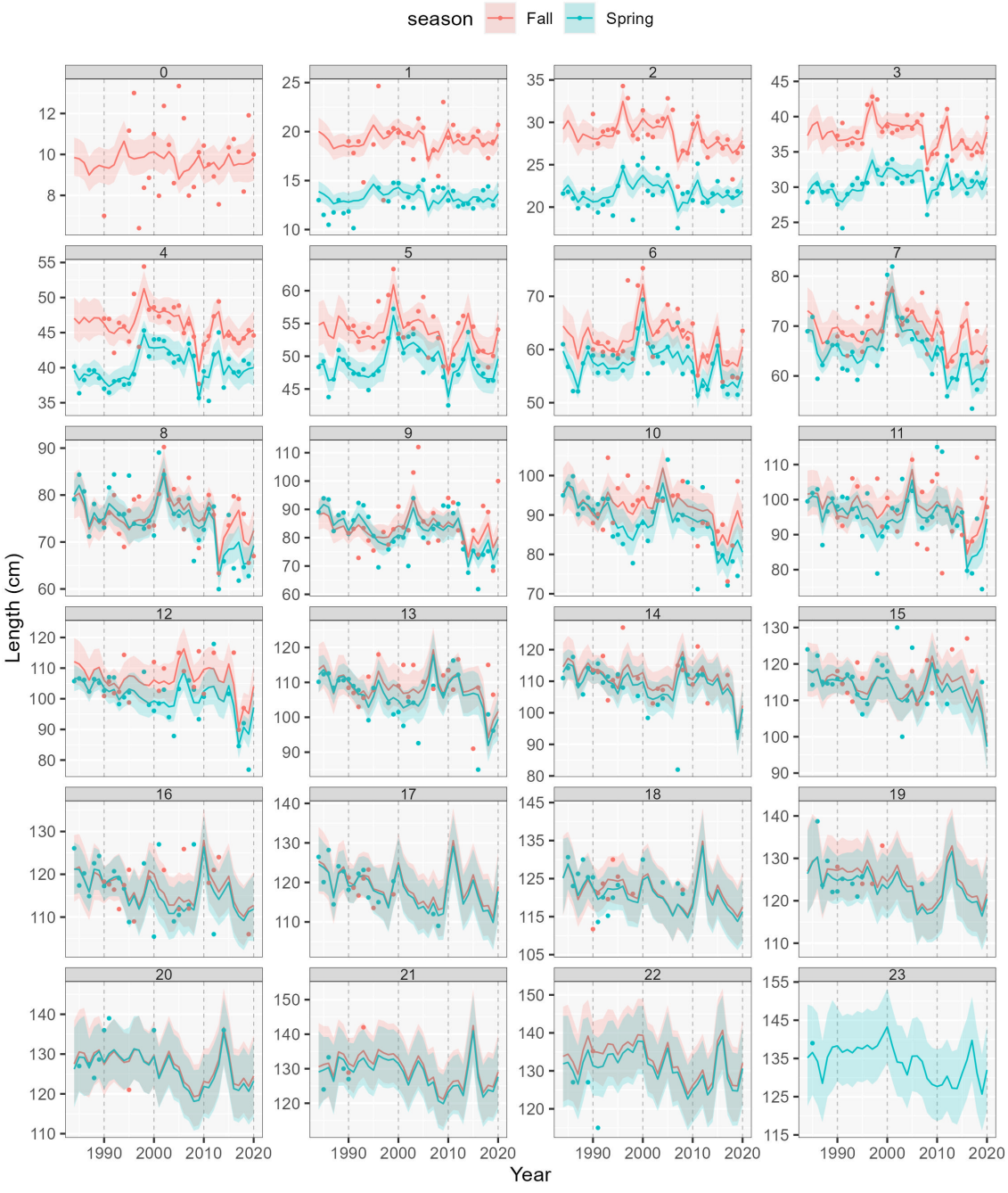

Figure 4.5: Time-series of observed (points) and model-predicted (lines) average length-at-age from Spring (green) and Fall (red) DFO bottom-trawl surveys in NAFO Divisions 3NO. Each panel is for an age class. Shaded regions indicate 95% confidence intervals.

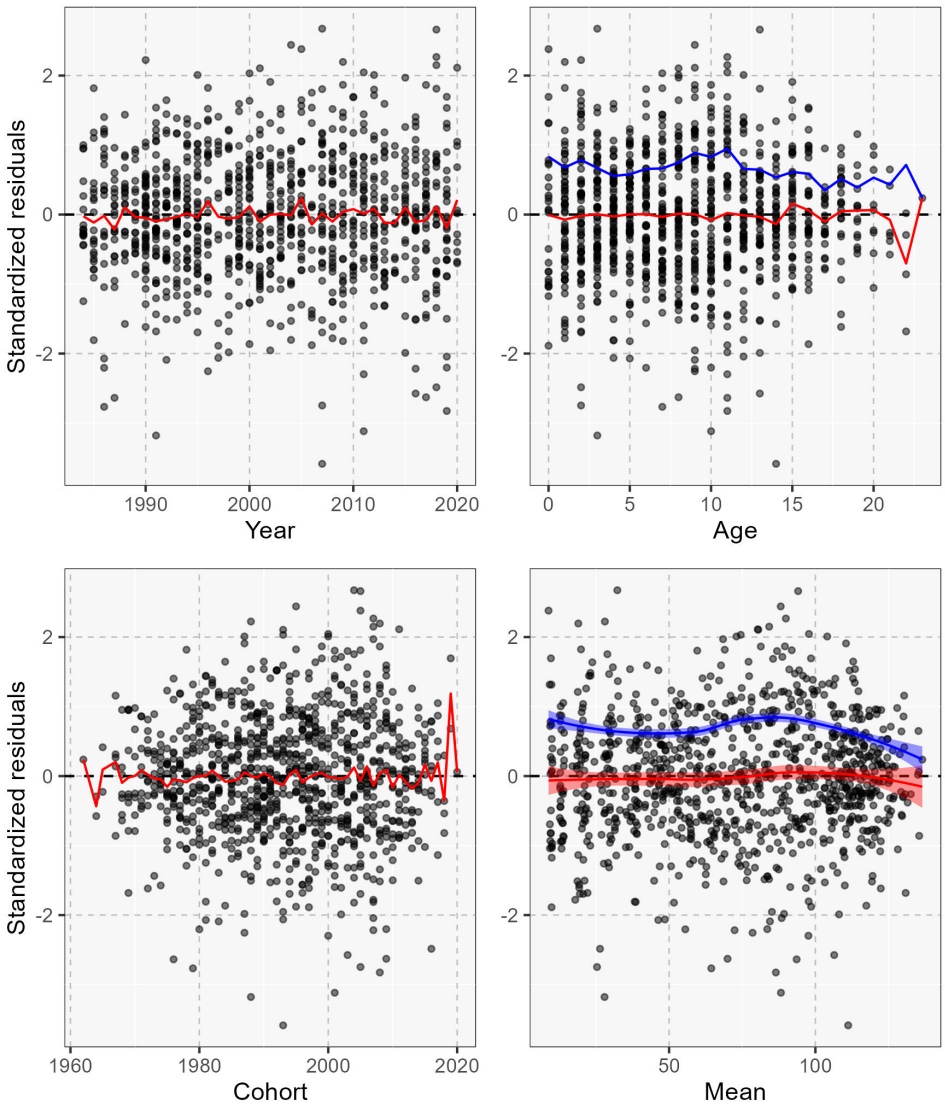

Figure 4.6: Pearson standardized residuals versus year (top left), age (top right), cohort (bottom left) and the mean (bottom right). Red lines indicate the average residual, and the blue line indicates the average absolute residual.

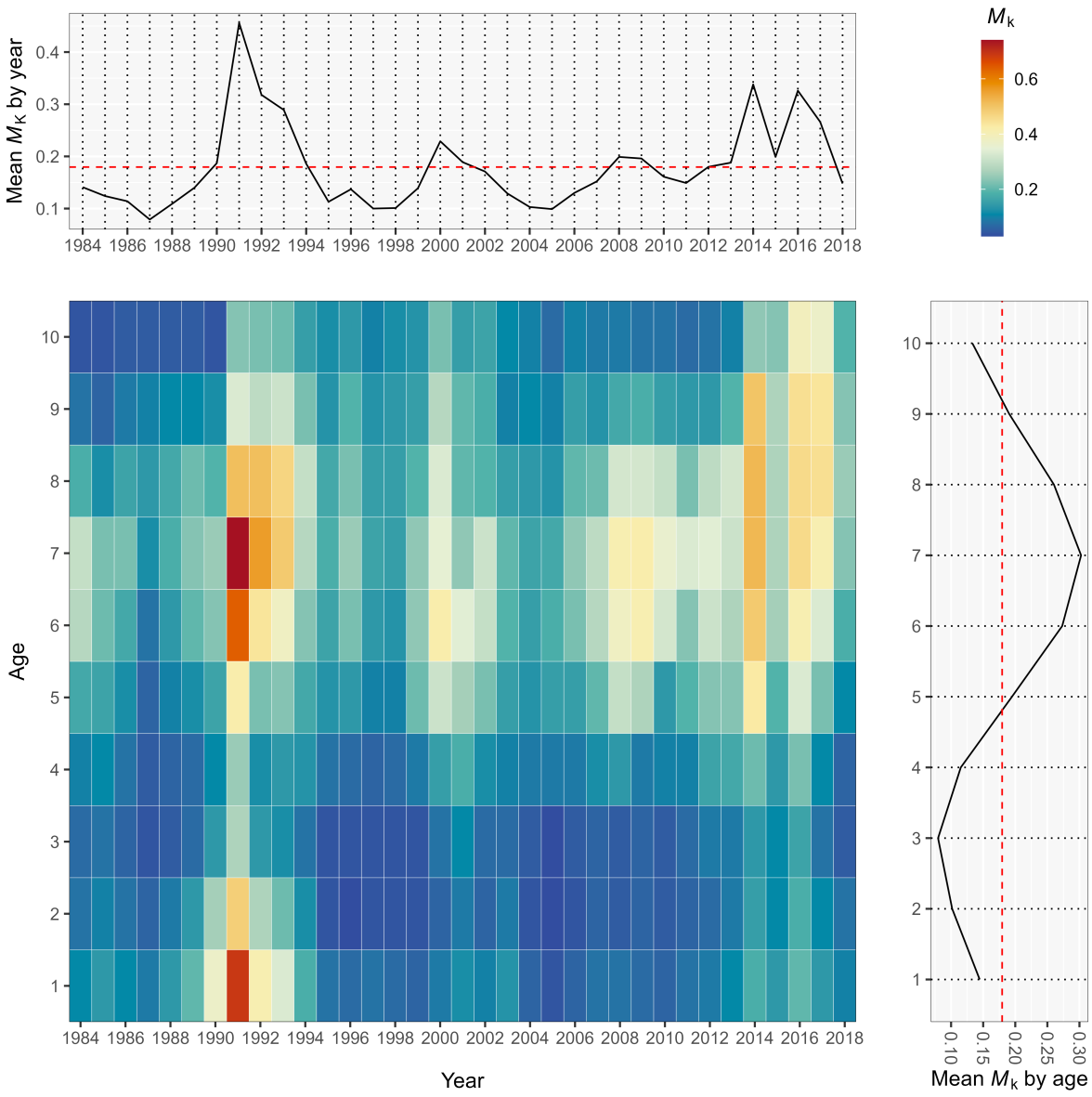

Figure 4.7: Condition mortality (M_{KI}) for each year and age. Colors indicate the magnitude of M_{KI} as indicated in the top right-hand legend. Average M_{KI} over years and ages are indicated at the top and right, respectively. Dashed lines in the marginal plots indicate the series average.

Chapter 5

Integrating an Age-based Starvation Mortality Index into a State-space Stock Assessment Model

The purpose of this chapter is to describe the integration of the age-based starvation mortality index (i.e., $M_{KI,a,y}$) calculated in Chapter 4 into a SSAM for SGB cod. Subsequently, I will compare the assessment results with those obtained from the initial SSAM model formulation of Cadigan et al. (2022a) and the results obtained using the NAFO assessment (*ADAPT*), as discussed in Rideout et al. (2021).

5.1 Rationale

Natural mortality plays a significant role in modern fisheries stock assessment models. However, it is among the most difficult parameters to estimate (Punt et al., 2021a; Hamel et al., 2023). Cadigan et al. (2022a) developed a State-space Stock Assessment Model (SSAM) for 3NO cod, where they treated M's as user-supplied model inputs, although the SSAM involved process errors that can partially account for uncertainty about M values. They used baseline M's derived from body weights (e.g., Lorenzen,

1996),

$$M_{a,y} = M_{B,a,y} = M_0 W_{a,y}^b, \tag{5.1}$$

where $M_{a,y}$ is the natural mortality rate at age a in year y, $W_{a,y}$ is the stock weight-at-age, M_0 is a scaling parameter, and b is an allometric scaling factor. The basic assumption with Eqn. (5.1) is that M's for small fish are larger due to predation effects. Cadigan et al. (2022a) used b = -0.305, which was the value for ocean systems in Lorenzen (1996). This value was also used in Miller and Hyun (2018) and Kumar et al. (2020). The scaling parameter was chosen so that $\min_{a,y} M_{a,y} = 0.15$. Cadigan et al. (2022a) identified these input M's as preliminary estimates. However, stock assessment models are sensitive to input values of M (Clark, 1999; Williams, 2002). For instance, M significantly affects estimates of stock size and productivity, which in turn determines optimal harvest rates (Clark, 1999). Therefore, it is crucial to update an age-based SSAM with improved estimates of M, and subsequently, investigate the changes to assessment model results. This process also provides valuable insights into the significance of including a starvation mortality index in age-based SSAM's as a component of M.

5.2 Research approach

In Chapter 2 I developed a spatiotemporal condition model for SGB cod and utilized it to derive a length-based starvation mortality index in Chapter 3. However, the natural mortality rates in Cadigan et al. (2022a) were estimated similar to Lorenzen (1996), and were age-based. Therefore, I converted the length-based starvation mortality index into an age-based index as described in Chapter 4, to use it in the SSAM of Cadigan et al. (2022a). In this chapter, I use two components of natural morality rates, the

starvation mortality rate and the so called "Lorenzen M", which may be considered as the predation mortality rate, to include in the SSAM and update the results. The SSAM described by Cadigan et al. (2022a) and the procedure to estimate new input M's for the SSAM are described in subsection 5.3.2. The results of the updated model are compared to the initial SSAM results and those obtained by Rideout et al. (2021) using the ADAPTive framework.

5.3 Methods

5.3.1 Data

The assessment period of the 3NO cod SSAM in Cadigan et al. (2022a) is 1959–2020. I used annual fisheries landing estimates and age compositions from 1959–2020, and indices from DFO's surveys in the fall (1990–2020), spring (1984–2019), and EU surveys conducted by Spain during 1997–2019. In addition, I used external estimates of catch weights-at-age, stock weights-at-age, and mature proportions-at-age for the assessment period as inputs for the SSAM. These are the same inputs used in the SSAM described in Cadigan et al. (2022a). The values calculated for age-based starvation morality indices are available from Chapter 4.

5.3.2 State-space stock assessment model

Model definitions, notations and parameters are summarized in Table B.4.

Population dynamics process model

Cadigan et al. (2022a) used the common stochastic cohort population dynamics model for SGB cod, which included a plus group at age $A = 10$,

$$\log(N_{a,y}) = \begin{cases} \log\left(N_{a-1,y-1}\right) - Z_{a-1,y-1} + \delta_{a,y}, & a < A, \\ \log\big\{N_{a-1,y-1}\exp(-Z_{a-1,y-1}) & y = 1, ..., Y, \\ \quad +N_{a,y-1}\exp(-Z_{a-1,y-1})\big\} + \delta_{a,y}, & a = A, \end{cases} \quad (5.2)$$

where $N_{a,y}$ is stock abundance at age a in year y and $Z_{a,y}$ is the total mortality rate, which is the sum of fishing morality ($F_{a,y}$) and natural mortality ($M_{a,y}$) rates; $Z_{a,y} = F_{a,y}+M_{a,y}$. For the first year, $\log(N_{a,y=1})$ were considered unknown and free parameters to estimate. They were modelled as random effects with no distribution. The process errors δ's were assumed to be independent for all ages and years and had a normal distribution with mean zero and variance σ^2_δ.

The recruitment vector $R = (N_{1,1}, ...N_{1,Y})$ was assumed to be a lognormal random vector variable,

$$\log(R) \sim MVN(\mu_R, \Sigma_R) \quad (5.3)$$

where μ_R is a parameter vector. To account for major changes in the level of recruitment over time, three time-blocks with constant μ_R's were selected; 1) $y < 1970$, 2) $1970 \leq y \leq 1991$, and 3) $y > 1991$. Σ_R is the stationary covariance matrix of an AR(1) process defined by μ_R and φ_R. The correlation between $\log(R_i)$ and $\log(R_j)$ is $\varphi_R^{|i-j|}$.

The main difference between my model and the SSAM in Cadigan et al. (2022a) involves how $M_{a,y}$ is treated. Cadigan et al. (2022a) used external assumed values of $M_{a,y}$'s (see Eqn. 5.1). However, I combine these external values with the starvation mortality indices, which is described in the next section.

Natural mortality

I assumed that the M is the sum of two components, a starvation mortality rate M_K, and a remainder term M_R, that will mostly represent the natural mortality rate due to predation of fish that are not in critical condition. That is,

$$M_{a,y} = M_{K,a,y} + M_{R,a,y}. \tag{5.4}$$

I assumed that $M_{R,a,y}$ is proportional to the baseline values (i.e., $M_{B,a,y}$'s in Eqn. 5.1) based on body weights (e.g., Lorenzen, 1996); that is, $M_{R,a,y} = \beta_y \times M_{B,a,y}$. The $M_{B,a,y}$ are shown in (Cadigan et al., 2022a, Fig. 14). They varied little and ranged from 0.6–0.8 at age 2, but ranged less at older ages and were essentially constant over time at ages 5–10+. However, preliminary analyses (i.e., retrospective runs) indicated that time variation in β is important. Thus, I assumed the $\log(\beta_y)$'s follow a Gaussian random walk with mean zero and standard deviation σ_β. I also assumed that $M_{K,a,y}$ is proportional to M_K indices based on critical body condition; that is, $M_{K,a,y} = \eta_a \times M_{KI,a,y}$, where $M_{KI,a,y}$ are the age-based starvation mortality indices. Finally, the total M I include in the extended SGB cod SSAM is

$$M_{a,y} = \eta_a M_{KI,a,y} + \beta_y M_{B,a,y}, \tag{5.5}$$

where $\eta_a, a = 1, ..., A$, and the SD of the β_y's, i.e., σ_β, are scalar parameters to estimate.

Catch equation

The Baranov catch equation,

$$C_{a,y} = N_{a,y} \frac{\{1 - \exp(-Z_{a,y})\} F_{a,y}}{Z_{a,y}}, \tag{5.6}$$

was used to model catches at ages 2 to 10+. The F at age 1 was assumed to be zero, as no catches were reported at this age for SGB cod. Other F's were modeled as a stochastic process about a small number of mean values μ_F, similar to recruitment. Six age-year blocks were used to map μ_F's, to account for shifts in mean F because of the moratorium on fishing that started in 1994, and ages 2 and 3 cod are historically not targeted the same as older and larger sized cod. Hence, there are six μ_F parameters for ages 2, 3, and 4+, each for pre- and post-moratorium. The F deviations at age 2, $\Delta_{F,2,y} = \log(F_{2,y}) - \mu_{F2,y}$, were modelled as independent normal random variables, $\Delta_{F,2,y} \sim N(0, \sigma^2_{F2})$. If $\boldsymbol{F}$ is an $(A-2)Y \times 1$ vector of all $F_{a,y}$'s for ages 3–10+, then

$$\log(\boldsymbol{F}) \sim MVN(\mu_F, \Sigma_F). \tag{5.7}$$

The $\Delta_F = \log(\boldsymbol{F}) - \mu_F$ was modeled as an AR(1) stochastic process in age and year, and the elements of Σ_F were based on

$$Cov\left\{\Delta_{F,a,y}, \Delta_{F,a-j,y-k}\right\} = \sigma^2_{F,3}\varphi^j_{F,age}\varphi^k_{F,yr}; \tag{5.8}$$

$$Corr\left\{\Delta_{F,a,y}, \Delta_{F,a-j,y-k}\right\} = \varphi^j_{F,age}\varphi^k_{F,yr}. \tag{5.9}$$

There was no correlation between F deviations at age 2 and those at ages 3 and older. In the SSAM, the catch-at-age in abundance and biomass were internally calculated, and summed over ages to calculate total catch-weight each year.

The state-space model latent random variables are the stock size (i.e., N's, whose distributions are derived using the δ's in Eqn. 5.2) and fishing mortality rates (i.e., F's). They have probability distributions and likelihood components with a small number of mean and covariance parameters that need to be estimated. Survey and catch data are used to estimate these parameters through observation equations as described below.

Observation equations

Marginal maximum likelihood and the Template Model Builder (TMB; Kristensen et al., 2016) package within R (R Core Team, 2022) was used to estimate the model parameters. This involves 1) modelling the probabilities of the data conditional on the states of N's and F's (i.e., observation equations), and then 2) integrating over all the likely states of N's and F's to get the marginal distribution of the data, which the marginal likelihood is based on. TMB was used to calculate the marginal negative loglikelihood (mnll). The model parameters were estimated using the R function, $nlminb()$. The mnll was derived from a "joint" nll which is the sum of conditional nll's of the data given N and F, and the nll's of N and F. TMB uses the Laplace approximation to integrate the joint nll over the random effects to calculate the mnll. Thus, the conditional nll's of the data are the observation equations.

TMB also provides predictions of random effects and functions of random effects and model parameters, and generalized delta-method "standard errors" for these derived quantities (i.e., model parameters). I generated these "standard errors" for N-weighted annual average F's at ages 4–6 and ages 6–9, among other derived quantities. With respect to the distributions of N and F, the "standard errors" are actually marginal mean squared errors. These marginal mean squared errors provide a more robust basis for inference about the values of N and F, as detailed in Zheng and Cadigan (2021). In some contexts, the marginal mean squared errors are also referred to as prediction standard errors.

Fishery catches

Fishery landings data and estimates of catch age-compositions were modeled separately because they originate from two different data sources (i.e., sampling programs). A censored likelihood approach (e.g., Cadigan, 2015; Van Beveren et al., 2017; Perreault

et al., 2020) was used to address uncertainties and possible bias associated with fishery landings information. The censored likelihood is based on subjective assumptions regarding potential inaccuracies in landings. However, I examined the sensitivity of key assessment outputs to a range of assumptions about these inaccuracies. The reliability of the landings is quantified by lower and upper landings bounds that are inputs to the assessment model. In fact, the SSAM does not directly use 3NO cod landings estimates; it only uses the bounds. Note that using landings bounds via a censored likelihood is very different than a sensitivity analyses with landings bounds as catch options, and the latter is an incomplete way to account for uncertainty in landings.

Let L_y be the true but unknown landings in year y, and $L_{lo,y}$ and $L_{hi,y}$ are the lower and upper bounds (i.e., the data). The conditional censored nll landings observation equation for the SSAM parameters, collected in a vector θ, is

$$nll = \left(\theta | L_{l_o,y}, L_{h_{i,y}}\right) = -\sum_{y=1}^{Y} \log\left[\Phi_N\left\{\frac{\log(L_{h_i,y}) - \log(L_y)}{\sigma_l}\right\} - \Phi_N\left\{\frac{\log(L_{lo,y}) - \log(L_y)}{\sigma_l}\right\}\right], \tag{5.10}$$

where Φ_N is the cumulative distribution function of a standard normal random variable, and σ_l is a parameter that controls the sharpness of the bounds. I set σ_l equal to 0.02 to ensure that the negative log-likelihood (nll) surface is nearly flat within the specified landings bounds and rises steeply outside of those bounds. This keeps the predicted landings within or just outside of the bounds, and otherwise predicted landings will be estimated to be consistent with other data sources.

Prior to 1994, the bounds on landings were assumed to be $L_{lo,y} = 0.9L_{obs,y}$, $L_{hi,y} = 1.5L_{obs,y}$, where $L_{obs,y}$'s are the reported (observed) landings. These were the same bounds used in Cadigan et al. (2022a). Note that they indicated in their report that the upper bound was $L_{hi,y} = 2L_{obs,y}$ prior to 1994, which was a text error and this

was not the model they implemented. The upper bound is too high for historic periods when landings were relatively high; it suggests the potential that large amounts (i.e., hundreds of kt's) of SGB cod could be misreported, which seems unreasonable. Thus, the upper bound $L_{hi,y} = 1.5L_{obs,y}$ seems like a more reasonable value. This was the bound that assessment results reported in Cadigan et al. (2022a) were based on. However, the bounds I assume are only illustrative, I recommend that better bounds should be provided during the NAFO assessment process when more expertise about the various fleets fishing for SGB cod is available. Since 1994 when by-catches have only been about 1 kt on average, Cadigan et al. (2022a) assumed that $L_{lo,y} = L_{obs,y}$, while 3 options were explored for $L_{hi,y\geq 1994}$:

1. M1: $L_{hi,y} = 1.25L_{obs,y}$,
2. M2: $L_{hi,y} = 1.5L_{obs,y}$, and
3. M3: $L_{hi,y} = 2.0L_{obs,y}$.

I also investigate the sensitivity of the model results to these choices for upper bounds on landings since 1994. Cadigan et al. (2022a) found that these choices of landings upper bounds since 1994 had little impact on estimates of SSB or average F values.

The time-series of catch abundance proportion at ages 2,..., 10+ (i.e., the catch age compositions) were modeled using the multiplicative logistic multivariate normal distribution based on the continuation ratio logit (crl) transformation of the proportions described in Cadigan (2015),Perreault et al. (2020), Cadigan et al. (2022a), among others. There are only $A-1$ crl's derived from A catch proportions because catch proportions only contribute $A-1$ independent observations since $\Sigma_{a=1}^{A} P_{a,y} = 1$. The observation equation nll for the vector $X_{o,y}$ of observed crl's in year y was based on

$$X_{oy} = X_y + \varepsilon_{X,y}, \quad \varepsilon_{X,y} \sim MVN(0, \Sigma_X), \tag{5.11}$$

where X_y is the vector of model predicted crl's and Σ_X was assumed to be an AR(1) process, with variance parameter σ_X^2 and correlation φ_X. Thus, the crl errors were assumed AR(1) correlated within years but independent between years.

No catches were reported at age 2 before 1987. Therefore, for that period the crl's were derived from ages 3 to 10+. However, for this time period, the SSAM predicted catches at age 2. Here, the catches were assumed to be missing but not zero. The crl was not defined when other observed catch-at-age proportions are zero (see Cadigan et al., 2022a). These values were replaced with half the minimum non-zero estimated catch.

Survey indices

Let $I_{s,a,y}$ denote the observed age-based abundance index for survey s. Let t be the midpoint of the survey dates which is expressed in a fraction of the year. The model predicted index is

$$E(I_{s,a,y}) = q_{s,a} N_{y,a} \exp(-t_{s,y} Z_{y,a}). \tag{5.12}$$

The $\exp(-t_{s,y} Z_{y,a})$ term projects beginning-of-year abundance to the time of the survey. The $q_{s,a}$'s are catchability parameters to estimate, with possible constraints or blocking among ages. Let

$$\mu_{s,y,a} = \log\{E(I_{s,a,y})\} = \log(q_{s,a}) + \log(N_{y,a}) - t_{s,y} Z_{y,a}. \tag{5.13}$$

The index observation equation is

$$\log(I_{s,a,y}) = \mu_{s,y,a} + \varepsilon_{s,y,a}. \tag{5.14}$$

I assumed the observation errors, $\varepsilon_{s,y,a}$ are independent, and follow a normal distribution with zero mean and variance, $\sigma^2_{s,a,y}$; $\varepsilon_{s,y,a} \sim N(0, \sigma^2_{s,a,y})$. For each survey, the error variances are blocked for all ages and years, but these variances can be split further if residual diagnostics indicate a need for this. Eqn. (5.14) can be used for all survey ages and years, including the plus group age for plus group survey indices. Within-year correlation in errors is common and the SSAM can be easily modified to account for such correlations. A small number of indices (zero's and age 1 prior to 1995) were excluded from estimation, as described by Cadigan et al. (2022a). I assumed survey q's were asymptotic for the fall survey because it covers the whole stock area and the trawl selectivity is expected to be flat-topped.

The EU-Spain survey covers a relatively small part of the total 3NO cod stock area. However, in recent years the majority of the DFO fall survey biomass has been located in the area covered by the EU-Spain survey. This suggests that the fraction of the stock available to this survey may have changed over time. I accommodate potential q-drift for the EU-Spain survey by using a separable q-model,

$$\log(q_{s,a,y}) = \log(q_{s,a}) + \gamma_{s,y}. \tag{5.15}$$

In the Eqn. 5.15 the $\gamma_{s,y}$'s were modelled as a zero mean normal random-walk with variance σ^2_γ. The $q_{s,a}$'s for the EU-Spain survey were treated as fixed-effects parameters to estimate, similar to the other surveys. Hence, the EU-Spain survey q's can change from year-to-year but the ratio of q's for any two years were assumed to be the same for all ages.

5.4 Results

The parameter estimates and fits of the $SSAM_B$ model from Cadigan et al. (2022a) and the new model with starvation M indices and time-varying predation M using Eq. 5.5 (i.e., $SSAM_M$) are shown in Tables 5.2 and 5.3. Overall, the $SSAM_M$ model fit better, as indicated by lower values of both AIC and BIC. This model exhibited a significantly lower cohort process error standard deviation ($\hat{\sigma}_\delta = 0.13$) compared to the $SSAM_B$ model ($\hat{\sigma}_\delta = 0.34$). This suggests that the inclusion of starvation mortality indices and time-varying predation M using Eq. (5.5) explained a substantial portion of the process error in the SGB assessment model. This is also evident in the model predicted process errors illustrated in Figure 5.1. Note that in Eq. (5.5) I included age-specific η parameters; however, in preliminary models I found that they were estimated with high uncertainty, they were not significantly different from each other, and produced high retrospective variability. As a result, I constrained all their values to be the same. The model fit with age-specific η's yielded an AIC value of 3625.02, which was substantially higher than the final model with the same η for each age ($SSAM_M$ AIC value in Table 5.2). In Section 5.4.5 below, I will also examine the retrospective variability of the estimates of the η and γ parameters in Eq. (5.5).

5.4.1 Natural mortality

The estimates of $M_{K,a,y}$, $M_{R,a,y}$, and $M_{a,y}$ ranged from 0.02–0.67, 0.09–2.31, and 0.16–2.47, respectively (Figure 5.2). At young ages (i.e., less than 6) the total M's were mostly due to predation mortality M_R, as expected; however, at ages 6–10+, starvation mortality M_K was approximately the same as M_R since the late 1980's. Note that M was assumed to be 0.2 for all ages in the NAFO $ADAPT$ model. In the $SSAM_B$ model M was modeled as a function of body weights (see Section 5.3.2); they varied with age but varied little over time and were close to 0.2 for ages 7 and older. The annual

variations in M_R are driven primarily by the β_y effects described in Eqn. (5.5) and shown in Figure 5.3, because the baseline values $M_{B,a,y}$ from Cadigan et al. (2022a) did not vary much over time, as described in Section 5.3.2. Figure 5.3 indicates that M_R (i.e., predation mortality) is important at younger ages but that M_K was also important at ages 6 and older. Figure 5.3 indicates several periods of higher predation mortality, during 1985–1989, 1991–1996, 2001–2004, and 2014–2020. Average M_K's at ages 6–10+ exceed 0.2 in 1991–1994, 2000–2002, 2008–2010, 2012–2017, and 2019–2020 (see Figure 4.7 and 5.2). I computed total M relative to the time-series average for each age, and averaged this over ages 1–10+ to give an overall indication of years with relatively high M's. These years were 1987–1989, 1991–1996, 2000–2003, and 2014–2020. M's in these years are substantially higher than the assumed value of 0.2 in the NAFO $ADAPT$ model.

5.4.2 Fishing mortality

The $\bar{F}_{4-6}$ estimates from the SSAMs (Figure 5.4) were lower overall than the $ADAPT$ estimates, which is consistent with the usually higher M's at these ages in the SSAMs. The $SSAM_M$ $\bar{F}_{4-6}$ were substantially lower in some years (i.e., 2005). The $\bar{F}_{6-9}$ estimates from the $SSAM_M$ model were usually lower as well. Since 1995, $\bar{F}_{6-9}$ from $SSAM_B$ were close to the $ADAPT$ estimates. The SSAM $\bar{F}$'s had less inter-annual variability, which is expected because the SSAMs use stochastic models with autocorrelation for F and observation errors for catches, whereas $ADAPT$ is a VPA and fits catches exactly.

5.4.3 Biomass

Prior to 1975, both $SSAM_B$ and $SSAM_M$ estimated substantially higher SSB and total biomass compared to $ADAPT$ (Figure 5.5). This is primarily because the SSAM's

included a plus group whereas the $ADAPT$ did not. However, since about 1995, the estimates from $ADAPT$ and $SSAM_B$ were more similar, while the $SSAM_M$ biomass values were substantially higher during this period. The inclusion of starvation mortality rates ($M_{K,a,y}$) had substantial impacts on SSB and total biomass compared to the $SSAM_B$ results, especially during 1980–1991 for SSB and between 1975–1991 for total biomass.

5.4.4 Recruitment

Recruitment estimates from the SSAMs are substantially different than those from $ADAPT$ (Figure 5.6). This is mostly due to the substantially different M's used by the two models, but also due to the different ages that recruitment represents; that is, age 1 for the SSAMs and age 2 for $ADAPT$. Recruitment estimates are more uncertain prior to the early 1980s when there are no survey indices. The recruitment trends relative to the mean during 1970–1990 are more similar; however, the $SSAM_M$ model does not indicate relatively high recruitment in the 1960's and early 1970's compared to $ADAPT$ and the $SSAM_B$ models. $SSAM_M$ produces much different stock-recruit scatter-plots (see Figure 5.7), including evidence of density-dependence, compared to $ADAPT$ or $SSAM_B$ (see Figures 37–38 in Cadigan et al., 2022a), where density-dependence was unclear. Hence, these models may produce much different management reference points and stock status evaluations. However, further exploration of this is beyond the focus of this thesis.

5.4.5 Retrospective patterns

All the model formulations exhibited some retrospective variability and patterns for SSB (Figure 5.8), average F (Figures 5.9 and 5.10), and recruitment (Figure 5.11). Mohn's rho's (see Table 5.4) for the $SSAM_M$ were usually closer to zero compared

to $ADAPT$ and $SSAM_B$. There were retrospective variation in the estimates of M's (Figure 5.12) caused by retrospective variation in the M parameter estimates $\hat{\eta}$ and $\hat{\gamma}$ (Figure 5.13) in Eqn. (5.5).

5.4.6 Upper catch bound sensitivity runs

The $SSAM_M$ model predicted higher catches since 1994 when the upper catch bound was increased (Figure 5.14). However, similar to Cadigan et al. (2022a), these choices of catch bounds made little difference to F (Figure 5.15) or biomass (Figure 5.16) estimates.

5.5 Discussion

It is widely recognized that M likely varies with the age, sex, and time (Punt et al., 2021a; Cadigan et al., 2022a; Hamel et al., 2023). However, incorporating time-varying M into stock assessment models is still a challenge and is uncommon (Hamel et al., 2023). I estimated time-varying starvation M in the SGB cod SSAM by utilizing the age-based starvation M index estimated in Chapter 4. The SGB cod SSAM proposed by Cadigan et al. (2022a) (i.e., $SSAM_B$) addressed concerns with the stock assessment model used by NAFO. However, Cadigan et al. (2022a) considered the values of M they used as preliminary (i.e., $M_{B,a,y}$), and suggested better values could be used if they were available. This was the purpose of this chapter. I incorporated age-based starvation mortality indices ($M_{KI,a,y}$) into the model (i.e., $SSAM_M$), which led to a reduction in process errors by approximately 62% compared to the assessment model that did not use starvation mortality indices. Moreover, AIC and BIC values indicated that $SSAM_M$ had higher goodness-of-fit compared to $SSAM_B$ (see Table 5.2). I conclude that starvation mortality is an important source of variation in the productivity of

SGB cod stock. Accounting for starvation mortality should improve the reliability of management advice derived from the SSAM.

Time-varying M, if not correctly accounted for in a stock assessment model, is a source of retrospective patterns, among others possible causes such as catch misreporting and changes in survey catchability (e.g., Mohn, 1999; Hurtado-Ferro et al., 2014). While Rideout et al. (2021) did not consider the retrospective patterns of their SGB cod assessment model to be large, the Mohn's rho values for $ADAPT$ F's (Table 5.4) were smaller than the -0.15 rule of thumb value proposed by Hurtado-Ferro et al. (2014) to indicate when a retrospective pattern should be addressed explicitly. Mohn's ρ for our $SSAM_M$ average F at ages 4–6 was close to zero but was -0.09 for ages 6–9, which is still smaller in absolute value than the rule of thumb and better than the $ADAPT$ or $SSAM_B$ models. The upper bound rule of thumb in Hurtado-Ferro et al. (2014) was 0.2, and none of the $SSAM_M$ ρ values were larger than 0.2. The $SSAM_B$ ρ value for SSB was slightly greater than 0.2 (i.e., Mohn's $\rho = 0.22$). I also conducted 7-year retrospective analyses, which the 7-year results in Figure 5.13 indicates, and overall ρ results were similar to Table 5.4. Positive Mohn's ρ for biomass and negative Mohn's ρ for F are indicators of overestimation of biomass and the highest risk for overfishing (Hurtado-Ferro et al., 2014). Hence, overall I conclude the $SSAM_M$ model had improved retrospective patterns for SSB and $\bar{F}$ compared to the $ADAPT$ or $SSAM_B$ models.

Since 1992, the SSB estimates from the $SSAM_B$ were more similar to those from the $ADAPT$. Conversely, the SSB estimates from the $SSAM_M$ were higher during this period. The increase in SSB was also more significant during 1980–1991 (see Figure 5.5). The level of fishing is a crucial factor that determines the productivity of a fish stock (Morgan et al., 2014a,b). The higher stock size estimates from the $SSAM_M$ model produced lower fishing morality rates estimates in the $SSAM_M$ compared to $SSAM_B$ and $ADAPT$ (see Figure 5.4). Moreover, the $ADAPT$ estimate for SSB in

2020 (see Rideout et al., 2021) was 7,279 t, which is only 12% of the SSB limit reference point (B_{lim} = 60,000 t; González-Costas and González-Troncoso, 2013). However, the $SSAM_M$ estimated an SSB of 13,655 t for 2020, which was 88% larger than the $ADAPT$ estimate. However, it is important to note that this estimate still falls far below the B_{lim}, representing about 23% of the B_{lim}. Although the $SSAM_M$ estimated a larger terminal SSB than $ADAPT$, it also estimated substantially larger initial SSB (>2 times SSB from $ADAPT$). This would affect the reference points (B_{lim}) and therefore may actually indicate that the stock has a similar (or even worse) status relative to B_{lim} than was estimated via the $ADAPT$ model.

A simulation study should be conducted to investigate the accuracy of the $SSAM_M$ estimates of time-varying M's and if the $SSAM_M$ provides improved estimates of stock size and F's compared to the $SSAM_B$ and $ADAPT$ models. This should include simulating data from the estimated $SSAM_M$ model, and then calculating the simulation bias for SSB and $\bar{F}$. An objective and rigorous simulation study is a substantial task and beyond the scope my thesis.

The $SSAM_B$ predicted substantially different recruitment estimates compared to those from $ADAPT$. The estimates from the $SSAM_M$ were also higher, that is almost doubling of the recruitment figures compared to those from $SSAM_B$ (or even more significant differences, such as in 1990, where $SSAM_M$ estimates were much higher than $SSAM_B$ estimates (see the top panel of Figure 5.6)). This difference is due to the different M values. However, it is also influenced by the different ages that recruitment represents; specifically, age 1 for the SSAMs and age 2 for $ADAPT$. Conversely, the estimates were similar since 1992. Thus, the recruitment estimates are highly affected by M, emphasizing the importance of estimating time-varying M accurately at all ages to model recruitment as a function of SSB (Cadigan et al., 2022a).

Both SSAMs (i.e., $SSAM_B$ and $SSAM_M$) did not produce different conclusions

about current SGB cod stock size. This is at a low level, as indicated by both the DFO Spring and Fall surveys, and the Spanish survey. This is a fact that assessment models cannot easily change. However, this does not mean that advice from these models will be the same. The stock-recruitment patterns from the $SSAM_M$ model provided evidence of density-dependence in recruitment and suggest that the common Beverton-Holt model may be fit reliably and fit the assessment data adequately. The stock-recruit scatterplots in Cadigan et al. (2022a) did not provide evidence of asymptotic recruitment and may not produce realistic management rebuilding projections. At the same time, managing fish stocks is more challenging when M varies with time Punt et al. (2021a); Hamel et al. (2023), especially when determining management targets and limits which are usually based on stationary assumptions for stock productivity. However, a new B_{lim} for $SSAM_M$ will need to be produced if the $SSAM_M$ were adopted by NAFO. This will include considering effects of time-varying M, and also need to forecast M for short-term projections.

5.6 Tables

Table 5.1: Description of acronyms and parameters.

$SSAM$	State-space assessment model
$SSAM_B$	$SSAM$ from Cadigan et al. (2022a)
$SSAM_M$	$SSAM$ including starvation mortality indices via Eqn. (5.5)
SD	Standard deviation
SGB	Southern Grand Banks
s	Survey (i.e., Fall, Juvenile, Spanish or Spring)
t	Fraction of year a survey occurs
a, y	Age and year
A	Age plus group
N	Stock abundance
R	Recruitment vector
Z, F, M	Total, fishing, and natural mortality rates
$\bar{F}_{4-6}$	Average fishing mortality at age group 4–6
$\bar{F}_{6-9}$	Average fishing mortality at age group 6–9
$q_{s,a}$	Survey catchability parameter
μ_R	Recruitment parameter vector
μ_F	Mean F
η_a	Scalar parameters for $M_{K,a,y} = \eta_a M_{KI,a,y}$
$M_{K,a,y}$	Starvation/ condition mortality at age a and in year y
$M_{KI,a,y}$	Starvation/ condition mortality index at age a and in year y
$M_{B,a,y}$	Preliminary M (or baseline M) at age a and in year y
$M_{R,a,y}$	M remainder component at age a and in year y
$M_{a,y}$	Total stock $M_{a,y} = M_{R,a,y} + M_{K,a,y}$
$C_{a,y}$	Catch-at-age in year y
L_y	Fish landings in year y
$L_{lo,y}$	Lower bounds of landings in year y
$L_{hi,y}$	Upper bounds of landings in year y
$P_{o,a,y}$	Observed catch-at-age proportion in year y
$P_{a,y}$	Model predicted catch-at-age proportion in year y
Φ_N	Cumulative distribution function of a standard normal random variable
$X_{o,y}$	Vector of observed continuation-ratio logits (crl's) of $P_{o,a,y}$ in year y
X_y	Vector of model predicted crl's of $P_{a,y}$ in year y
$\pi_{a,y}$	Catch-at-age proportion
$I_{s,a,y}$	Observed age-based abundance index for survey s in year y
$\delta_{a,y}$	Process error at age a and in year y
$\Delta_{F,2,y}$	F deviation at age 2 and in year y
$\Delta_{F,3-10+,y}$	F deviation at age 3–10+ and in year y
$\varepsilon_{X,y}$	Error term for $X_{o,y}$
$\varepsilon_{s,y,a}$	Observation error for $I_{s,a,y}$
$\gamma_{s,y}$	Error term for EU–Spanish survey catchability drift
β_y	Random M effect, $M_{R,a,y} = \beta_y M_{B,a,y}$
σ_s	SD of $\varepsilon_{s,y,a}$
σ_β	SD of β_y random walk
σ_R	Stationary SD of Σ_R AR1 process
σ_δ	SD of the process errors
σ_{F2}	SD of $\Delta_{F,2,y}$
σ_{F3-10+}	SD of $\Delta_{F,3-10+,y}$
σ_l	User–specified parameter for landings bounds
Σ_X	SD of X_y
σ_γ	SD of $\gamma_{s,y}$
φ_R	Autocorrelation for R AR1 process
φ_X	Autocorrelation for X_y

Table 5.2: Estimates (EST) of model parameters from the SSAM with baseline M's ($SSAM_B$) and the model with M estimated using condition indices ($SSAM_M$). CV stands for coefficient of variation.

Parameter	Condition	$SSAM_B$		$SSAM_M$	
		EST	CV	EST	CV
μ_R	$y < 1970$	1060.09	0.15	1794.89	0.69
	$1970 \leq y \leq 1991$	337.58	0.45	1057.41	0.72
	$y > 1991$	25.62	0.23	141.95	0.49
μ_F	$y < 1995$, $a = 2$	<0.01	0.54	<0.01	0.68
	$y < 1995$, $a = 3$	0.08	0.85	0.03	0.51
	$y < 1995$, $a \geq 4$	0.50	0.83	0.20	0.45
	$y \geq 1995$, $a = 2$	<0.01	0.29	<0.01	0.39
	$y \geq 1995$, $a = 3$	0.01	0.86	0.01	0.48
	$y \geq 1995$, $a \geq 4$	0.02	0.83	0.02	0.43
σ_s	Fall survey	0.70	0.06	0.65	0.05
	Juvenile survey	0.40	0.14	0.42	0.13
	Spanish survey	0.90	0.06	0.93	0.05
	Spring survey	0.76	0.04	0.80	0.04
σ_F	$a = 2$	1.36	0.11	1.43	0.15
	$a > 2$	1.33	0.30	0.87	0.09
$2\sigma_{X,y}$	$y \neq 1995$	0.73	0.08	0.74	0.07
	$y = 1995$	4.39	0.28	4.13	0.27
σ_R	–	0.78	0.12	0.68	0.17
σ_δ	–	0.34	0.08	0.13	0.22
σ_γ	–	0.40	0.28	0.32	0.34
σ_β	–	–	–	0.31	0.26
φ_R	–	0.33	0.45	0.51	0.31
φ_X	–	0.76	0.07	0.72	0.07
$\varphi_{F,a}$	$a = 2$	0.97	0.02	0.85	–
$\varphi_{F,y}$	$a = 3$–$10+$	0.94	0.04	0.85	–
η_a	$a = 1$–$10+$	–	–	0.86	0.16
	AIC/BIC	3700.42	3964.97	3616.05	3880.61

Table 5.3: Estimates (EST) of survey catchability parameters ($q_{s,a}$) from the $SSAM_B$ and $SSAM_M$ models. SE stands for the standard error of the estimate.

Survey	Age	Cathability ($q_{s,a}$)			
		$SSAM_B$		$SSAM_M$	
		EST	CV	EST	CV
Fall	1	0.13	0.19	0.03	0.38
Fall	2–10	0.42	0.09	0.16	0.29
Juvenile	1	0.22	0.25	0.03	0.50
Juvenile	2	0.98	0.22	0.26	0.41
Juvenile	3	0.74	0.21	0.28	0.36
Juvenile	4	0.83	0.20	0.27	0.34
Juvenile	5	0.87	0.20	0.25	0.33
Juvenile	6	0.69	0.21	0.21	0.33
Juvenile	7	0.55	0.21	0.19	0.33
Juvenile	8	0.50	0.22	0.19	0.34
Juvenile	9	0.37	0.26	0.15	0.36
Spain	1	0.01	0.54	0.00	0.60
Spain	2	0.09	0.53	0.03	0.56
Spain	3	0.41	0.52	0.16	0.54
Spain	4	0.74	0.52	0.30	0.54
Spain	5	0.83	0.52	0.36	0.54
Spain	6	0.70	0.52	0.33	0.54
Spain	7	0.61	0.53	0.31	0.54
Spain	8	0.31	0.53	0.18	0.54
Spain	9	0.26	0.54	0.16	0.55
Spain	10	0.12	0.55	0.06	0.55
Spring	1	0.05	0.20	0.01	0.42
Spring	2	0.36	0.15	0.10	0.37
Spring	3	0.68	0.15	0.21	0.33
Spring	4	0.46	0.15	0.15	0.30
Spring	5	0.38	0.15	0.13	0.29
Spring	6	0.31	0.14	0.11	0.29
Spring	7	0.35	0.14	0.13	0.30
Spring	8	0.37	0.15	0.15	0.30
Spring	9	0.40	0.16	0.18	0.31
Spring	10	0.57	0.17	0.23	0.33

Table 5.4: Mohn's rho statistics for SSB, Recruitment, and Average F.

Quantity	Mohn's rho		
	$ADAPT$	$SSAM_B$	$SSAM_M$
SSB	0.10	0.22	0.08
Recruitment	0.39	0.07	-0.16
Average F_{4-6}	-0.25	-0.13	0.01
Average F_{6-9}	-0.25	-0.26	-0.09

5.7 Figures

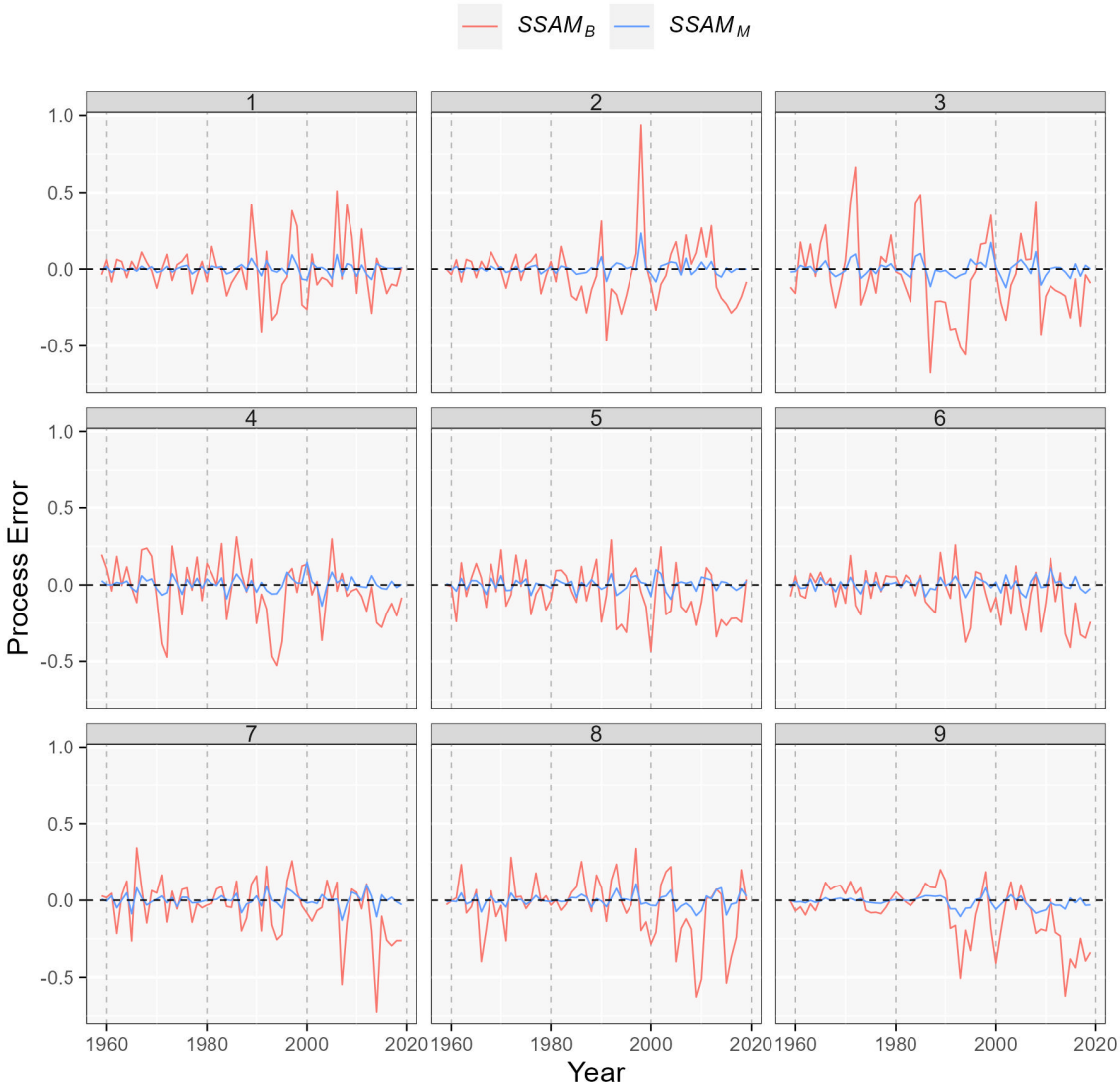

Figure 5.1: Process errors estimated by the $SSAM_B$ and $SSAM_M$ models. Line colors indicate the models, which are defined at the top.

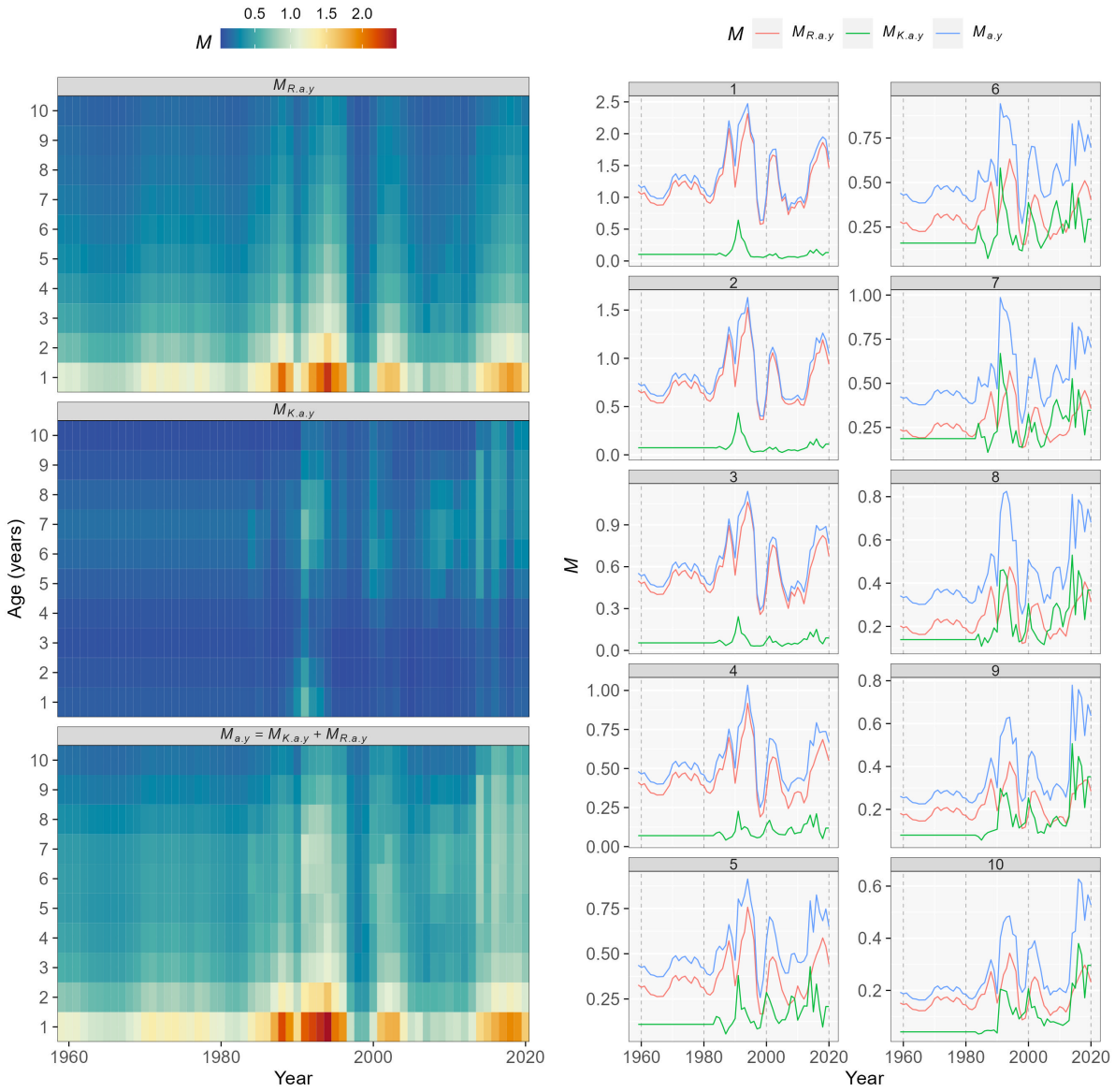

Figure 5.2: Natural mortality rate estimates, $M_{a,y} = M_{K,a,y} + M_{R,a,y}$, over time and across ages. Notations are defined in Table B.4.

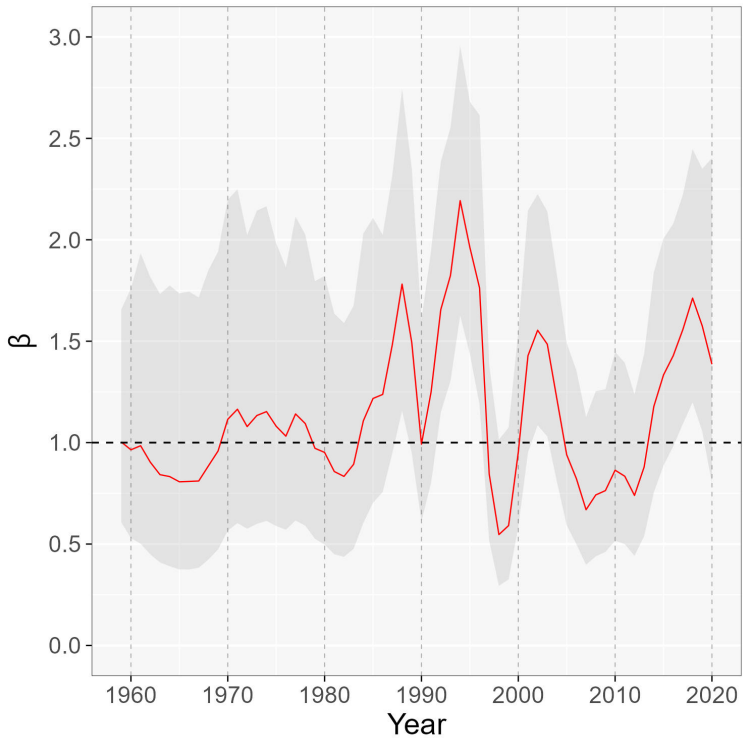

Figure 5.3: Estimates of predation M β scaling effects, $M_{R,a,y} = \beta_y M_{B,a,y}$. Shaded regions indicate 95% confidence intervals.

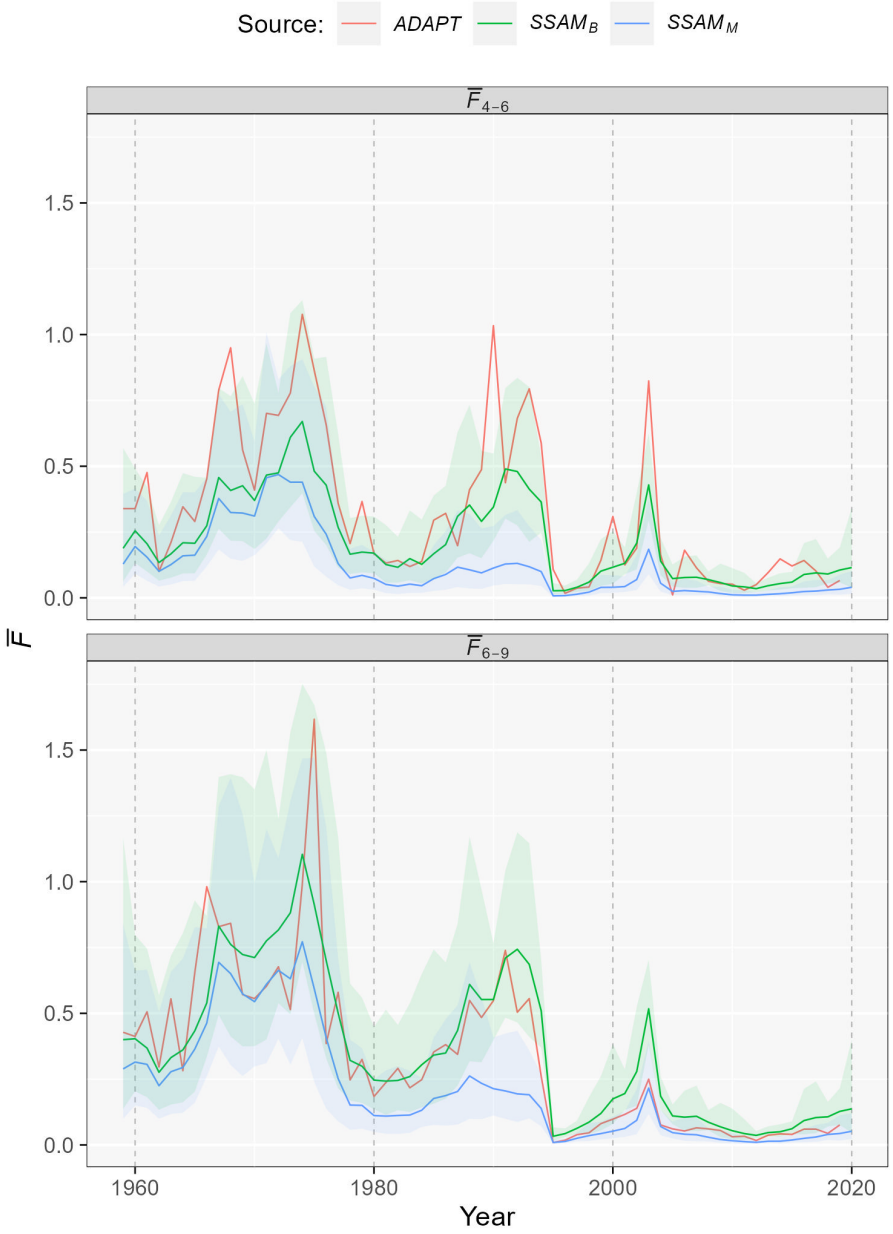

Figure 5.4: SSAM estimates of average F at ages 4–6 (F_{4-6}) and 6–9 (F_{6-9}) compared to $ADAPT$ results. Line colors indicate assessment models, which are defined at the top. Shaded regions indicate 95% confidence intervals. $SSAM_B$ used baseline M's provided by Cadigan et al. (2022a), and $SSAM_M$ included time-varying M's, $M_{a,y} = M_{K,a,y} + M_{R,a,y}$.

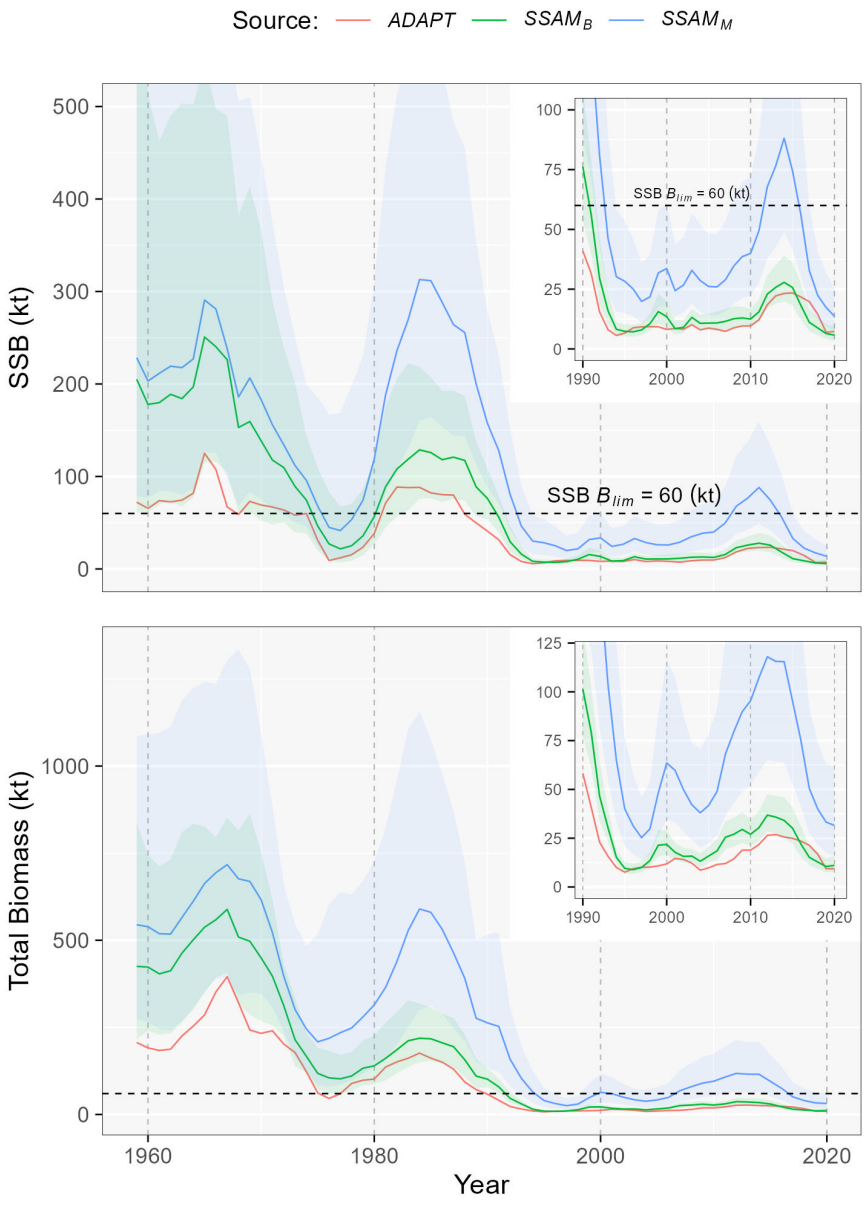

Figure 5.5: SSAM estimates of SSB and total biomass compared to *ADAPT* results. Line colors indicate assessment models, which are defined at the top. Shaded regions indicate 95% confidence intervals. Inset figures focus on estimates since 1990. $SSAM_B$ used baseline M's provided by Cadigan et al. (2022a), and $SSAM_M$ included time-varying M's, $M_{a,y} = M_{K,a,y} + M_{R,a,y}$. Dashed line represents the NAFO SSB limit reference point for SGB cod.

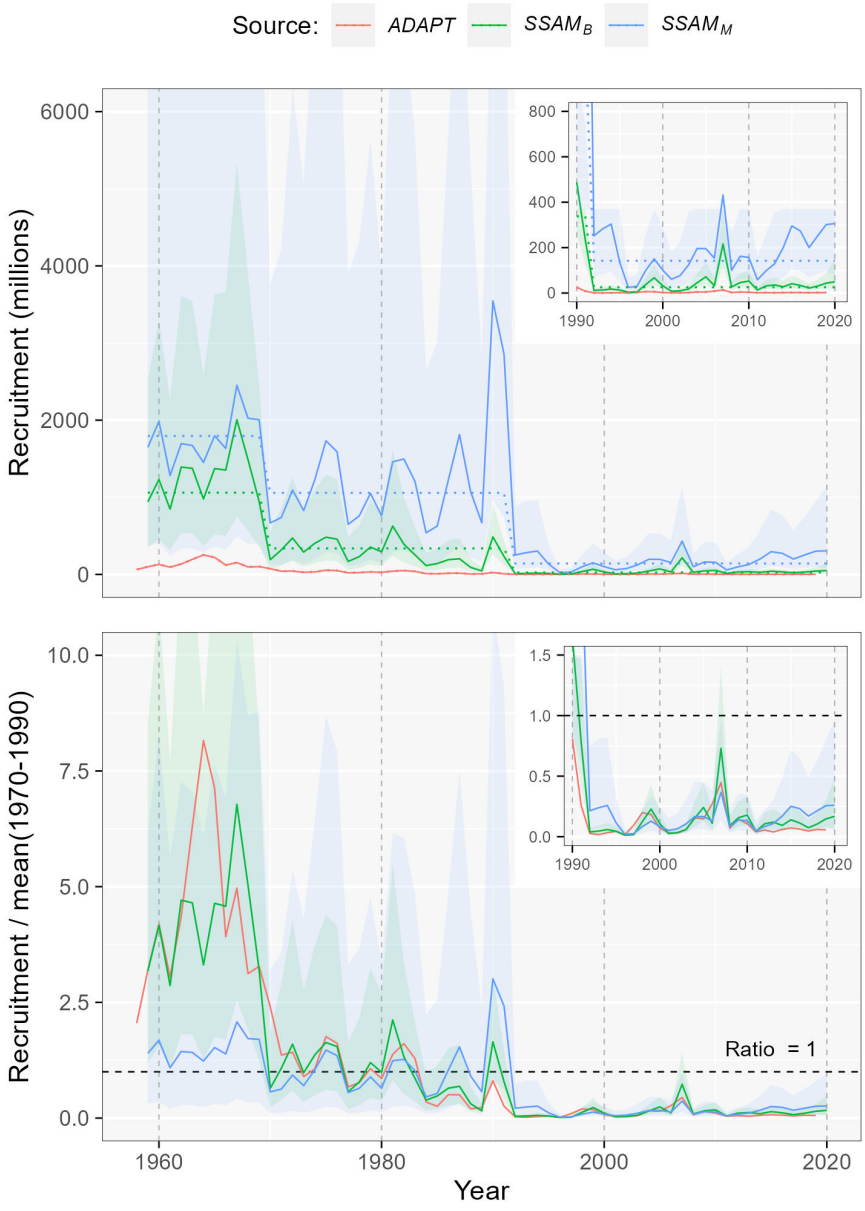

Figure 5.6: Top panel: SSAM estimates of recruitment at age 1 compared to *ADAPT* results. Line colors indicate assessment models, which are defined at the top. Shaded regions indicate 95% confidence intervals. The dashed blue and green lines indicate the recruitment mean estimates for three time-blocks. Shaded regions indicate 95% confidence intervals. Inset figures focus on estimates since 1990. *ADAPT* recruitment is at age 2 and it was back shifted one year to indicate the same cohorts as the *SSAM*'s. Bottom panel: Recruitment relative to the overall mean for each series (i.e., *SSAM*'s and *ADAPT*) during 1970–1990. $SSAM_B$ used baseline M's provided by Cadigan et al. (2022a), and $SSAM_M$ included time-varying M's, $M_{a,y} = M_{K,a,y} + M_{R,a,y}$.

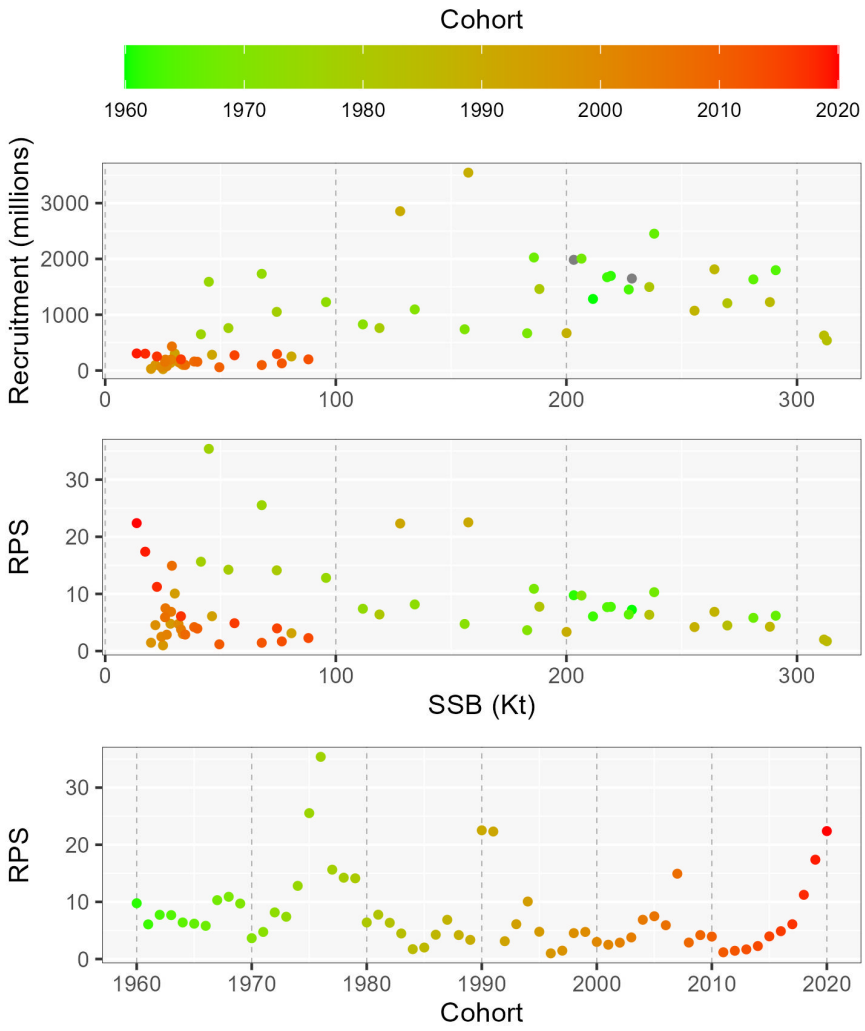

Figure 5.7: Stock-recruit relationship from $SSAM_M$. Top panel: recruitment versus SSB; middle panel: Recruits per spawner (RPS) versus SSB; bottom panel: RPS versus year. Plotting symbol colors indicate cohort which is described at the top of the figure.

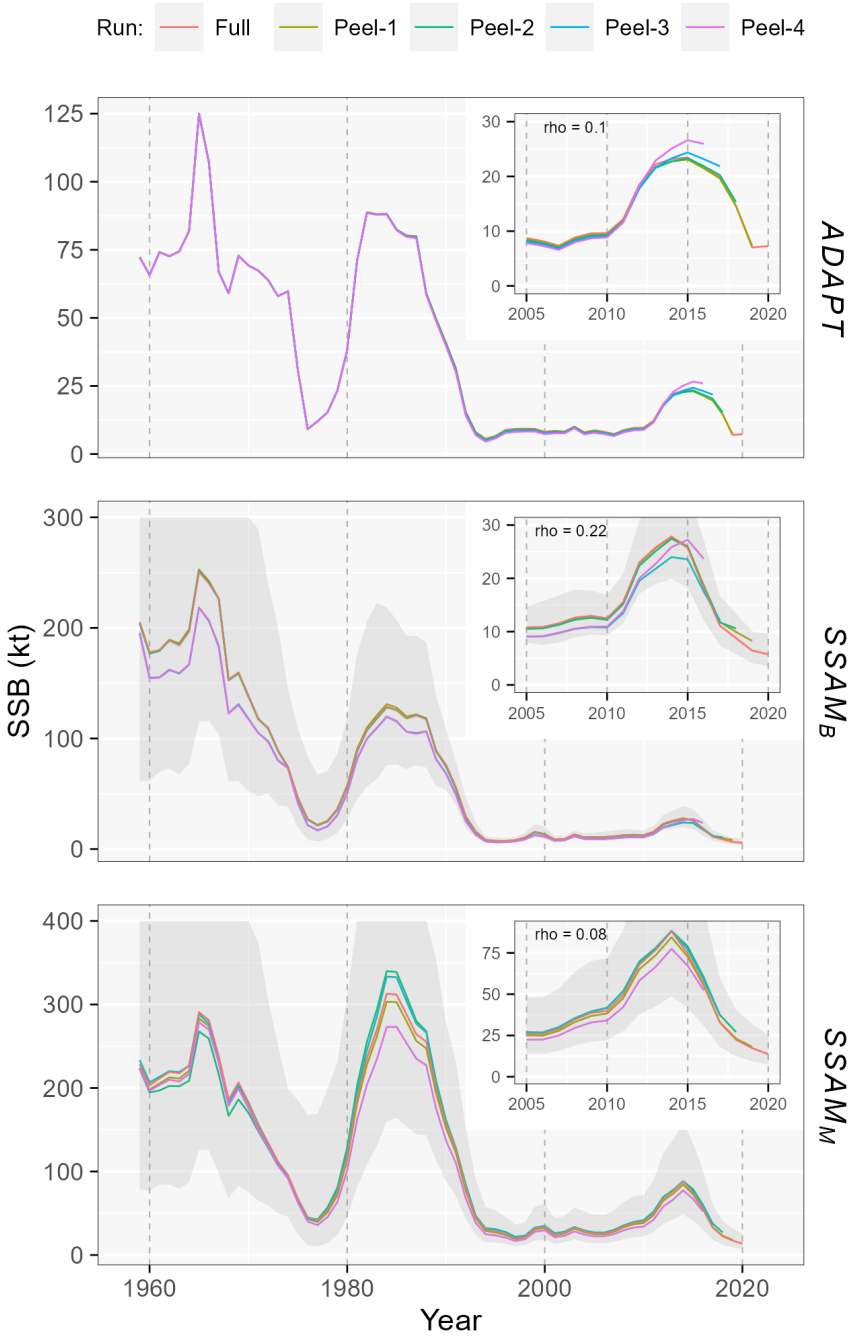

Figure 5.8: Retrospective estimates for SSB from three assessment models defined in Fig. 5.5. Shaded regions indicate 95% confidence intervals based on the full time-series of data. Inset figures show trends since 2005, with Mohn's rho listed in the top left-hand corner.

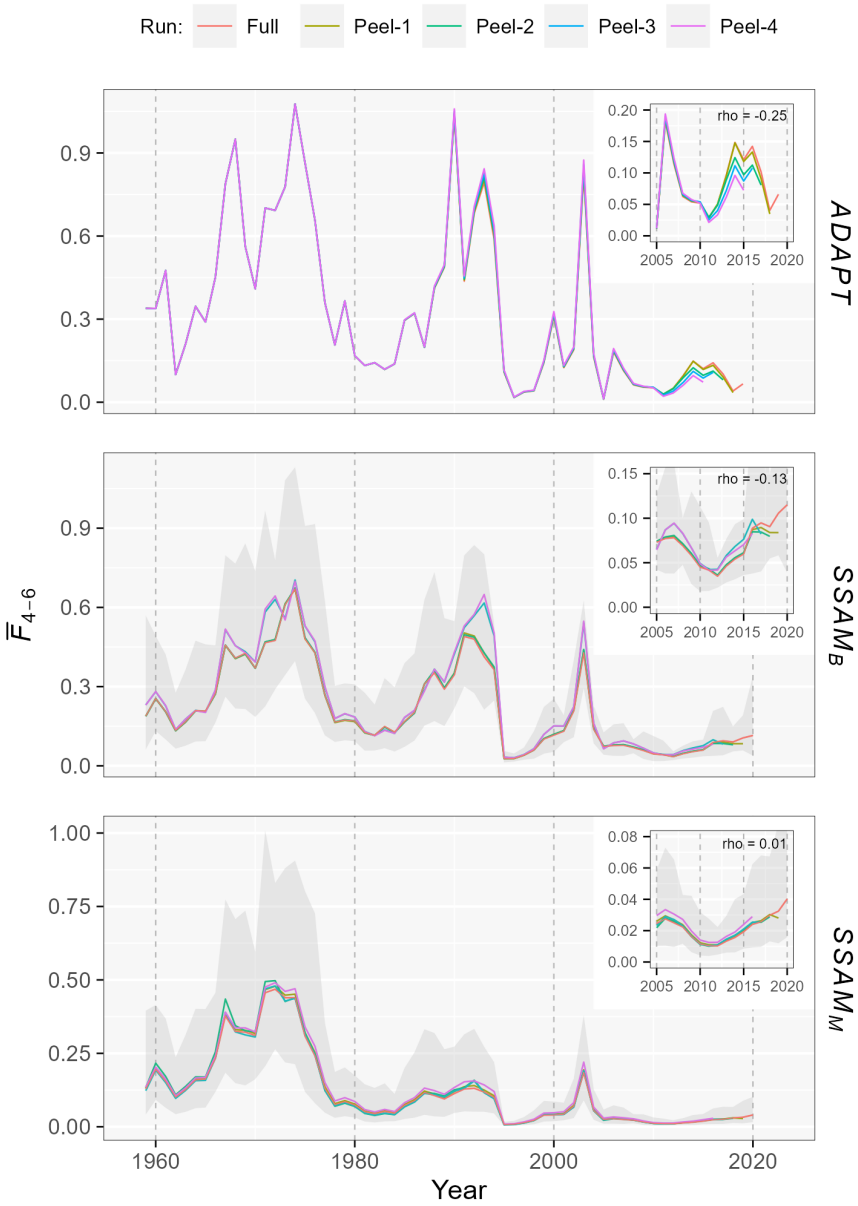

Figure 5.9: Retrospective estimates for average F at ages 4–6 from three assessment models defined in Fig. 5.5. Shaded regions indicate 95% confidence intervals based on the full time-series of data. Inset figures show trends since 2005, with Mohn's rho listed at the top.

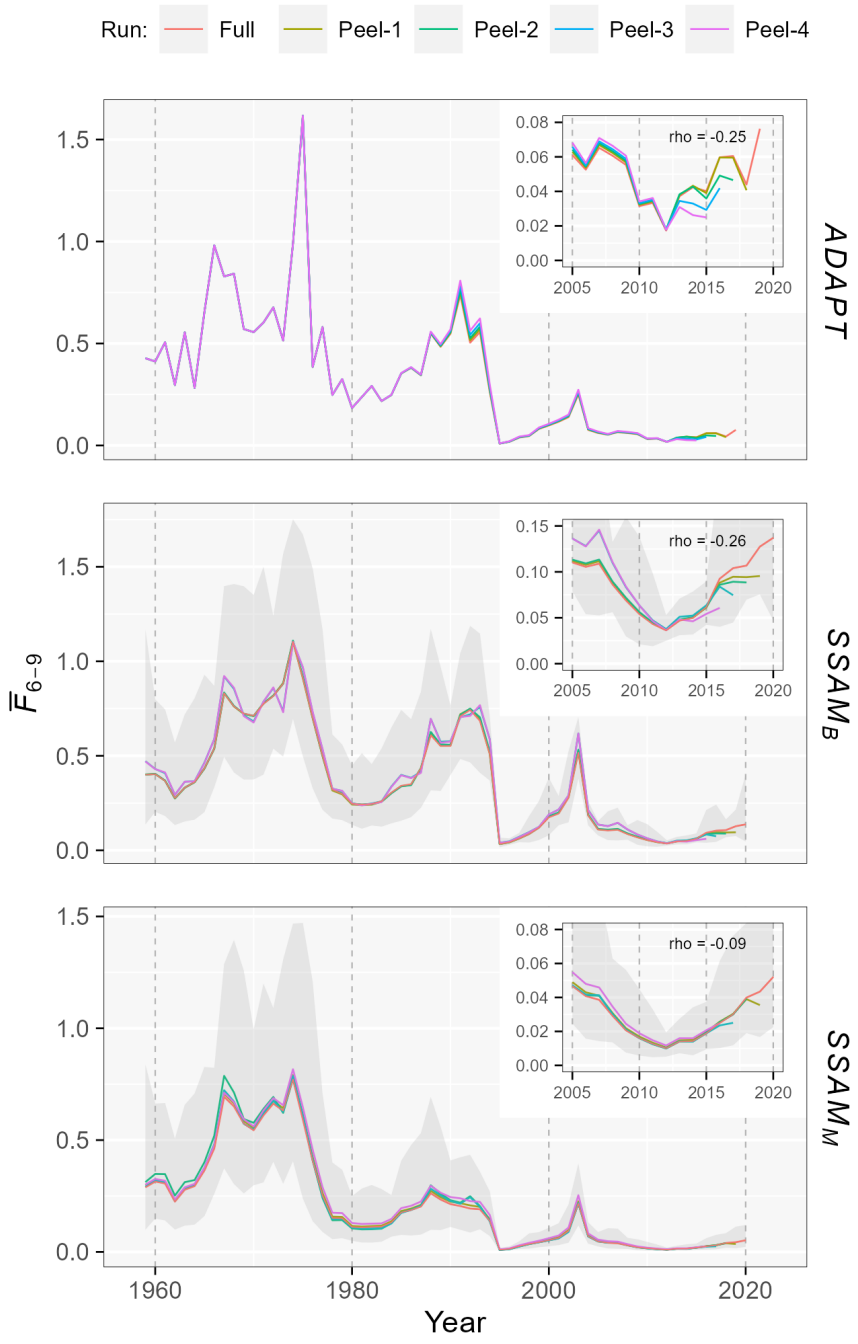

Figure 5.10: Retrospective estimates for average F at ages 6–9 from three assessment models defined in Fig. 5.5. Shaded regions indicate 95% confidence intervals based on the full time-series of data. Inset figures show trends since 2005, with Mohn's rho listed at the top.

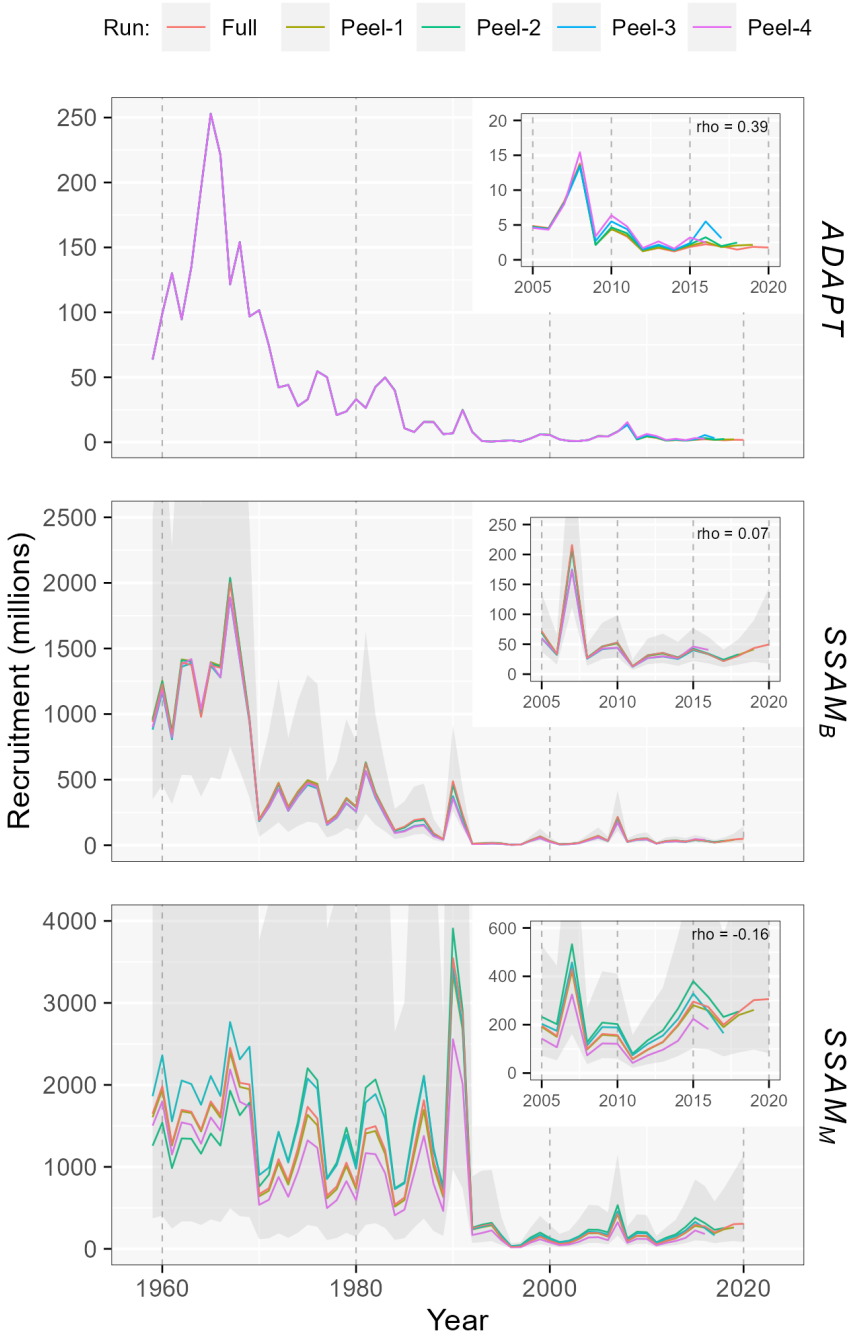

Figure 5.11: Retrospective estimates of recruitment from three assessment models defined in Fig. 5.5. Shaded regions indicate 95% confidence intervals based on the full time-series of data. Inset figures show trends since 2005, with Mohn's rho listed at the top right-hand corner.

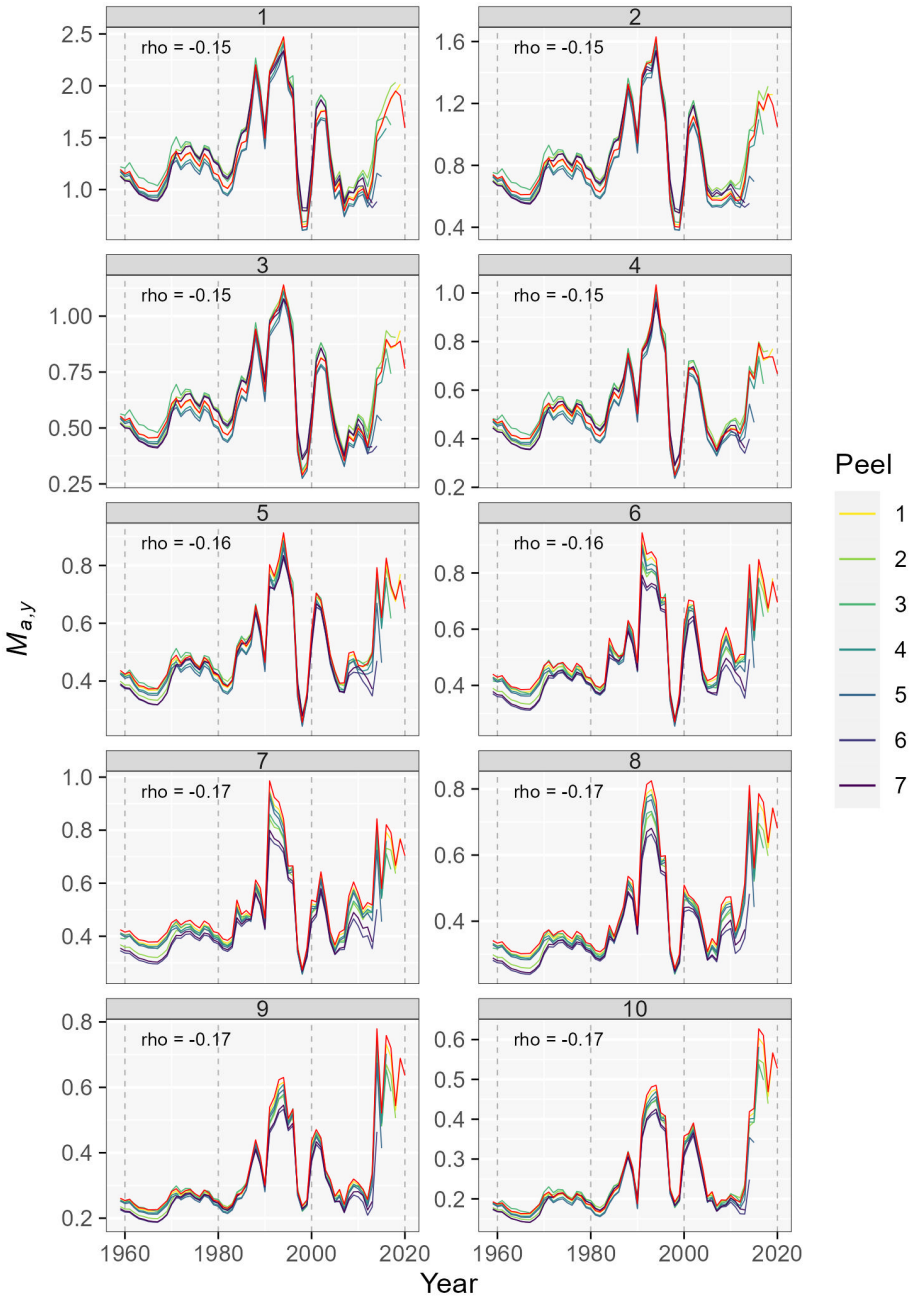

Figure 5.12: Retrospective estimates of $M_{a,y}$ from the $SSAM_M$ model. Each panel indicates an age. Red lines indicate estimates from the full time-series. Seven retrospective peels were used. Mohn's rho listed at the top left-hand corner.

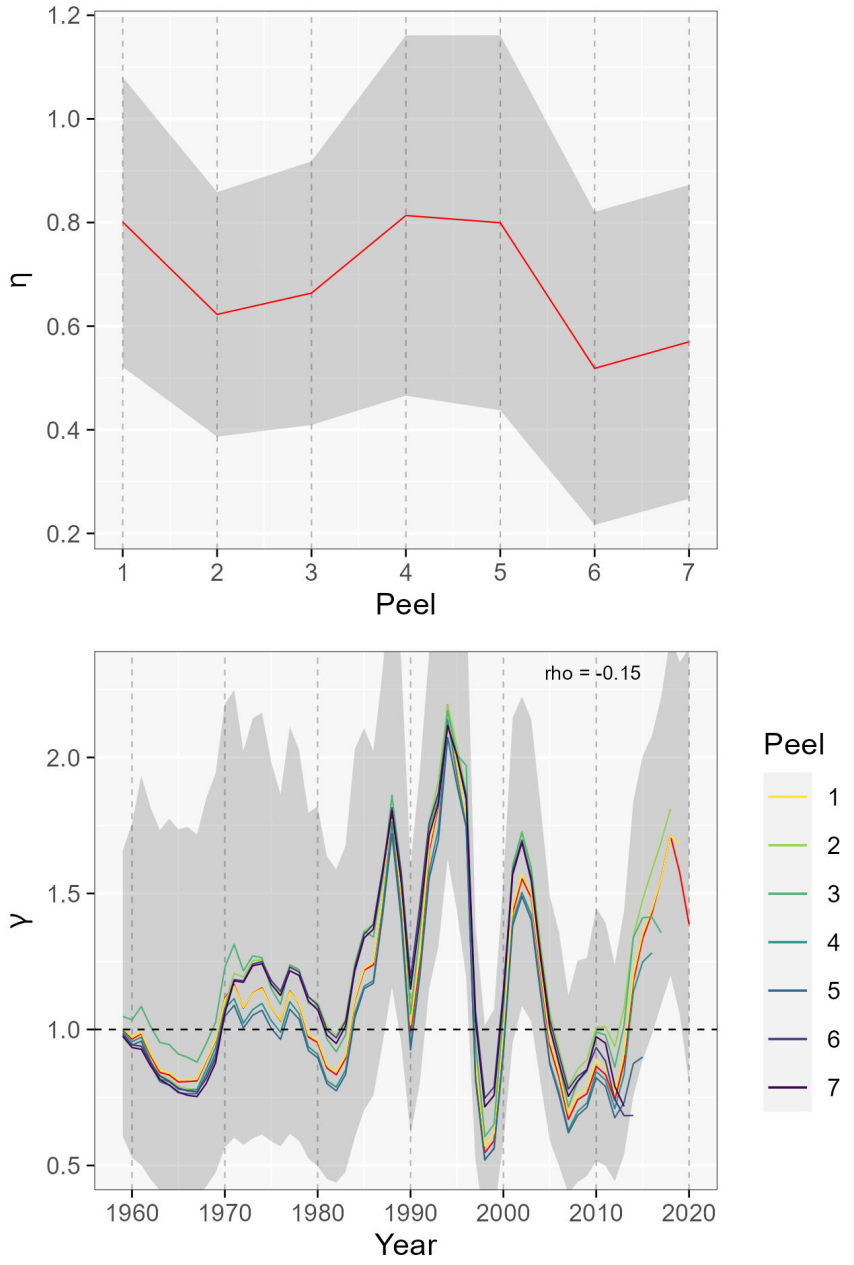

Figure 5.13: Retrospective estimates of the M parameters and effects in Equation 5.5) for the $SSAM_M$ model. Top panel: η parameter and 95% confidence intervals. Bottom panel: β effects and 95% confidence intervals based on the full time-series. Seven retrospective peels were used.

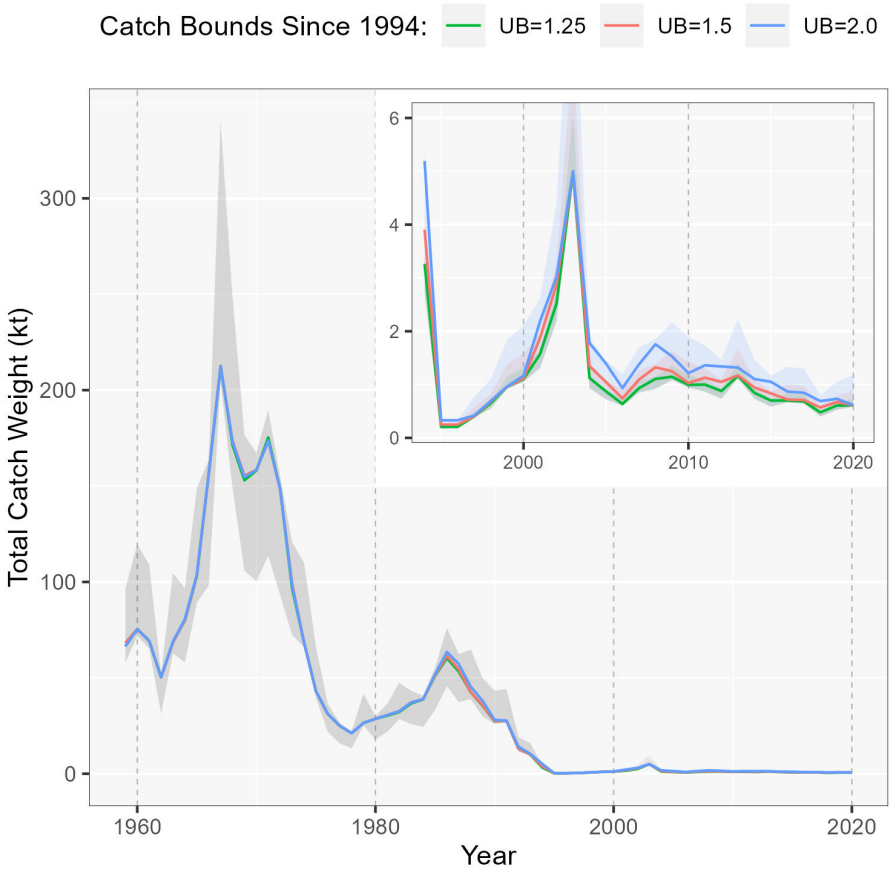

Figure 5.14: Model predicted catches from the sensitivity runs for the $SSAM_M$ with $L_{hi,y} = 1.25 \times L_{obs,y}$ and $L_{hi,y} = 2 \times L_{obs,y}$ since 1994, compared to the $SSAM_M$ with $L_{hi,y} = 1.5 \times L_{obs,y}$. Shaded regions indicate 95% confidence intervals. Inset figures show results since 1994. UB in the legend stands for upper bound of catch (i.e., $L_{hi,y}$).

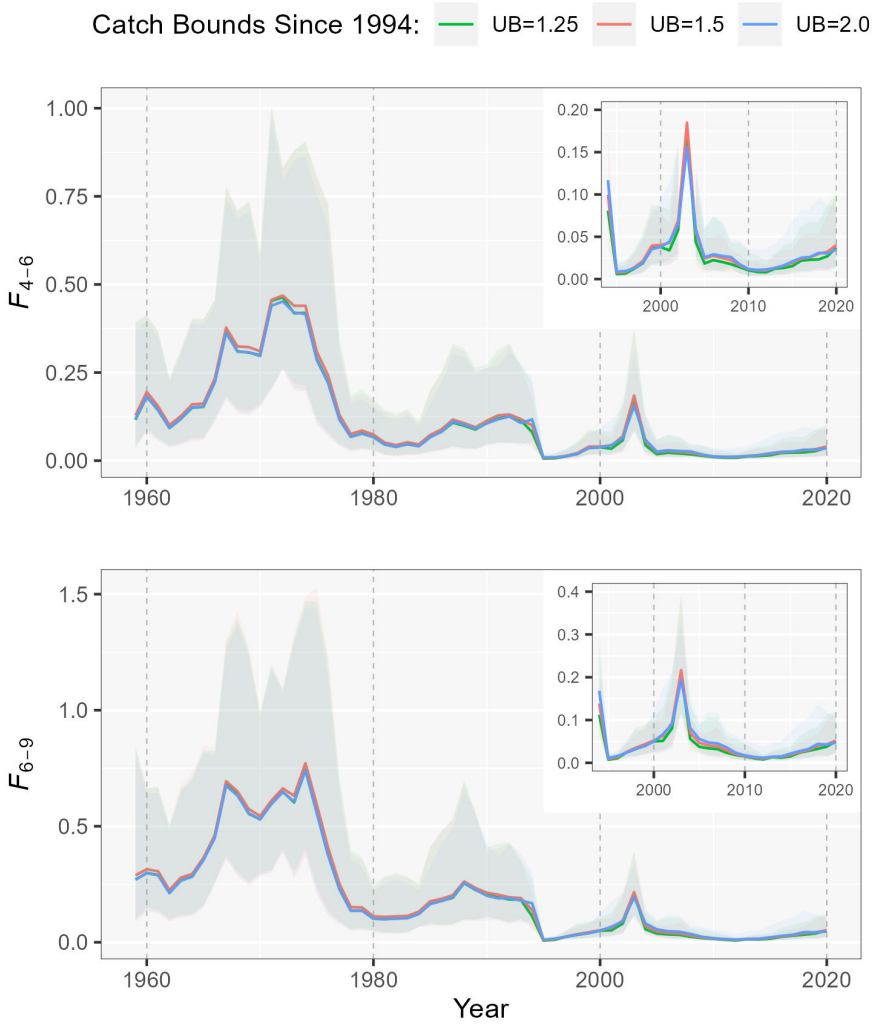

Figure 5.15: Model predicted average F at ages 4–6 and 6–9 from the sensitivity runs for the $SSAM_M$ with $L_{hi,y} = 1.25 \times L_{obs,y}$ and $L_{hi,y} = 2 \times L_{obs,y}$ since 1994, compared to the $SSAM_M$ with $L_{hi,y} = 1.5 \times L_{obs,y}$. Shaded regions indicate 95% confidence intervals. Inset figures show results since 1994. UB in the legend stands for upper bound of catch (i.e., $L_{hi,y}$).

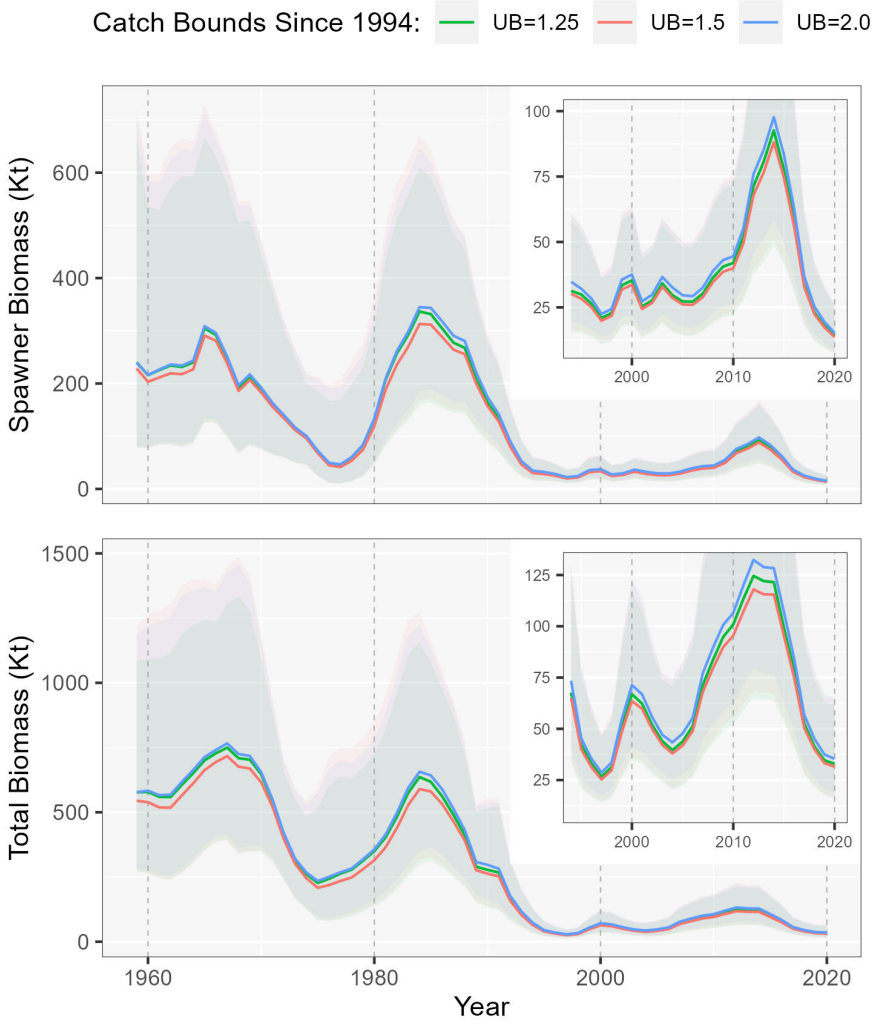

Figure 5.16: Model predicted average SSB (top panel) and biomass (bottom panel) from the sensitivity runs for the $SSAM_M$ with $L_{hi,y} = 1.25 \times L_{obs,y}$ and $L_{hi,y} = 2 \times L_{obs,y}$ since 1994, compared to the $SSAM_M$ with $L_{hi,y} = 1.5 \times L_{obs,y}$. Shaded regions indicate 95% confidence intervals. Inset figures show results since 1994. UB in the legend stands for upper bound of catch (i.e., $L_{hi,y}$).

Chapter 6

Conclusions and Research Recommendations

6.1 Conclusions

The spatiotemporal model I developed using the length and gutted-weight can be utilized for deriving a fish condition index.

The results of the spatiotemporal condition model indicate that the starvation mortality index is higher in the spring compared to the fall. It is elevated for cod in the size range of 55 to 80 cm and for those greater than 120 cm. Notably, the index is higher during 1991–1993 when the stock experienced a substantial decline, and also high in 2016.

The starvation mortality index is a significant source of variation in natural mortality (M), and therefore, it can be considered as a crucial component influencing the productivity of the SGB cod stock.

A better model of M in the SSAM should also improve the reliability of the model estimates. This could ultimately improve the reliability of the management decisions based on assessment model results.

6.2 Research recommendations

During the spatiotemporal modeling of cod condition, I assumed that starvation mortality indices, derived from changes in fish condition, were linearly related to a population's starvation M, without considering any error. To account for this, it may be beneficial to consider utilizing an errors-in-variables approach, similar to the methods available in the Woods Hole Assessment Model (WHAM; Stock and Miller, 2021). According to Stock and Miller (2021) "WHAM can estimate time- and age-varying random effects on annual transitions in numbers at age, M, and selectivity, as well as fit environmental time-series with process and observation errors, missing data, and nonlinear links to R and M. WHAM can also be configured as a traditional statistical catch-at-age model in order to easily bridge from status quo models and test them against models with state-space and environmental effects, all within a single framework" (p. 1). This approach would offer more realistic representation of the relationship between fish condition and starvation mortality.

The estimation of spatial correlations was based on the centroid distance between spatial strata, following the similar approach described in Cadigan et al. (2022b). Cadigan et al. (2022b) also suggested the possibility of using depth information to compute 3-dimensional centroid distances of the strata. However, it's worth noting that incorporating depth information in this manner can introduce complexities, particularly when it comes to weighting vertical and horizontal distances appropriately. Nevertheless, this could be a consideration need to be taken into account in any future extensions of the model.

Bibliography

Aanes, S., Engen, S., Sæther, B.-E., and Aanes, R. (2007). Estimation of the parameters of fish stock dynamics from catch-at-age data and indices of abundance: can natural and fishing mortality be separated? *Canadian Journal of Fisheries and Aquatic Sciences*, 64(8):1130–1142.

Abdulhafedh, A. (2017). How to detect and remove temporal autocorrelation in vehicular crash data. *Journal of transportation technologies*, 7(2):133–147.

Aeberhard, W. H., Mills Flemming, J., and Nielsen, A. (2018). Review of state-space models for fisheries science. *Annual Review of Statistics and Its Application*, 5:215–235.

Ajiad, A., Jakobsen, T., and Nakken, O. (1999). Sexual difference in maturation of Northeast Arctic cod. *Journal of Northwest Atlantic Fishery Science*, 25.

Albikovskaya, L. K., Gerasimova, O. V., and Kotlyarov, S. M. (1991). Estimates of Consumption of Major Food Objects by Cod in Grand Bank Areas in Spring-Summer 1990. *NAFO SCR Doc.*, 91/121, Serial No. N2014, 11 pp.

Anderson, E. D. (1998). The history of fisheries management and scientific advice-the ICNAF/NAFO history from the end of World War II to the present. *Journal of Northwest Atlantic Fishery Science*, 23.

Anderson, J. T. and Gregory, R. S. (2000). Factors regulating survival of northern cod (NAFO 2J3KL) during their first 3 years of life. *ICES Journal of Marine Science*, 57(2):349–359.

Auger-Méthé, M., Newman, K., Cole, D., Empacher, F., Gryba, R., King, A. A., Leos-Barajas, V., Mills Flemming, J., Nielsen, A., Petris, G., et al. (2021). A guide to state–space modeling of ecological time series. *Ecological Monographs*, 91(4):e01470.

Baird, J. W. and Bishop, C. A. (1988). Assessment of the Cod Stock in NAFO Div. 3NO. *NAFO SCR Doc.*, 88/19, Serial No. N1455, 47 p.

Baird, J. W. and Bishop, C. A. (1989). The Assessment of the Cod Stock in NAFO Div. 3NO. *NAFO SCR Doc.*, 89/35, Serial No. N1611, 61 p.

Bar, N. (2014). Physiological and hormonal changes during prolonged starvation in fish. *Canadian journal of fisheries and aquatic sciences*, 71(10):1447–1458.

Bishop, C. A. (1977). Cod stock evaluation - Div. 3NO. *ICNAF Res. Doc.*, 77/VI/17, Serial No. 5037, 08 p.

Bishop, C. A. and Wells, R. (1978). Status of the cod stock in Division 3NO. *ICNAF Res. Doc.*, 78/VI/59, Serial No. 5227, 08 p.

Bishop, C. A. and Wells, R. (1979). Status of the cod stock in Division 3NO. *ICNAF Res. Doc.*, 79/VI/67, Serial No. 5409, 24 p.

Björnsson, B., Sólmundsson, J., and Woods, P. J. (2022). Natural mortality in exploited fish stocks: Annual variation estimated with data from trawl surveys. *ICES Journal of Marine Science*, 79:1569–1582.

Bolger, T. and Connolly, P. L. (1989). The selection of suitable indices for the measurement and analysis of fish condition. *Journal of Fish Biology*, 34(2):171–182.

Brander, K. M. (1994). Patterns of distribution, spawning, and growth in North Atlantic cod: the utility of inter-regional comparisons. In *ICES Mar. Sci. Symp.*, volume 198, pages 406–413.

Brander, K. M. (1995). The effect of temperature on growth of Atlantic cod (*Gadus morhua*). *ICES Journal of Marine Science*, 52(1):1–10.

Bulatova, A. Y. (1990). Assessment of the Cod Stock in Div. 3NO and Div. 3KL from the 1989 Trawl-Acoustic Survey. *NAFO SCR Doc.*, 90/05, Serial No. N1716, 14 p.

Bundy, A. and Fanning, L. P. (2005). Can Atlantic cod (*Gadus morhua*) recover? Exploring trophic explanations for the non-recovery of the cod stock on the eastern Scotian Shelf, Canada. *Canadian Journal of Fisheries and Aquatic Sciences*, 62(7):1474–1489.

Buren, A. D., Koen-Alonso, M., and Stenson, G. B. (2014). The role of harp seals, fisheries and food availability in driving the dynamics of northern cod. *Marine Ecology Progress Series*, 511:265–284.

Cadigan, N. G. (2015). A state-space stock assessment model for northern cod, including under-reported catches and variable natural mortality rates. *Canadian Journal of Fisheries and Aquatic Sciences*, 73(2):296–308.

Cadigan, N. G. (2016). Weight-at-age growth models and forecasts for Northern cod (*Gadus morhua*). *DFO Can. Sci. Advis. Sec. Res. Doc.*, 2016/016. v + 19 p.

Cadigan, N. G. (2023a). A Simple Mixed-Effects Model to Smooth and Extrapolate Weights-at-Age for 3Ps Cod. *DFO Can. Sci. Advis. Sec. Res. Doc.*, 2023/024. iv + 49 p.

Cadigan, N. G. (2023b). A State-Space Assessment Model for 3Ps Cod (3PsSSAM). *DFO Can. Sci. Advis. Sec. Res. Doc.*, 2023/017. iv + 68 p.

Cadigan, N. G. and Konrad, C. (2016). A cohort time-series Von Bertalanffy growth model for Northern cod (*Gadus morhua*), and estimation of the age of tagged cod. *DFO Can. Sci. Advis. Sec. Res. Doc.*, 2016/017. v + 37 p.

Cadigan, N. G. and Rideout, R. (2022). Mixed-Effects Model to Smooth and Interpolate Survey Weights-at-Age for 3NO Cod. *NAFO SCR Doc.*, 22/040, Serial No. N7316.

Cadigan, N. G., Rideout, R., and Regular, P. (2022a). A State-Space Assessment Model for 3NO Cod. *NAFO SCR Doc.*, 22/039, Serial No. N7315.

Cadigan, N. G., Robertson, M. D., Nirmalkanna, K., and Zheng, N. (2022b). The complex relationship between weight and length of Atlantic cod off the south coast of Newfoundland. *Canadian Journal of Fisheries and Aquatic Sciences*, 79(11):1798–1819.

Camp, E. V., Collins, A. B., Ahrens, R. N. M., and Lorenzen, K. (2020). Fish population recruitment: What recruitment means and why it matters. *EDIS*, 2020(2):6–6.

Casini, M., Eero, M., Carlshamre, S., and Lövgren, J. (2016). Using alternative biological information in stock assessment: Condition-corrected natural mortality of Eastern Baltic cod. *ICES Journal of Marine Science*, 73.

Chambers, R. C. and Waiwood, K. G. (1996). Maternal and seasonal differences in egg sizes and spawning characteristics of captive Atlantic cod, *Gadus morhua*. *Canadian Journal of Fisheries and Aquatic Sciences*, 53(9):1986–2003.

Chekhova, V. A. and Postolaky, A. I. (1981). Abundance and Biomass of Cod on the Grand Bank (Divisions 3NO) and Flemish Cap (Division 3M). *NAFO Res. Doc.*, 81/II/09, Serial No. N273, 09 p.

Chumakov, A. K. and Serebrov, L. I. (1978). The determination of the catchability coefficient of bottom trawl for cod and Greenland halibut. *ICNAF Res. Doc.*, 78/VI/24, Serial No. 5185, 08 p.

Clark, D. S. and Green, J. M. (1990). Activity and movement patterns of juvenile Atlantic cod, it Gadus morhua, in Conception Bay, Newfoundland, as determined by sonic telemetry. *Canadian Journal of Zoology*, 68(7):1434–1442.

Clark, W. G. (1999). Effects of an erroneous natural mortality rate on a simple age-structured stock assessment. *Canadian Journal of Fisheries and Aquatic Sciences*, 56(10):1721–1731.

COSEWIC (2003). COSEWIC assessment and update status report on the Atlantic cod (*Gadus morhua*) in Canada. Technical report, Committee on the Status of Endangered Wildlife in Canada, Ottawa.

Cote, D., Ollerhead, L., Scruton, D., and McKinley, R. (2003). Microhabitat use of juvenile Atlantic cod in a coastal area of Newfoundland determined by 2D telemetry. *Marine Ecology Progress Series*, 265:227–234.

Coutant, C. C. (1987). Thermal preference: when does an asset become a liability? *Environmental biology of fishes*, 18:161–172.

Cren, E. D. L. (1951). The Length-Weight Relationship and Seasonal Cycle in Gonad Weight and Condition in the Perch (*Perca fluviatilis*). *Journal of Animal Ecology*, 20(2):201–219.

Dale, M. R. T. and Fortin, M. J. (2014). *Spatial analysis : a guide for ecologists*. Cambridge University Press, Cambridge, 2 edition.

Dalley, E. L. and Anderson, J. T. (1997). Age-dependent distribution of demersal juvenile Atlantic cod (*Gadus morhua*) in inshore/offshore northeast Newfoundland. *Canadian Journal of Fisheries and Aquatic Sciences*, 54(S1):168–176.

Dawe, E., Koen-Alonso, M., Chabot, D., Stansbury, D., and Mullowney, D. (2012). Trophic interactions between key predatory fishes and crustaceans: comparison of

two Northwest Atlantic systems during a period of ecosystem change. *Marine Ecology Progress Series*, 469:233–248.

Dean, M. J., Hoffman, W. S., and Armstrong, M. P. (2012). Disruption of an Atlantic cod spawning aggregation resulting from the opening of a directed gill-net fishery. *North American Journal of Fisheries Management*, 32(1):124–134.

DeYoung, B. and Rose, G. A. (1993). On recruitment and distribution of Atlantic cod (*Gadus morhua*) off Newfoundland. *Canadian Journal of Fisheries and Aquatic Sciences*, 50(12):2729–2741.

DFO (2007). *The Grand Banks of Newfoundland: Atlas of Human Activities*. DFO, Newfoundland and Labrador Region, Communications Branch and Oceans Division, Oceans and Habitat Management Branch, St. John's, NL A1C 5X1.

DFO (2021). Rebuilding plan for Atlantic Cod - NAFO Divisions 2J3KL. `https://www.dfo-mpo.gc.ca/fisheries-peches/ifmp-gmp/cod-morue/2020/cod-atl-morue-2020-eng.html`. Accessed: 2022-10-17.

Doubleday, W. (1981). Manual of groundfish surveys in the Northwest Atlantic. *NAFO Sci. Council Stud.*, 2:7–55.

Drinkwater, K. F. (2005). The response of Atlantic cod (*Gadus morhua*) to future climate change. *ICES Journal of Marine Science*, 62(7):1327–1337.

Duarte, C. M. and Alcaraz, M. (1989). To produce many small or few large eggs: a size-independent reproductive tactic of fish. *Oecologia*, 80:401–404.

Dutil, J. D., Castonguay, M., Gilbert, D., and Gascon, D. (1999). Growth, condition, and environmental relationships in Atlantic cod (*Gadus morhua*) in the northern Gulf of St. Lawrence and implications for management strategies in the Northwest Atlantic. *Canadian Journal of Fisheries and Aquatic Sciences*, 56(10):1818–1831.

Dutil, J. D., Godbout, G., Blier, P. U., and Groman, D. (2006). The effect of energetic condition on growth dynamics and health of Atlantic cod (*Gadus morhua*). *Journal of Applied Ichthyology*, 22.

Dutil, J.-D. and Lambert, Y. (2000). Natural mortality from poor condition in Atlantic cod (*Gadus morhua*). *Canadian Journal of Fisheries and Aquatic Sciences*, 57(4):826–836.

Echave, K. B., Hanselman, D. H., Adkison, M. D., and Sigler, M. F. (2012). Interdecadal change in growth of sablefish (*Anoplopoma fimbria*) in the northeast Pacific Ocean. *Fisheries Bulletin*, 210:361–374.

Fahay, M. P. (1999). Essential fish habitat source document. Atlantic cod, *Gadus morhua*, life history and habitat characteristics. *NOAA Technical Memorandum NMFSNE-124*.

Fomin, K. and Pochtar, M. (2019). Russian Research Report for 2018. *NAFO SCS Doc.*, 19/11, Serial No. N6929, 25 pp.

Fomin, K. and Pochtar, M. (2020). Russian Research Report for 2019. *NAFO SCS Doc.*, 20/13, Serial No. N7077, 52 pp.

Fomin, K. Y. (2021). Capelin Stock Assessment in NAFO Divisions 3NO Based on Data from Trawl Surveys. *NAFO SCR Doc.*, 21/029, Serial No. N7197.

Fournier, D. A., Skaug, H. J., Ancheta, J., Ianelli, J., Magnusson, A., Maunder, M. N., Nielsen, A., and Sibert, J. (2012). AD Model Builder: using automatic differentiation for statistical inference of highly parameterized complex nonlinear models. *Optimization Methods and Software*, 27(2):233–249.

Fox, W. W. (1975). Fitting the generalized stock production model by least-squares and equilibrium approximation. *Fish. Bull*, 73(1):23–37.

Froese, R. and Pauly, D. (2023). FishBase. World Wide Web electronic publication. `https://www.fishbase.org`. Accessed: 2023-02-26.

Fudge, S. B. and Rose, G. A. (2008). Life history co-variation in a fishery depleted Atlantic cod stock. *Fisheries Research*, 92(1):107–113.

Garrido, I., González-Troncoso, D., González-Costas, F., Román, E., and Ramilo, L. (2023). Results of the Spanish survey in NAFO Div. 3NO. *NAFO SCR Doc.*, 23/002, Serial No. N7379, 74 p.

Gavaris, S. (1979). Update of the Cod Stock Assessment for Divisions 3NO. *ICNAF Res. Doc.*, 79/VI/45, Serial No. 5384, 6 p.

Gavaris, S. (1988). An adaptive fraework for the estimation of population size. *CAFSAC Res. Doc.*, 12 p.

Geissinger, E. A., Gregory, R. S., Laurel, B. J., and Snelgrove, P. V. (2021). Food and initial size influence overwinter survival and condition of a juvenile marine fish (age-0 Atlantic cod). *Canadian Journal of Fisheries and Aquatic Sciences*, 78(4):472–482.

Getis, A. (2008). A history of the concept of spatial autocorrelation: A geographer's perspective. *Geographical analysis*, 40(3):297–309.

González-Costas, F. and González-Troncoso, D. (2013). Biological Reference Points for Cod Div. 3NO. *NAFO SCR Doc.*, 13/040, Serial No. N6195, 10 pp.

González, C., Paz, X., Román, E., and Hermida, M. (1998). Feeding Habits of Fish Species Distributed on the Grand Bank (NAFO Divisions 3NO, 2002-2005). *NAFO SCR Doc.*, 06/31, Serial No. N5251, 22 pp.

González-Costas, F., Ramilo, G., Román, E., Lorenzo, J., Gago, A., González-Troncoso, D., J. L. del Rio, J. L., and Sacau, M. (2019). Spanish Research Report for 2018. *NAFO SCS Doc.*, 19/10, Serial No. N6922, 44 pp.

González-Costas, F., Ramilo, G., Román, E., Lorenzo, J., Gago, A., González-Troncoso, D., Sacau, Duran, P., Casas, M., and del Rio, J. L. (2020). Spanish Research Report for 2019. *NAFO SCS Doc.*, 20/07, Serial No. N7045, 42 pp.

González-Troncoso, D., Román, E., and Paz, X. (2012). Results for Greenland halibut, American plaice and Atlantic cod of the Spanish survey in NAFO Div. 3NO for the period 1997-2011. *NAFO SCR Doc.*, 12/012, Serial No. N6036, 54 pp.

Grabowski, T. B. and Grabowski, J. H. (2004). Early life history. In Rose, G. A., editor, *Atlantic cod: a bio-ecology*, pages 133–168. John Wiley and Sons, Inc., Hoboken, NJ, USA.

Gregory, R. S. and Anderson, J. T. (1997). Substrate selection and use of protective cover by juvenile Atlantic cod *Gadus morhua* in inshore waters of Newfoundland. *Marine Ecology Progress Series*, 146:9–20.

Gudmundsson, G. (1994). Time series analysis of catch-at-age observations. *Journal of the Royal Statistical Society: Series C (Applied Statistics)*, 43(1):117–126.

Gudmundsson, G. and Gunnlaugsson, T. (2012). Selection and estimation of sequential catch-at-age models. *Canadian Journal of Fisheries and Aquatic Sciences*, 69(11):1760–1772.

Haberle, I., Bavčević, L., and Klanjscek, T. (2023). Fish condition as an indicator of stock status: Insights from condition index in a food-limiting environment. *Fish and Fisheries,*, 00(2):1–15.

Hamel, O. S., Ianelli, J. N., Maunder, M. N., and Punt, A. E. (2023). Natural mortality: Theory, estimation and application in fishery stock assessment models. *Fisheries Research*, 261:106638.

Healey, B. and Parrill, E. (2019). Canadian Research Report for 2018 Newfoundland and Labrador Region. *NAFO SCS Doc.*, 19/13, Serial No. N6953, 28 pp.

Healey, B., Tobin, J., Ings, D. W., and Regular, P. M. (2020). *Rstrap: Stratified Analysis Package*. R package version 1.14.1.

Healey, B. P., Murphy, E. F., Brattey, J., Cadigan, N. G., Morgan, M. J., Parsons, D. M., Power, D. J., Rideout, R. M., Colbourne, E. B., and Mahé, J. C. (2013). Assessing the status of the cod (*Gadus morhua*) stock in NAFO Subdivision 3Ps in 2011. *DFO Can. Sci. Advis. Sec. Sci. Advis. Rep.*, 2012/158, iv + 81 p.

Healey, B. P., Murphy, E. F., Stansbury, D. E., and Brattey, J. (2003). An assessment of the cod stock in NAFO Divisions 3NO. *NAFO SCR Doc.*, 03/059, Serial No. N4878 60 pp.

Hubert, L. J., Golledge, R. G., and Costanzo, C. M. (1981). Generalized procedures for evaluating spatial autocorrelation. *Geographical analysis*, 13(3):224–233.

Hurtado-Ferro, F., Szuwalski, C. S., Valero, J. L., Anderson, S. C., Cunningham, C. J., Johnson, K. F., Licandeo, R., McGilliard, C. R., Monnahan, C. C., Muradian, M. L., Ono, K., Vert-Pre, K. A., Whitten, A. R., and Punt, A. E. (2014). Looking in the rear-view mirror: bias and retrospective patterns in integrated, age-structured stock assessment models. *ICES Journal of Marine Science*, 72(1):99–110.

Hutchings, J. A., Myers, R. A., and Lilly, G. R. (1993). Geographic variation in the spawning of Atlantic cod, *Gadus morhua*, in the Northwest Atlantic. *Canadian Journal of Fisheries and Aquatic Sciences*, 50(11):2457–2467.

Höffle, H. and Planque, B. (2023). Natural mortality estimations for beaked redfish (*Sebastes mentella*) – A long-lived ovoviviparous species of the Northeast Arctic. *Fisheries Research*, 260:106581.

ICES (2005). Spawning and life history information for North Atlantic cod stocks. ICES Cooperative Research Report. Technical Report 274, ICES.

Jellyman, P. G., Booker, D. J., Crow, S. K., Bonnett, M. L., and Jellyman, D. J. (2013). Does one size fit all? An evaluation of length-weight relationships for New Zealand's freshwater fish species. *New Zealand Journal of Marine and Freshwater Research*, 47.

Jobling, M. (1988). A review of the physiological and nutritional energetics of cod, *Gadus morhua* L., with particular reference to growth under farmed conditions. *Aquaculture*, 70(1-2):1–19.

Kalman, R. E. (1960). A New Approach to Linear Filtering and Prediction Problems. *Journal of Basic Engineering*, 82(1):35–45.

Kalman, R. E. and Bucy, R. S. (1961). New Results in Linear Filtering and Prediction Theory. *Journal of Basic Engineering*, 83(1):95–108.

Keys, A. B. (1928). The weight-length relation in fishes. *Proceedings of the National Academy of Sciences*, 14(12):922–925.

Kjesbu, O. S., Solemdal, P., Bratland, P., and Fonn, M. (1996). Variation in annual egg production in individual captive Atlantic cod (*Gadus morhua). Canadian Journal of Fisheries and Aquatic Sciences*, 53(3):610–620.

Kristensen, K., Nielsen, A., Berg, C. W., Skaug, H., and Bell, B. M. (2016). TMB: Automatic Differentiation and Laplace Approximation. *Journal of Statistical Software*, 70(5):1–21.

Krohn, M., Reidy, S., and Kerr, S. (1997). Bioenergetic analysis of the effects of temperature and prey availability on growth and condition of northern cod (*Gadus morhua*). *Canadian Journal of Fisheries and Aquatic Sciences*, 54(S1):113–121.

Kumar, R., Cadigan, N. G., Zheng, N., Varkey, D. A., and Morgan, M. J. (2020). A state-space spatial survey-based stock assessment (SSURBA) model to inform spatial variation in relative stock trends. *Canadian Journal of Fisheries and Aquatic Sciences*, 77(10):1638–1658.

Lambert, Y. and Dutil, J. D. (1997). Can simple condition indices be used to monitor and quantify seasonal changes in the energy reserves of cod (*Gadus morhua*)? *Canadian Journal of Fisheries and Aquatic Sciences*, 54(S1):104–112.

Lambert, Y., Kjesbu, O. S., Kraus, G., Marteinsdottir, G., and Thorsen, A. (2005). How variable is the fecundity within and between cod stocks? In *ICES CM Doc. 2005*. ICES.

Langton, R. W. (1982). Diet overlap between Atlantic cod, *Gadus morhua* , silver hake, *Merluccius bilinearis* , and fifteen other Northwest Atlantic finfish. *Fishery bulletin (Washington, D.C.)*, 80(4):745–759.

Latour, R. J., Gartland, J., and Bonzek, C. F. (2017). Spatiotemporal trends and drivers of fish condition in Chesapeake Bay. *Marine Ecology Progress Series*, 579.

Lear, W. H. (1998). History of fisheries in the Northwest Atlantic: the 500-year perspective. *Journal of Northwest Atlantic Fishery Science*, 23.

Lee, H. H., Maunder, M. N., Piner, K. R., and Methot, R. D. (2011). Estimating natural mortality within a fisheries stock assessment model: an evaluation using simulation analysis based on twelve stock assessments. *Fisheries Research*, 109(1):89–94.

Lilly, G. R. (2005). Southern Grand Bank (NAFO Division 3NO). In Brander, K., editor, *ICES Cooperative Research Report*, pages 114–118. ICES, ICES, Denmark.

Lilly, G. R. and Fleming, A. M. (1981). Size Relationships in Predation by Atlantic Cod, *Gadus morhua*, on Capelin, *Mallotus villosus*, and Sand Lance, *Ammodytes dublus*, in the Newfoundland Area. *NAFO Sci. Coun. Stud.*, 1:41–45.

Lilly, G. R. and Meron, S. (1986). Propeller clam (*Cyrtodaria siliqua*) from stomachs of Atlantic cod (*Gadus morhua*) on the Southern Grand Bank (NAFO Div 3NO) natural prey or an instance of net feeding. In *ICES Demersal Fish Committee. CM 1986:36*. ICES.

Lilly, G. R., Murphy, E. F., and Simpson, M. (2000). Distribution and abundance of demersal juvenile cod (*Gadus morhua*) on the Northeast Newfondland shelf and the Grand Banks (Divsions 2J3KLNOP): implications for stock identity and monitoring. *DFO Can. Stock Assess. Sec. Res. Doc.*, 2000/092, 41 p.

Link, J. S. and Auster, P. J. (2013). The challenges of evaluating competition among marine fishes: who cares, when does it matter, and what can one do about it? *Bulletin of Marine Science*, 89(1):213–247.

Link, J. S. and Sherwood, G. D. (2004). Feeding, growth, and trophic ecology. In Rose, G. A., editor, *Atlantic cod : a bio-ecology*, pages 219–286. John Wiley and Sons, Inc., Hoboken, NJ, USA.

Lloret, J. and Planes, S. (2003). Condition, feeding and reproductive potential of white seabream (*Diplodus sargus*) as indicators of habitat quality and the effect of reserve protection in the northwestern Mediterranean. *Marine Ecology Progress Series*, 248:197–208.

Lorenzen, K. (1996). The relationship between body weight and natural mortality in juvenile and adult fish: a comparison of natural ecosystems and aquaculture. *Journal of fish biology*, 49(4):627–642.

Marshall, C. T., Yaragina, N. A., Ådlandsvik, B., and Dolgov, A. V. (2000). Reconstructing the stock-recruit relationship for Northeast Arctic cod using a bioenergetic index of reproductive potential. *Canadian Journal of Fisheries and Aquatic Sciences*, 57(12):2433–2442.

Marteinsdottir, G. and Begg, G. A. (2002). Essential relationships incorporating the influence of age, size and condition on variables required for estimation of reproductive potential in Atlantic cod *Gadus morhua*. *Marine Ecology Progress Series*, 235:235–256.

Marteinsdottir, G., Gudmundsdottir, A., Thorsteinsson, V., and Stefansson, G. (2000). Spatial variation in abundance, size composition and viable egg production of spawning cod (*Gadus morhua* L.) in Icelandic waters. *ICES Journal of Marine Science*, 57(4):824–830.

May, A. W. (1967). Fecundity of Atlantic cod. *Journal of the Fisheries Board of Canada*, 24(7):1531–1551.

Meager, J. J., Skjæraasen, J. E., Fernö, A., and Løkkeborg, S. (2010). Reproductive interactions between fugitive farmed and wild Atlantic cod (*Gadus morhua)* in the field. *Canadian Journal of Fisheries and Aquatic Sciences*, 67(8):1221–1231.

Mieszkowska, N., Genner, M. J., Hawkins, S. J., and Sims, D. W. (2009). Effects of climate change and commercial fishing on Atlantic cod *Gadus morhua*. In Sims, D. W., editor, *Advances in Marine Biology*, volume 56, pages 213–273. Elsevier.

Miller, T. J. and Hyun, S. Y. (2018). Evaluating evidence for alternative natural mortality and process error assumptions using a state-space, age-structured assessment model. *Canadian Journal of Fisheries and Aquatic Sciences*, 75(5):691–703.

Mohn, R. (1999). The retrospective problem in sequential population analysis: an investigation using cod fishery and simulated data. *ICES Journal of Marine Science*, 56(4):473–488.

Morgan, M. J., Colbourne, E. B., and Shelton, P. A. (2007). An examination of growth and condition of Div. 3NO cod at different environmental temperatures. *NAFO Res. Doc.*, 07/24, Serial No. N5375, 31 p.

Morgan, M. J., DeBlois, E. M., and Rose, G. A. (1997). An observation on the reaction of Atlantic cod (*Gadus morhua*) in a spawning shoal to bottom trawling. *Canadian Journal of Fisheries and Aquatic Sciences*, 54(S1):217–223.

Morgan, M. J., Koen-Alonso, M., Rideout, R. M., Buren, A. D., and Maddock Parsons, D. (2018). Growth and condition in relation to the lack of recovery of northern cod. *ICES Journal of Marine Science*, 75(2):631–641.

Morgan, M. J., Rideout, R. M., and Colbourne, E. B. (2010). Impact of environmental temperature on Atlantic cod *Gadus morhua* energy allocation to growth, condition and reproduction. *Marine Ecology Progress Series*, 404:185–195.

Morgan, M. J., Shelton, P. A., and Rideout, R. M. (2014a). An evaluation of fishing mortality reference points under varying levels of population productivity in three Atlantic cod (*Gadus morhua*) stocks. *ICES Journal of Marine Science*, 71(6):1407–1416.

Morgan, M. J., Shelton, P. A., and Rideout, R. M. (2014b). Varying components of productivity and their impact on fishing mortality reference points for Grand Bank Atlantic cod and American plaice. *Fisheries Research*, 155:64–73.

Morgan, M. J., Shelton, P. A., Stansbury, D. P., Brattey, J., and Lilly, G. R. (2000). An examination of the possible effect of spawning stock characteristics on recruitment in four Newfoundland groundfish stocks. *DFO CSAS Research Document*, 2000/28, 29 pp.

Mu, X., Zhang, C., Xu, B., Ji, Y., Xue, Y., and Ren, Y. (2021). Accounting for the fish condition in assessing the reproductivity of a marine eel to achieve fishery sustainability. *Ecological Indicators*, 130:108116.

Mullowney, D. R. and Rose, G. A. (2014). Is recovery of northern cod limited by poor feeding? The capelin hypothesis revisited. *ICES Journal of Marine Science*, 71(4):784–793.

Myers, R. A., Mertz, G., and Fowlow, P. S. (1997). Maximum population growth rates and recovery times for Atlantic cod, *Gadus morhua*. *Fishery Bulletin*, 95(4):762–772.

NAFO (2001). Report of the Standing Committee on International Control (STACTIC). Technical report, Northwest Atlantic Fisheries Organization, Halifax. N.S., Canada.

NAFO (2021). Report of the Scientific Council, 27 May -11 June 2021. *NAFO SCS Doc.*, 21/14REV.

Newman, K. B., Buckland, S. T., Morgan, B. J. T., King, R., Borchers, D. L., Cole, D. J., Besbeas, P., Gimenez, O., and Thomas, L. (2014). *Modelling Population Dynamics: Model Formulation, Fitting and Assessment using State-Space Methods*. Methods in Statistical Ecology. Springer New York.

Nielsen, A. and Berg, C. W. (2014). Estimation of time-varying selectivity in stock assessments using state-space models. *Fisheries Research*, 158:96–101.

O'Brien, L., Burnett, J., and Mayo, R. K. (1993). Maturation of nineteen species of finfish off the northeast coast of the United States, 1985-1990. Technical report, NMFS 113, NOAA, Seattle, WA.

Pante, E. and Simon-Bouhet, B. (2013). marmap: A Package for Importing, Plotting and Analyzing Bathymetric and Topographic Data in R. *PLoS ONE*, 8(9):e73051. doi:10.1371/journal.pone.0073051.

Pardoe, H., Thórdarson, G., and Marteinsdóttir, G. (2008). Spatial and temporal trends in condition of Atlantic cod *Gadus morhua* on the Icelandic shelf. *Marine Ecology Progress Series*, 362:261–277.

Pedersen, E. J., Thompson, P. L., Ball, R. A., Fortin, M. J., Gouhier, T. C., Link, H., Moritz, C., Nenzen, H., Stanley, R. R. E., and Taranu, Z. E. (2017). Signatures of the collapse and incipient recovery of an overexploited marine ecosystem. *Royal Society open science*, 4(7):170215.

Perreault, A. M. J., Zheng, N., and Cadigan, N. G. (2020). Estimation of growth parameters based on length-stratified age samples. *Canadian Journal of Fisheries and Aquatic Sciences*, 77(3):439–450.

Pinhorn, A. T. and Wells, R. (1973). Virtual population assessment of the cod stock in ICNAF Divisions 3NO. *ICNAF Res. Doc.*, 73/04, Serial No. 2904, 04 p.

Portner, H. O. and Knust, R. (2007). Climate change affects marine fishes through the oxygen limitation of thermal tolerance. *Science*, 315(5808):95–97.

Punt, A. E., Castillo-Jordán, C., Hamel, O. S., Cope, J. M., Maunder, M. N., and Ianelli, J. N. (2021a). Consequences of error in natural mortality and its estimation in stock assessment models. *Fisheries Research*, 233:105759.

Punt, A. E., Castillo-Jordán, C., Hamel, O. S., Cope, J. M., Maunder, M. N., and Ianelli, J. N. (2021b). Consequences of error in natural mortality and its estimation in stock assessment models. *Fisheries Research*, 233:105759.

R Core Team (2022). *R: A Language and Environment for Statistical Computing*. R Foundation for Statistical Computing, Vienna, Austria.

Regular, P. M., Buren, A. D., Dwyer, K. S., Cadigan, N. G., Gregory, R. S., Koen-Alonso, M., Rideout, R. M., Robertson, G. J., Robertson, M. D., Stenson, G. B., et al. (2022). Indexing starvation mortality to assess its role in the population regulation of northern cod. *Fisheries Research*, 247:106180.

Ricker, W. E. (1954). Stock and Recruitment. *Journal of the Fisheries Research Board of Canada*, 11(5):559–623.

Ridanovic, S., Nedic, Z., and Ridanovic, L. (2015). First observation of fish condition from Sava river in Bosnia and Herzegovina. *Survey in Fisheries Sciences*, 1.

Rideout, R., Rogers, B., and Ings, D. (2018). An assessment of the cod stock in NAFO Divisions 3NO. *NAFO SCR Doc.*, 18/28, Serial No. N6812, 52 pp.

Rideout, R. M. and Morgan, M. J. (2010a). Relationships between maternal body size, condition and potential fecundity of four north-west Atlantic demersal fishes. *Journal of Fish Biology*, 76(6):1379–1395.

Rideout, R. M. and Morgan, M. J. (2010b). Relationships between maternal body size, condition and potential fecundity of four north-west Atlantic demersal fishes. *Journal of Fish Biology*, 76.

Rideout, R. M., Rogers, R., and Ings, D. W. (2021). An Updated Assessment of the Cod Stock in NAFO Divisions 3NO. *NAFO SCR Doc.*, 21/031, Serial No. N7199, 57 pp.

Rideout, R. M. and Rose, G. A. (2006). Suppression of reproduction in Atlantic cod *Gadus morhua*. *Marine Ecology Progress Series*, 320.

Righton, D. and Metcalfe, J. (2004). Migration. In Rose, G. A., editor, *Atlantic cod: a bio-ecology*, pages 169–218. John Wiley and Sons, Inc., Hoboken, NJ, USA.

Rikardsen, A., Amundsen, P. A., Knudsen, R., and Sandring, S. (2006). Seasonal marine feeding and body condition of sea trout (*Salmo trutta*) at its northern distribution. *ICES Journal of Marine Science*, 63(3):466–475.

Robertson, M. D., Koen-Alonso, M., Regular, P. M., Cadigan, N. G., and Zhang, F. (2022). Accounting for a nonlinear functional response when estimating prey dynamics using predator diet data. *Methods in Ecology and Evolution*, 13(4):880–893.

Rogers, B. and Simpson, M. (2020). Canadian Research Report for 2019. *NAFO SCS Doc.*, 20/11, Serial No. N7064, 51 pp.

Rose, G. A. (2019). *Atlantic cod : a bio-ecology*. John Wiley and Sons, Inc., Hoboken, NJ, USA, 1 edition.

Rose, G. A., Atkinson, B. A., Baird, J., Bishop, C. A., and Kulka, D. W. (1994). Changes in distribution of Atlantic cod and thermal variations in Newfoundland waters, 1980-1992. In *ICES Marine Science Symposia*, volume 198, pages 542–552. Copenhagen, Denmark: International Council for the Exploration of the Sea, 1991-.

Rose, G. A. and O'Driscoll, R. (2002). Capelin are good for cod: can the northern stock rebuild without them? *ICES Journal of Marine Science*, 59(5):1018–1026.

Rue, H. and Held, L. (2005). *Gaussian Markov random fields: theory and applications*. Chapman & Hall/CRC.

Rätz, H. J. and Lloret, J. (2003). Variation in fish condition between Atlantic cod (*Gadus morhua*) stocks, the effect on their productivity and management implications. *Fisheries Research*, 60.

Sandeman, L. R., Yaragina, N. A., and Marshall, C. T. (2008). Factors contributing to inter-and intra-annual variation in condition of cod *Gadus morhua* in the Barents Sea. *Journal of Animal Ecology*, 77(4):725–734.

Sherwood, G. D., Rideout, R. M., Fudge, S. B., and Rose, G. A. (2007). Influence of diet on growth, condition and reproductive capacity in Newfoundland and Labrador cod (*Gadus morhua*): Insights from stable carbon isotopes (δ^{13}C). *Deep Sea Research Part II: Topical Studies in Oceanography*, 54(23-26):2794–2809.

Smedbol, R. K. and Wroblewski, J. S. (1997). Evidence for inshore spawning of northern Atlantic cod (*Gadus morhua*) in Trinity Bay, Newfoundland, 1991-1993. *Canadian Journal of Fisheries and Aquatic Sciences*, 54(S1):177–186.

Sober, E. (2002). Instrumentalism, parsimony, and the Akaike framework. *Philosophy of Science*, 69(S3):S112–S123.

Stansbury, D. E., Shelton, P. A., Murphy, E. F., Healey, B., and Brattey, J. (1998a). An Assessment of the Cod Stock in NAFO Divisions 3NO. *NAFO SCR Doc.*, 01/72, Serial No. N4450, 64 pp.

Stansbury, D. E., Shelton, P. A., Murphy, E. F., Lilly, G. R., and Brattey, J. (1998b). An Assessment of the Cod Stock in NAFO Divisions 3NO. *NAFO SCR Doc.*, 98/65, Serial No. N3057, 38 pp.

Stansbury, D. E., Shelton, P. A., Murphy, E. F., P., H. B., and P., B. (2001). An Assessment of the Cod Stock in NAFO Divisions 3NO. *NAFO SCR Doc.*, 01/072, Serial No. N4450, 64 pp.

Stares, J. C., Rideout, R. M., Morgan, M. J., and Brattey, J. (2007). Did population collapse influence individual fecundity of Northwest Atlantic cod? *ICES Journal of Marine Science*, 64(7):1338–1347.

Stock, B. C. and Miller, T. J. (2021). The Woods Hole Assessment Model (WHAM): A general state-space assessment framework that incorporates time-and age-varying processes via random effects and links to environmental covariates. *Fisheries Research*, 240:105967.

Stokesbury, K. D. E., Cadrin, S. X., Calabrese, N., Keiley, E., Lowery, T. M., Rothschild, B. J., and DeCelles, G. R. (2017). Towards an improved system for sampling New England groundfish using video technology. *Fisheries*, 42(8):432–439.

Sullivan, P. J. (1992). A Kalman filter approach to catch-at-length analysis. *Biometrics*, pages 237–257.

Sundby, S. (2000). Recruitment of Atlantic cod stocks in relation to temperature and advectlon of copepod populations. *Sarsia*, 85(4):277–298.

Taggart, C. T., Anderson, J., Bishop, C., Colbourne, E., Hutchings, J., Lilly, G., Morgan, J., Murphy, E., Myers, R., Rose, G., et al. (1994). Overview of cod stocks,

biology, and environment in the Northwest Atlantic region of Newfoundland, with emphasis on northern cod. In *ICES Mar. Sci. Symp.*, volume 198, pages 140–157.

Templeman, W. (1981). Vertebral numbers in Atlantic cod, *Gadus morhua*, of the Newfoundland and adjacent areas, 1947-71, and their use for delineating cod stocks. *Journal of Northwest Atlantic Fishery Science*, 2.

Thorson, J. T. (2015). Spatio-temporal variation in fish condition is not consistently explained by density, temperature, or season for California Current groundfishes. *Marine Ecology Progress Series*, 526.

Trippel, E. A. (1995). Age at maturity as a stress indicator in fisheries. *Bioscience*, 45(11):759–771.

Trippel, E. A., Joanne, M., Fréchet, A., Rollet, C., Sinclair, A. F., Annand, C., Beanlands, D., and Brown, L. (1997). Changes in Age and Length at Sexual Maturity of Northwest Atlantic Cod, Haddock and Pollock Stocks, 1972-1995 . Technical report, Canadian Technical Report of Fisheries and Aquatic Sciences No. 2157, Biological Station St. Andrews, NB EOG 2XO.

Van Beveren, E., Duplisea, D., Castonguay, M., Doniol-Valcroze, T., Plourde, S., and Cadigan, N. G. (2017). How catch underreporting can bias stock assessment of and advice for northwest Atlantic mackerel and a possible resolution using censored catch. *Fisheries Research*, 194:146–154.

Varkey, D., Babyn, J., Regular, P., Ings, D., Kumar, R., Rogers, B., Champagnat, J., and Morgan, M. (2022). A state-space model for stock assessment of cod (*Gadus morhua*) stock in NAFO Subdivision 3Ps. *DFO Can. Sci. Advis. Sec. Res. Doc.*, 2022/022. v + 78 p.

Vazquez, A. and Larraneta, M. G. (1980). Assessment of Cod Stock in Divisions 3NO. *NAFO Res. Doc.*, 80/II/10, Serial No. N042, 11 p.

Vincent, M. T. and Pilling, G. M. (2023). Assumptions influencing the estimation of natural mortality in a tag-integrated statistical model for western and central pacific ocean skipjack. *Fisheries Research*, 261:106612.

Walsh, P. and Hiscock, W. (2005). Fishing for Atlantic Cod (*Gadus mohrua*) using Experimental Baited Pots. Technical report, Centre for Sustainable Aquatic Resources, Fisheries and Marine Institute of Memorial University of Newfoundland, P.O. Box 4920, St. John's, NL, Canada, A1C 5R3.

Walsh, S. J., Brodie, W. B., Bishop, C. A., and Murphy, E. F. (1995). Fishing on juvenile groundfish nurseries on the Grand Bank: a discussion of technical measures of conservation. *Marine Protected Areas and Sustainable Fisheries*, pages 54–73.

Warren, W., Brodie, W., Stansbury, D., Walsh, S., Morgan, J., and Orr, D. (1996). Analysis of the 1996 Comparative Fishing Trial between the Alfred Needier with the Engel 145 trawl and the Wilfred Templeman with the Campelen 1800 trawl. *NAFO SCR Doc.*, 97/68, Serial No. N2902, 12 pp.

Warren, W. G. (1996). Report on the Comparative Fishing Trial Between the Gadus Atlantica and Teleost. *NAFO SCR Doc.*, 96/028, Serial No. N2701, 16 pp.

Wikle, C. K. (2015). Modern perspectives on statistics for spatio-temporal data. *Wiley Interdisciplinary Reviews: Computational Statistics*, 7(1):86–98.

Wikle, C. K., Zammit-Mangion, A., and Cressie, N. (2019). *Spatio-temporal statistics with R*. CRC Press, FL.

Williams, E. H. (2002). The effects of unaccounted discards and misspecified natural mortality on harvest policies based on estimates of spawners per recruit. *North American Journal of Fisheries Management*, 22(1):311–325.

Wright, P. J. and Rowe, S. (2004). Reproduction and spawning. In Rose, G. A., editor, *Atlantic cod: a bio-ecology*, pages 87–132. John Wiley and Sons, Inc., Hoboken, NJ, USA.

Xiao, Y. (2001). Formulae for calculating the instantaneous rate of natural mortality of animals from its surrogates. *Mathematical and Computer Modelling*, 33.

Zemeckis, D. R., Dean, M. J., and Cadrin, S. X. (2014). Spawning dynamics and associated management implications for Atlantic cod. *North American Journal of Fisheries Management*, 34(2):424–442.

Zheng, N. and Cadigan, N. (2021). Frequentist delta-variance approximations with mixed-effects models and TMB. *Computational Statistics & Data Analysis*, 160:107227.

Zheng, N., Cadigan, N., and Morgan, M. J. (2020a). A spatiotemporal richards–schnute growth model and its estimation when data are collected through length-stratified sampling. *Environmental and Ecological Statistics*, 27:415–446.

Zheng, N., Robertson, M., Cadigan, N., Zhang, F., Morgan, J., and Wheel, L. (2020b). Spatiotemporal variation in maturation: a case study with American plaice (*Hippoglossoides platessoides*) on the Grand Bank off Newfoundland. *Canadian Journal of Fisheries and Aquatic Sciences*, 77(10):1688–1699.

Appendix A

Atlantic cod at a glance

Figure A.1: Atlantic cod (*Gadus morhua*). Source: https://www.istockphoto.com

Kingdom:	Animalia	Dorsal spines:	0	L_{50} = 65.4 cm (31–74 cm)
Phylum:	Chordata	Anal spines:	0	L_{max} = 200 cm
Class:	Teleostei	Dorsal soft rays:	44–55	A_{50} = 2–7 yrs
Order:	Gadiformes	Anal soft rays:	33–45	A_{max} = 25 yrs
Family:	Gadidae	Vertebrae*:	51–55	W_{max} = 96 kg
Genus:	Gadus			
Species:	*Gadus morhua*			

*individual bones that interlock with each other to form the spinal code

Fecundity: 2.5 million (5 kg Female) to 9 million (34 kg Female)

Appendix B

Tables

Table B.1: Summary of data processed for the analysis.

Survey years	1984–2018			
No of survey strata	47			
Survey seasons	Spring: April–June			
	Fall: September–December			
No of observations	26,660			
Statistic	Mean	SD	Min.	Max.
Gutted-Weight (kg)	2.12	3.45	0.01	27.18
Length (cm)	51.75	26.18	15.00	148.00

Table B.2: Summary statistics for spatial strata.

Count	Area (km^2)		
	Mean	Min.	Max.
47	2,128.35	33.72	8,837.18

Table B.3: Definition of mathematical notations, including symbols used, their type (Index, Data, Parameter, Random Effect "RE", Derived Quantity "DQ", and Assumed Value "AV"), and dimension.

Name	Symbol	Type	Dimension
Number of observations	n	Data	1
Number of spatial strata	G	Data	1
Number of years	T	Data	1
Number of months	S	Data	1
Number of length bins (Size = 1)	L	Data	1
Number of length bins (Size = 3)	L_3	Data	1
Spatial strata for observation number i	g_i	Data	n
Year for observation number i	t_i	Data	n
Length for observation number i	l_i	Data	n
Month for observation number i	s_i	Data	S
Length bin (size = 3 cm) for l_i	l_{3i}	Data	n
Weight for observation number i	W_i	Data	n
Area of stratum g	A_g	Data	G
Distance between centroids of strata g and g'	$d_{gg'}$	Data	$G \times G$
Observation number	$i = 1, \ldots, n$	Index	-
Spatial stratum	$g = 1, \ldots, G$	Index	-
Year	$t = 1, \ldots, T$	Index	-
Month (Season)	$s = 1, \ldots, S$	Index	-
Length bin (Size = 1 cm) number	$l = 1, \ldots, L$	Index	-
Length bin (Size = 3 cm) number	$l_3 = 1, \ldots, L_3$	Index	-
Length-Weight intercept	A_{g,t,l_3}	RE	$G \times T \times L_3$
Stratum effect for $A(g,t,l_3)$	Δ_g	RE	G
Year effect for $A(g,t,l_3)$	Δ_t	RE	T
Length effect for $A(g,t,l_3)$	Δ_{l_3}	RE	L_3
Year and stratum interaction effect for $A(g,t,l_3)$	Δ_{gt}	RE	$G \times T$
Stratum and length interaction effect for $A(g,t,l_3)$	Δ_{gl_3}	RE	$G \times L_3$
Year and length interaction effect for $A(g,t,l_3)$	Δ_{tl_3}	RE	$T \times L_3$
Month (season)-length interaction effect	Δ_{sl_3}	RE	$S \times L_3$
Weight measurement error for observation number i	ε_{wi}	RE	n
Main effect for $A(g,t,l_3)$	a	Parameter	1
Length-Weight slope	b	Parameter	1
Variance of Δ_t	$\sigma^2_{\mathcal{T}}$	Parameter	1
Variance of Δ_{l_3}	$\sigma^2_{\mathcal{L}_3}$	Parameter	1
Variance of Δ_{tl_3}	$\sigma^2_{\mathcal{T}\mathcal{L}_3}$	Parameter	1
Variance of Δ_{sl_3}	$\sigma^2_{\mathcal{S}\mathcal{L}_3}$	Parameter	1
Autocorrelation for Δ_t	$\varphi_{\mathcal{T}}$	Parameter	1
Autocorrelation for Δ_{l_3}	$\varphi_{\mathcal{L}_3}$	Parameter	1
Autocorrelation for Δ_{gt}	$\varphi_{\mathcal{G}\mathcal{T}}$	Parameter	1
Autocorrelation for Δ_{gl_3}	$\varphi_{\mathcal{G}\mathcal{L}_3}$	Parameter	1
Autocorrelation for rows of Δ_{tl_3}	$\varphi_{\mathcal{T}^*\mathcal{L}_3}$	Parameter	1
Autocorrelation for columns of Δ_{tl_3}	$\varphi_{\mathcal{T}\mathcal{L}^*_3}$	Parameter	1
Autocorrelation for rows of Δ_{sl_3}	$\varphi_{\mathcal{S}^*\mathcal{L}_3}$	Parameter	1
Autocorrelation for columns of Δ_{sl_3}	$\varphi_{\mathcal{S}\mathcal{L}^*_3}$	Parameter	1
Spatial precision matrix for Δ_g	$\Omega_{\mathcal{G}}$	Parameter	$G \times G$
Spatial precision matrix for Δ_{gt}	$\Omega_{\mathcal{G}\mathcal{T}}$	Parameter	$G \times G$
Spatial precision matrix for Δ_{gl_3}	$\Omega_{\mathcal{G}\mathcal{L}_3}$	Parameter	$G \times G$
$\Omega_{\mathcal{G}}$ decorrelation	$\omega_{\mathcal{G}}$	Parameter	1
$\Omega_{\mathcal{G}\mathcal{T}}$ decorrelation	$\omega_{\mathcal{G}\mathcal{T}}$	Parameter	1
$\Omega_{\mathcal{G}\mathcal{L}_3}$ decorrelation	$\omega_{\mathcal{G}\mathcal{L}_3}$	Parameter	1
$\Omega_{\mathcal{G}}$ scale	$q_{\mathcal{G}}$	Parameter	1
$\Omega_{\mathcal{G}\mathcal{T}}$ scale	$q_{\mathcal{G}\mathcal{T}}$	Parameter	1
$\Omega_{\mathcal{G}\mathcal{L}_3}$ scale	$q_{\mathcal{G}\mathcal{L}_3}$	Parameter	1
Parameters in σ^2_w	c, d, e	Parameter	1, 1, 1
Precision matrix parameter	τ	Parameter	1
Variance of ε_{wi}	σ^2_w	DQ	1
Distance (km) when spatial correlation of $\Delta_{g,t} = 0.5$	$\bar{d}_{0.5\mathcal{G}\mathcal{T}}$	DQ	1
Distance (km) when spatial correlation of $\Delta_{g,l_3} = 0.5$	$\bar{d}_{0.5\mathcal{G}\mathcal{L}_3}$	DQ	1
Critical fish condition	K_{crit}	AV	1

Table B.4: Definitions, model notations, and parameters.

SSAM	state-space assessment model
s	Survey (i.e., Fall, Juvenile, Spanish or Spring)
t	Survey fraction
a	Age
y	Year
A	Age plus group
N	Stock abundance
R	Recruitment vector
Z, F, M	Total, fishing, and natural mortality rates
F_{4-6}	Fishing mortality at age group 4–6
F_{6-9}	Fishing mortality at age group 6–9
$M_{a,y}$	Total stock M at age a and in year y
$M_{K,a,y}$	Starvation/ condition mortality at age a and in year y
$M_{KI,a,y}$	Starvation/ condition mortality index at age a and in year y
$M_{B,a,y}$	Preliminary M (or Base M) at age a and in year y
$M_{R,a,y}$	M remainder component at age a and in year y
$C_{a,y}$	Catch-at-age in year y
L_y	Fish landings in year y
$L_{lo,y}$	Lower bounds of landing data in year y
$L_{hi,y}$	Upper bounds of landing data in year y
$P_{a,y}$	Catch-at-age proportion in year y
ϕ_N	Cumulative distribution function of a standard normal random variable
$X_{o,y}$	Vector of observed continuation-ratio logit (crl) in year y
X_y	Vector of model predicted crl in year y
$I_{s,a,y}$	Observed age-based abundance index for survey s in year y
X_y	Vector of model predicted crl in year y
$\delta_{a,y}$	Process error at age a and in year y
Σ_R	Stationary covariance matrix of R
μ_R	Recruitment parameter vector
μ_F	Mean F
$\Delta_{F,2,y}$	F deviation at age 2 and in year y
$\Delta_{F,3-10+,y}$	F deviation at age 3–10+ and in year y
$\pi_{a,y}$	Probability of $P_{a,y}$
$\varepsilon_{X,y}$	Error term for $X_{o,y}$
$\varepsilon_{s,y,a}$	Observation error for $I_{s,a,y}$
$\gamma_{s,y}$	Error term for EU–Spanish survey catchability
γ	Scalar parameter for $M_{B,a,y}$
η_a	Scalar parameter for $M_{KI,a,y}$
σ_{γ_y}	Standard deviation of time varying γ
σ_R	Standard deviation of Σ_R AR1 process
φ_R	Autocorrelation parameter for Σ_R AR1 process
σ^2_δ	Variance of the process errors
σ^2_{F2}	Variance of $\Delta_{F,2,y}$
σ^2_{F3-10+}	Variance of $\Delta_{F,3-10+,y}$
σ_l	Parameter for landing data bounds
Σ_X	SD of $\varepsilon_{X,y}$
σ^2_X	Variance parameter for Σ_X
φ_X	Autocorrelation parameter for Σ_X AR1 process
$q_{s,a}$	Survey catchability parameter
$\sigma^2_{s,a,y}$	Variance of $\varepsilon_{s,y,a}$
σ^2_γ	Variance of $\gamma_{s,y}$

Appendix C

Figures

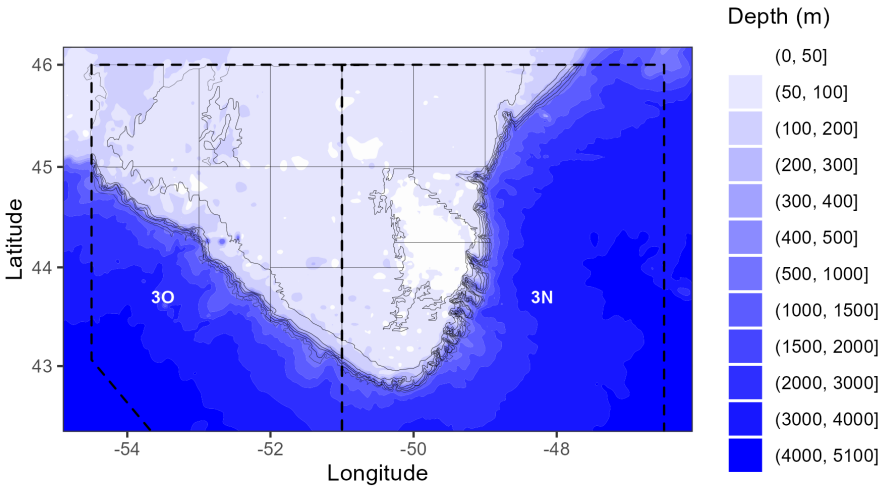

Figure C.1: DFO strata (solid lines) in NAFO Divisions 3NO (dashed lines) and depth intervals. The strata boundaries were provided as shapefiles by DFO. The bathymetric data were obtained from the NOAA server through the R package "marmap" (Pante and Simon-Bouhet, 2013). The map projection is WGS84.

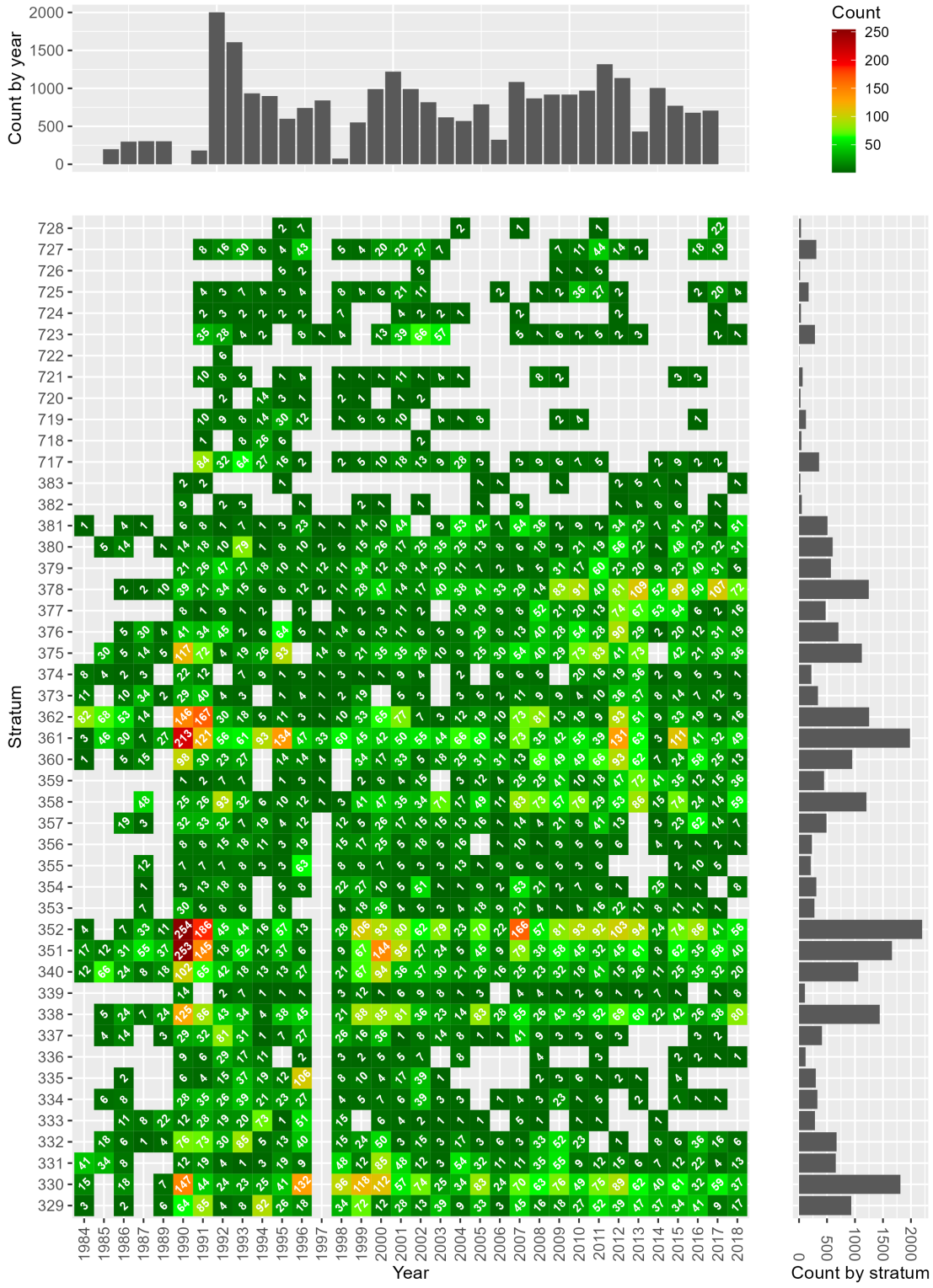

Figure C.2: The number of weight samples (white text) per stratum and year. Blank cells indicate no samples. Totals for years are shown at the top and for strata at the right.

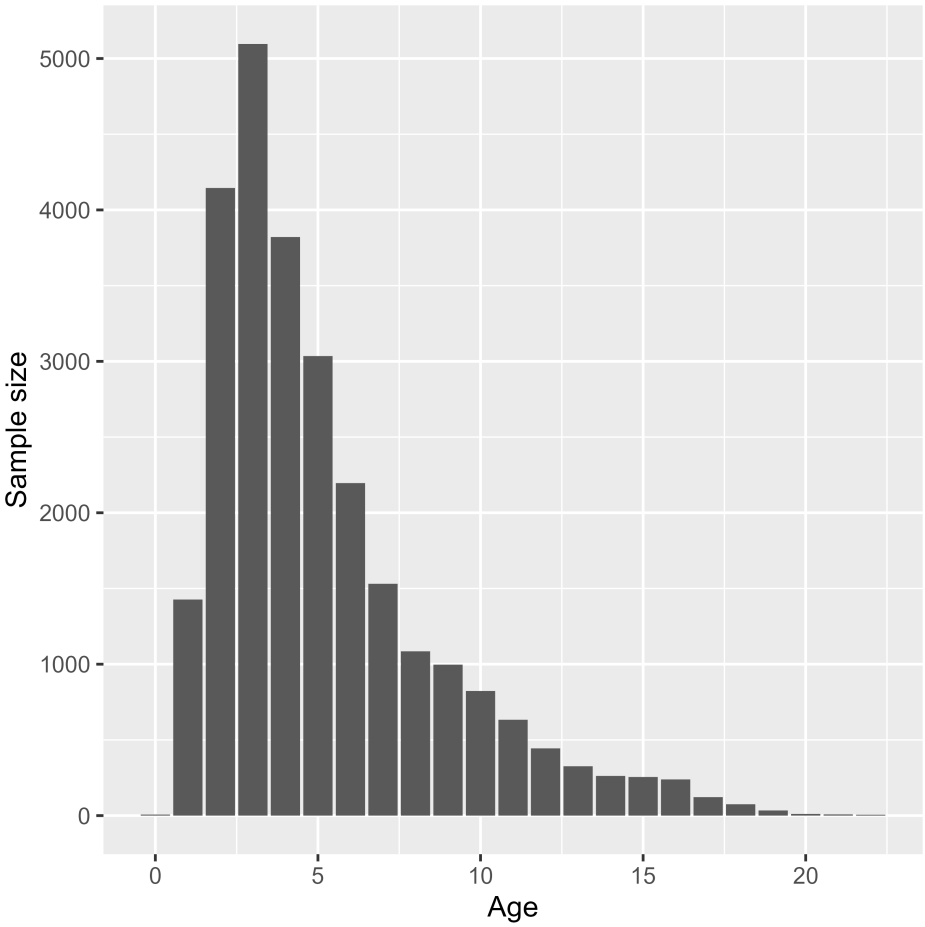

Figure C.3: Total number of length samples by age.

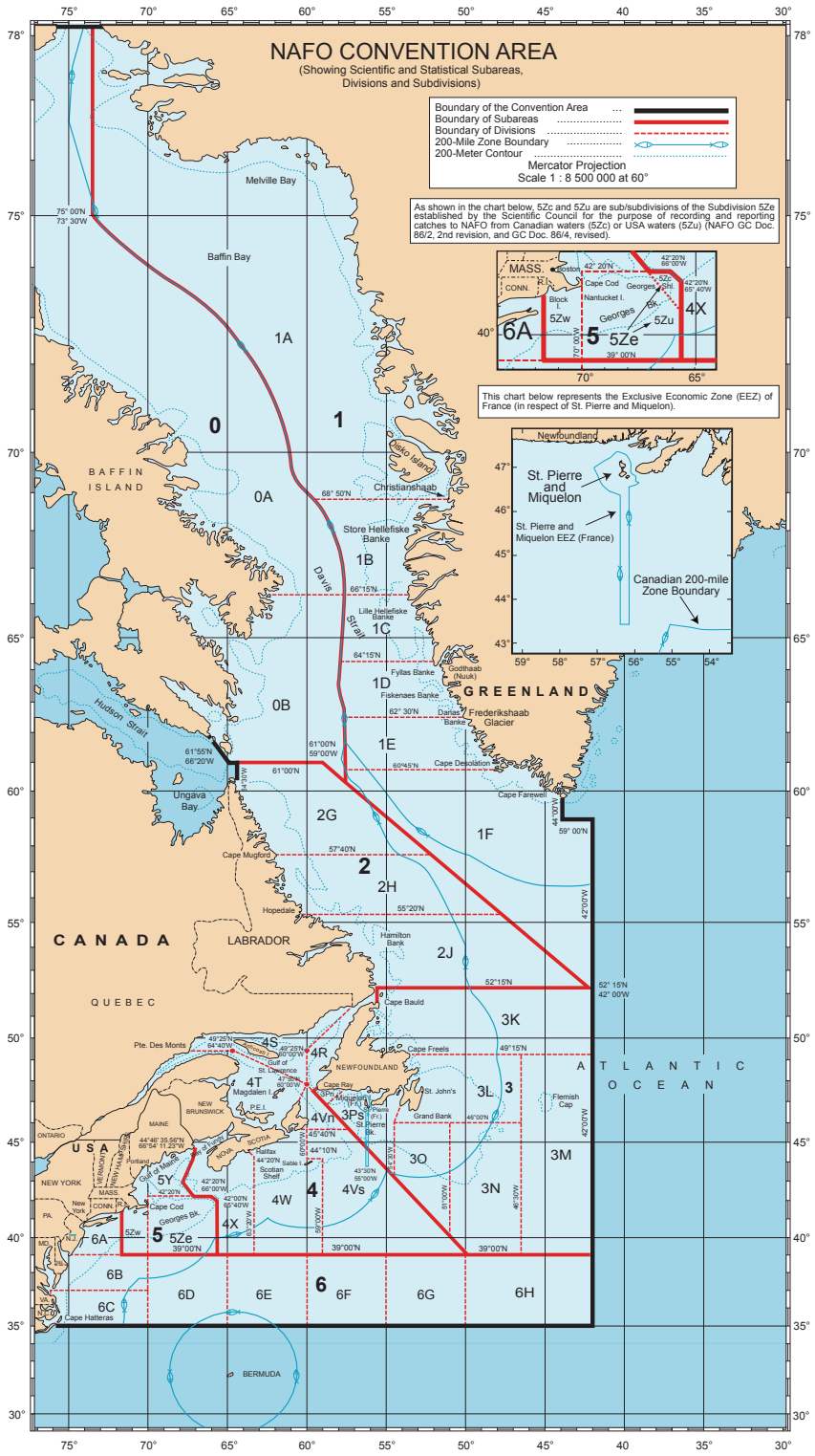

Figure C.4: NAFO convention area. ©*Northwest Atlantic Fisheries Organization.*